SYNTHESIS AND MODIFICATION OF MICRO AND MESOPOROUS MATERIALS AS CO2 ADSORBENTS

(SINTESIS DAN PENGUBAHSUAIAN BAHAN MIKRO AND MESOPOROS SEBAGAI BAHAN PENJERAP CO_2)

KHAIRUL SOZANA NOR KAMARUDIN
HANAPI MAT

FAKULTI KEJURUTERAAN KIMIA DAN KEJURUTERAAN SUMBER ASLI

UNIVERSITI TEKNOLOGI MALAYSIA

2009

ACKNOWLEDGEMENT

The financial support from the Ministry of Higher Education (MOHE) on the project (vot 78207) is gratefully acknowledged.

ABSTRACT

SYNTHESIS AND MODIFICATION OF MICRO AND MESOPOROUS MATERIALS AS CO2 ADSORBENTS

(Keyword: Microporous, Mesoporous, Zeolite, Amines, CO_2 adsorption)

Carbon dioxide (CO_2) removal from natural gas attracts more attention than other impurities due to its corrosiveness and inert property. Amine based chemical absorption has been used commercially for CO_2 separation. However, the liquid amine based processes pose operating difficulties due to high regeneration energy, large equipment size, solvent leakage and corrosion problem. Therefore, recent studies have introduced a promising approach which is the incorporation of organic amines into porous supports for CO_2 adsorption. This research studies the modification of porous materials by grafting amine functional groups directly to the surface of a solid sorbents. Amines (MEA, DEA, TEA, MDEA, and PEI) have been chosen as modification agents for mesoporous supports (MCM-41 and SBA-15) and microporous supports (zeolites NaY and 13X). The structures of the modified adsorbents were characterized by powder X-Ray Diffraction (XRD), nitrogen adsorption at 77K and Fourier Transform Infrared (FTIR) spectroscopy. Gas adsorption measurements were carried out using Thermal Gravimetric Analyzer (TGA). Investigation on the physicochemical properties and gas CO_2 adsorption characteristics of the amines modified adsorbents were thoroughly studied. Results revealed that types of amines and supports, amine loading concentration, metals loading, adsorption and heating temperatures significantly affect both structural and gas adsorption characteristics of the amine modified adsorbents. MEA modified MCM-41 shows the highest CO_2 adsorption capacity (40.91 mg/g sorbent) which is 2.2 times higher than MCM-41 support itself (18.58 mg/g sorbent). Although zeolites NaY and 13X show high adsorption but after modification, the adsorption capacity was reduced by 50 %. Cu modified MCM-41 also shows moderate adsorption (25.11 mg/g sorbent) but not much increment can be observed after grafting of MEA. As of operating temperatures of the adsorption process, the adsorption temperature at 25˚C and heating temperature at 100˚C show the highest adsorption capacity. Furthermore, adsorption bands observed in FTIR spectra demonstrated that the CO_2 interact strongly with the amine modified adsorbents.

Key Researchers:
Dr. Khairul Sozana Nor Binti Kamarudin
Associate Professor Dr. Hanapi Bin Mat
Chua Chung Lieh
Siti Syahida Binti Mohd Yassin
Mohd Hanafi Bin Abd. Rahim
Nur Hashimah Binti Alias
Umar Mokhtar Baba

ABSTRAK

SINTESIS DAN PENGUBAHSUAIAN BAHAN MIKRO AND MESOPOROS SEBAGAI BAHAN PENJERAP CO_2

(Kata kunci: Mikroporos, Mesoporos, Zeolite, Amin, Penjerapan CO_2)

Pemisahan karbon dioksida (CO_2) daripada gas asli lebih menarik perhatian berbanding bendasing lain kerana sifat menghakis dan merangkumi banyak ruang. Penjerapan secara kimia berasaskan bahan amina telah digunakan dalam pemisahan CO_2 secara komersil. Walau bagaimanapun, proses berasaskan cecair amina menunjukkan beberapa kekurangan seperti penggunaan tenaga yang tinggi, saiz alat yang besar, kebocoran bahan pelarut dan masalah kehakisan. Oleh sebab itu, kajian terbaru telah memperkenalkan satu kaedah baru untuk penjerapan CO_2 iaitu penggabungan bahan amina dengan bahan penyokong berliang. Tujuan kajian ini adalah untuk mensintesis pelbagai bahan penjerap seperti MCM-41, SBA-15, zeolit NaY dan 13X yang diubahsuai dengan amina seperti MEA, DEA, TEA, MDEA, dan PEI. Struktur bahan penjerap yang telah diubahsuai oleh amina dikaji dengan menggunakan Pembelaun X-Ray (XRD), penjerapan nitrogen pada suhu 77K dan infra merah pengubahan Fourier (FTIR) spektroskopi. Pengukuran penjerapan gas dijalankan menggunakan Penganalisa Termogravimetrik (TGA). Hasil kajian menunjukkan bahawa faktor-faktor seperti jenis amina, jenis bahan penyokong, kepekatan amina, penambahan logam dan suhu penjerapan mempengaruhi sifat penjerapan bahan penjerap yang diubahsuai dengan amina. MCM-41 yang diubahsuai dengan MEA menunjukkan nilai penjerapan CO_2 yang paling tinggi (40.91 mg/g sorbent) iaitu 2.2 kali lebih tinggi dari bahan penyokong MCM-41(18.58 mg/g sorbent). Walaupun zeolit NaY dan 13X menunjukkan kuantiti penjerapan yang tinggi, tetapi selepas pengubahsuaian dengan amina MEA menyebabkan pengurangan kuantiti penjerapan sebanyak 50 %. Sementara itu, MCM-41 yang diubahsuai dengan logam Cu menunjukkan penjerapan yang sederhana (25.11 mg/g sorbent). Walau bagaimanapun, selepas diubahsuai dengan MEA, tak banyak peningkatan yang diperolehi. Selain itu, suhu penjerapan pada 25˚C dan suhu pemanasan pada 100˚C menunjukkan kuantiti penjerapan yang paling tinggi. Selain itu, spektra daripada alat FTIR menunjukkan gas CO_2 mempunyai ikatan yang kuat terhadap permukaan bahan penjerap yang diubahsuai dengan amina.

Penyelidik Utama:
Dr. Khairul Sozana Nor Binti Kamarudin
Associate Professor Dr. Hanapi Bin Mat
Chua Chung Lieh
Siti Syahida Binti Mohd Yassin
Mohd Hanafi Bin Abd. Rahim
Nur Hashimah Binti Alias
Umar Mokhtar Baba

TABLE OF CONTENTS

LIST OF TABLES

LIST OF FIGURES

LIST OF SYMBOLS

^{0}C	-	Degree Celsius
T	-	Temperature (K)
d	-	Spacing of indices planes
h	-	Miller indices planes
k	-	Miller indices planes
l	-	Miller indices planes
%	-	Percentage
θ	-	Angle
λ	-	Wavelength
I_{rel}	-	Relative Intensity
wt.	-	Weight
Å	-	Angstrom (1Å = 10^{-10} m)
A	-	Absorbance
a.u.	-	Arbitrary unit

LIST OF ABBREVIATIONS

FTIR	-	Fourier Transform Infrared Spectroscopy
US	-	United State
BET	-	Brunauer, Emmett, Teller
XRD	-	X-Ray Diffraction
SEM	-	Scanning Electron Microscope
TEM	-	Transmission Electron Microscope
TGA	-	Thermogravimetric Analyzer
MEA	-	Monoethanolamine
DEA	-	Diethanolamine
TEA	-	Triethanolamine
MDEA	-	Methyl diethanolamine
PEI	-	Polyethylenimine

LIST OF APPENDICES

CHAPTER 1

INTRODUCTION

1.1 Introduction to CO_2 Adsorption

Malaysia has a vast reserve of natural gas, which places the country as the 13th largest gas reserves in the world in year 2001 (Anon,2005). As at 31 December 2003, Malaysia's gas reserves stood at 89.02 trillion standard cubic feet. At the current production rate, the gas reserve is estimated to last another 50 years (Anon, 2005). Recently, Malaysia is increasingly turning to natural gas from oil, not only as a source of energy, but also as a raw material in the manufacture of various petrochemical products. Natural Gas for Vehicle (NGV) program has diversified the use of natural gas into a new era.

However, before natural gas reaches the market place, numerous separation processes must be performed because the naturally occurring natural gas is a complex mixture containing many diverse components such as hydrocarbons (light, heavy, aromatic), water, sulfur components, carbon dioxide, nitrogen, mercury and other impurities. Therefore, there is a need to exploit cost-effective separation processes to

produce good quality gas (Daiminger, 2004). Carbon dioxide removal from natural gas attracts more attention than other impurities due to its corrosiveness and inert property. Up to date, the capture and separation of CO_2 can be achieved by different approaches, namely chemical and physical absorption using solvents, solid physical adsorption, cryogenic techniques and membrane separation (Gray *et al*., 2004; Meisen and Shuai, 1997). Among the approaches used, amine based chemical absorption have been used commercially for CO_2 capturing plant. However, the liquid amine based processes pose operating difficulties due to the challenge of keeping the solvent clean and operating within the process constraints of the system (Daiminger, 2004). Besides, this process also suffers from high regeneration energy, large equipment size, solvent leakage from piping system and also equipment corrosion problem (Xu *et al*., 2005). Therefore, many researchers have switched the work to another promising method, which is adsorption process due to its low energy requirement, cost advantage and ease of applicability over a relatively wide range of temperatures and pressures (Xu *et al*., 2003; Xu *et al*., 2005). Developing an adsorbent with high CO_2 adsorption capacity and high selectivity has now become the major challenge in the research of adsorption separation.

The discovery of zeolites by the Swedish scientist Cronstedt in 1756 until the introduction of synthetic zeolites in 1954 by Union Carbide as a new class of industrial adsorbents has proved the versatility of zeolites as good molecular sieve (Ghobarkar *et al*., 1999). Besides, zeolites also possess large internal pore volumes, molecular-size pores, regularity of crystal structures and diverse framework chemical composition, which enable them to be tailor-made into different structure and properties. Therefore, zeolites have been widely investigated as adsorbents for carbon dioxide separation (Sherman, 1999; Weitkamp, 2000; Ghobarkar *et al*., 1999).

In addition, the continuous research on the literature of design, synthesis, characterization and property evaluation of zeolites and molecular sieves for catalysis, adsorption and separation has driven the discovery of the M41S family of ordered

mesoporous adsorbents by scientists at Mobil Oil (Zhao *et al*., 1996; Kumar *et al*., 2001; Kresge *et al*., 1992). Among the M41S family, the two most investigated materials are the MCM-41 with a 2-D hexagonal structure and the MCM-48 with a 3-D cubic structure (Kumar *et al*., 2001). These highly ordered pore systems with tunable pore sizes, large specific surface areas and pore volumes, and high density of surface silanols provide excellent opportunities in inclusion chemistry. A large number of functionalizing entities including both organic and inorganic ligands have been introduced in the channels to generate catalysts, adsorbents, and to improve the hydrothermal and mechanical stabilities (Zhao *et al*., 1996; Zhao *et al*., 2000).

Discovery of the M41S family of molecular sieves has led to significant progress in the synthesis and characterization of ordered mesoporous materials. Large pore-size molecular sieves are much in demand for reactions or separations and the development of mesoporous structure has resulted in the preparation of well-ordered hexagonal mesoporous silica structures (SBA-15) with uniform pore sized up to approximately 300 angstroms (Stucky *et al*., 1998). SBA-15 which is a polymer-templated silica with hexagonally ordered mesopores has larger pore size, thicker pore walls and higher hydrothermal stability in comparison to MCM-41, which is surfactant-templated ordered mesoporous material.

The polymer employ to obtain SBA-15, poly(ethylene oxide)-poly(propylene oxide)-poly(ethylene oxide) (PEO-PPO-PEO), is biodegradable and cheaper than the surfactant used in the synthesis of MCM-41 (Fulvio *et al*., 2005). Another feature of SBA-15 is the existence of micropores interconnecting hexagonally ordered mesopores, which make it more suitable for catalysis because these interconnections facilitate diffusion inside the entire porous structure (Tatiana Klimova *et al*., 2006; Fulvio *et al*., 2005). These ordered structure with various pore sizes characteristic are suitable for either microporous or mesoporous materials to be use as support materials in modification of adsorbents.

Physical sorbents such as zeolites and carbon molecular sieves can reversibly adsorb a large quantity of CO_2 at room temperature. However, their capacity diminishes quickly at elevated temperature and the selectivity over water is poor. Amine functional groups are useful for CO_2 removal because of their ability to form ammonium carbamates and carbonates reversibly at moderate temperature (Gray *et al*., 2005). The incorporation of organic amines into a porous support is a promising approach for CO_2 sorbents combining good capacity and selectivity at moderate temperature (Zheng *et al*., 2005; Xu *et al*., 2002; Xu *et al*., 2003; Khatri *et al*., 2005).

Recently, the latest development of zeolites has been proposed with their new concept of CO_2 "molecular basket" for developing high-capacity, highly-selective CO_2 adsorbents, which can be operated at elevated temperature (Xu *et al*., 2003). This novel CO_2 "molecular basket" adsorbents are developed based on polyethyleimine (PEI)-modified mesoporous molecular sieve of MCM-41 type and shows high CO_2 adsorption capacity, which is 30 times higher than MCM-41 and more than twice of the pure PEI (Xu *et al*., 2003). Therefore, the proposed research will use the above mentioned concept to develop new amine modified porous materials as CO_2 adsorbents. Different alkanolamines including primary, secondary and tertiary amines will be used as the amine source and incorporated onto different type of support materials.

1.2 Research Background

Current technologies deploy at commercial scale for CO_2 removal use processes based on chemical absorption with alkanoamine such as monoethanolamine (MEA) solvent. However, the liquid amine-based processes suffer from high regeneration

energy, large equipment size, solvent degradation and equipment corrosion (Xu *et al*., 2005).

To overcome these disadvantages, several other separation technologies, such as adsorption, membrane and cryogenic separation have been studied. Over all the technologies, adsorption separation attracts more interest because of the low energy requirement, cost advantage, and ease of applicability over a relatively wide range of temperature and pressure. Therefore, regenerable solid sorbents will be a promising alternative that can potentially offer several advantages over liquid amine systems such as ease in handling of solids, reduced toxicity and corrosiveness (Rajesh *et al*., 2005). Besides that, regenerable solid CO_2 sorbents are also favorable for applications in enclosed environments, such as submarines and spacecraft.

Various porous supports impregnated with liquid amines have been reported and such hybrid sorbents have been used successfully onboard space vehicles for crew air scrubbing (Zheng *et al*., 2005). However, loss of amine components due to evaporation is a problem at moderate temperature. By grafting of amine functional groups directly to the surface of a physical sorbent, the evaporation problem can be eliminated and the overall thermal stability can be improved (Khatri *et al*., 2005; Xu *et al*., 2002). The key issue for adsorption separation is to develop an adsorbent with high CO_2 adsorption capacity and high CO_2 selectivity which will be the main objectives of this study.

1.3 Objectives and Scopes of Study

Several objectives have been specified in this research including synthesis of amine-modified adsorbents for carbon dioxide adsorption, the characterization of the physical and chemical properties of the synthesized adsorbents and the study of the carbon dioxide adsorption and desorption capacity. To be specific, two main objectives of this research are to study the effects of different type of amines on the adsorbents and the effects of different supporting materials, mesoporous materials and microporous materials by using one specific amine as standard (which is monoethanolamine, MEA) on the performance of carbon dioxide adsorption.

The main scopes in this research work is to achieve the specified objectives comprises of research activities such as preparation and modification of the adsorbents, the characterization of the adsorbents and the adsorption capacity study specifically for carbon dioxide separation. Two types of mesoporous adsorbents will be synthesis in this study as the supporting materials are MCM-41 and SBA-15. Meanwhile, other support materials such as zeolite NaY and 13X are obtained commercially.

After preparation of the support materials, the modification step is implemented by loading different types of amine groups into the adsorbents using freeze drying method. The characterization of chemical and physical properties of modified adsorbents such as the structure properties, the pore diameter distribution, the pore volume as well as the surface area are determined by X-ray diffraction (XRD) and N_2 adsorption/ desorption method using Quantachrome equipment. Meanwhile, thermal gravimetric analyzer (TGA) is used to study the performance of carbon dioxide adsorption for the modified adsorbents.

Other than adsorption capacity study, the modified adsorbents that have a good physical and chemical properties as well as adsorption properties such as good structure and high adsorption capacity is used as the standard adsorbent for the study of other parameters by varying amine concentration, adsorption temperatures, heating temperatures and carbon dioxide gas pressure for in situ adsorption study.

1.4 Report Outline

This thesis consists of five chapters which describes the research in a sequential order. Chapter 1 introduces the research background on amine modified adsorbents, problems encountered by the industry, and underlined objectives to solve the problems. Chapter 2 provides the literature review of the general aspects related to the field of research study. This includes natural gas processing, adsorption isotherms and mechanism, fundamental of microporous and mesoporous materials, modification of adsorbents and gas adsorption characteristics. Chapter 3 describes the materials and methods applied in the experimental study and adsorbents characterization in detail while the results and discussion of the findings are included in Chapter 4. Lastly, Chapter 5 summarized the results as well as the findings of the study and some recommendations for future work.

1.5 Summary

Ordered mesoporous and microporous materials on its own may have high performance as catalysts or as highly selective adsorbents. The modification of these adsorbents using different type of amines will create a combination of various physicochemical properties to produces more advance materials in many fields with additional functionality. Through this study, carbon dioxide adsorptive characteristics of amine modified adsorbents are well study and explain thoroughly for clear understanding. The fundamental results and findings obtained will enable researchers to carry on the work to design new gas adsorbents with higher adsorption capacity, selectivity and reversibility.

CHAPTER 2

LITERATURE REVIEW

2.1 Introduction to Natural Gas

Natural gas is nothing new. In fact, most of the natural gas that is brought out from under the ground is millions and millions of years old. However, it was not until recently that methods for obtaining this gas, bringing it to the surface, and putting it to use were developed.

Natural gas is a colorless, shapeless, and odorless gas in its pure form. Natural gas is combustible, and when burned it gives off a great deal of energy. Unlike other fossil fuels, however, natural gas is clean burning and emits lower levels of potentially harmful byproducts into the air. Energies are required constantly in various fields, for transportations, cooking, generate electricity and many more. It is this need for energy that has elevated natural gas to such a level of importance in our society and in our lives (Anon, 2005).

2.1.1 Fundamental of Natural Gas

Natural gas is a combustible mixture of hydrocarbon gases. While natural gas is formed primarily of methane, it can also include ethane, propane, butane and pentane. The composition of natural gas can vary widely, below is a chart outlining the typical makeup of natural gas before it is refined. From Table 2.1, it is clearly shows that carbon dioxide is the highest impurities (up to 8%) compare to others. Since the presence of carbon dioxide tend to cause corrosive and inert property problem, therefore it is necessary to remove this unwanted gas.

Table 2.1: Typical composition of natural gas (Anon, 2005).

Composition	Molecule Formula	Percentage
Methane	CH_4	70 – 90%
Ethane	C_2H_6	0 – 20%
Propane	C_3H_8	
Butane	C_4H_{10}	
Carbon Dioxide	CO_2	0 – 8%
Oxygen	O_2	0 – 0.2%
Nitrogen	N_2	0 – 5%
Hydrogen Sulphide	H_2S	0 – 5%
Rare Gases	A, He, Ne, Xe	trace

In its purest form, such as the natural gas used in Natural Gas Vehicles (NGV), it is almost pure methane. Methane is a molecule made up of one carbon atom and four hydrogen atoms, and is referred to as CH_4. Ethane, propane, and the other hydrocarbons commonly associated with natural gas have different chemical formulas.

Natural gas is considered 'dry' when it is almost pure methane, having had most of the other commonly associated hydrocarbons removed. When other hydrocarbons are present, the natural gas is considered 'wet' gas.

Natural gas has many uses, residentially, commercially, and industrially. Natural gas can be found in reservoirs underneath the earth and is commonly associated with oil deposits. Production companies search for evidence of these reservoirs by using sophisticated technology that helps to find the location of the natural gas, and drill wells in the earth where it is likely to be found. Once brought from underground, the natural gas is refined to remove impurities like water, other gases, sand, and other compounds. Some hydrocarbons are removed and sold separately, including propane and butane. Other impurities are also removed, like hydrogen sulfide (the refining of which can produce sulfur, which is then also sold separately). After refining, the clean natural gas is transmitted through a network of pipelines. From these pipelines, natural gas is delivered to its point of use.

2.1.2 Uses of Natural Gases

For hundreds of years, natural gas has been known as a very useful substance. The Chinese discovered a very long time ago that the energy in natural gas could be harnessed, and used to heat water. In the early days of the natural gas industry, the gas was mainly used to light streetlamps, and the occasional house. However, with much improved distribution channels and technological advancements, natural gas is being used in ways never thought possible.

There are so many different applications for the fossil fuel that it is hard to provide a complete list of everything it is used for. New uses are being discovered all time and in a wide range of area. Natural gas has many applications, commercially, for household, in industry, and even in the transportation sector. While the uses described in Figure 2.1 are not extensive, it may help to show just how much useful natural gas can be.

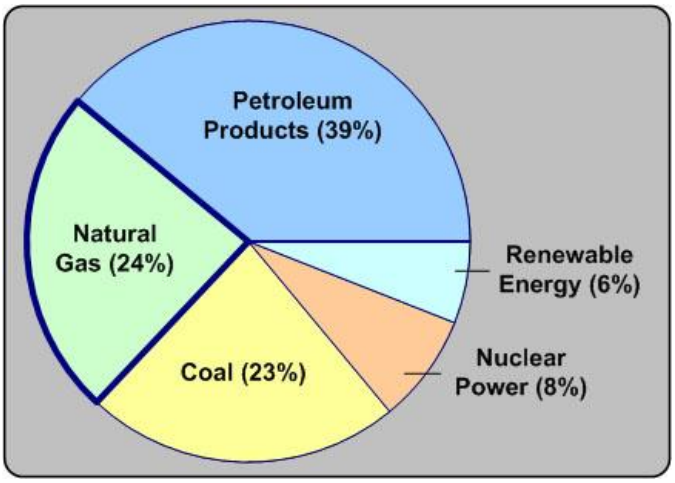

Figure 2.1: Total sources of energy consumed in U.S. for 2000 (Source: EIA - Annual Energy Outlook 2002).

According to the Energy Information Administration, energy from natural gas accounts for 24 percent of total energy consumed in the United States, making it a vital component of the nation's energy supply. Natural gas is used across all sectors, in varying amounts. Figure 2.2 gives an idea of the proportion of natural gas use per sector. The industrial sector accounts for the greatest proportion of natural gas use in the United States, with the residential sector consuming the second greatest quantity of natural gas. Other than United States, natural gas is also estimated to expand its share in the European energy market, from 22% in 2000 to 29% in 2030 (Mavrakis *et al.*, 2006). Although Asian countries like Malaysia, Thailand, China and others developing countries does not consume as much natural gas as of developed countries, however, it

cannot be deny that the application of natural gas in a wide range of areas is increasing gradually in the Asian region especially in transportation. Therefore, there is a necessity to continually developing new and improve method of natural gas processing.

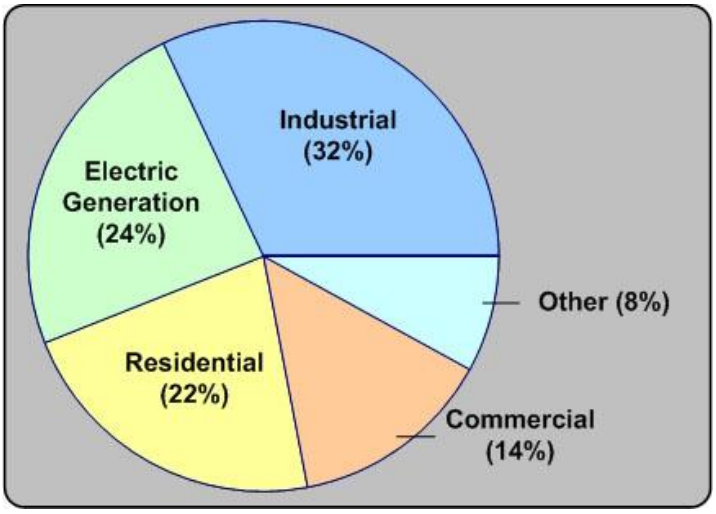

Figure 2.2: Natural gas use by sector (Source: EIA - Annual Energy Outlook 2002).

Natural gas has long been considered an alternative fuel for the transportation sector. In fact, natural gas has been used to fuel vehicles since the 1930's. According to the Natural Gas Vehicle Coalition, there are currently 130,000 Natural Gas Vehicles (NGVs) on the road in the United States today, and more than 2.5 million NGVs worldwide. In fact, the transportation sector accounts for 3 percent of all natural gas used in the United States. In recent years, technology has improved to allow for a proliferation of natural gas vehicles, particularly for fuel intensive vehicle fleets, such as taxicabs and public buses. However, virtually all types of natural gas vehicles are either in production today for sale to the public or in development, from passenger cars, trucks, buses, vans, and even heavy-duty utility vehicles. Despite these advances, a number of disadvantages of NGVs prevent their mass-production. Limited range, trunk space, higher initial cost, and lack of refueling infrastructure pose barriers to the future spread of natural gas vehicles.

Most natural gas vehicles operate using compressed natural gas (CNG). This compressed gas is stored in similar fashion to a car's gasoline tank, attached to the rear, top, or undercarriage of the vehicle in a tube shaped storage tank. A CNG tank can be filled in a similar manner, and in a similar amount of time, to a gasoline tank. This natural gas fuels a combustion engine similar to engines fueled by other sources. However, in a NGV, several components require modification to allow the engine to run efficiently on natural gas. In addition to using CNG, some natural gas vehicles are fueled by Liquefied Natural Gas (LNG). Some natural gas vehicles that exist today are bi-fuel vehicles, meaning they can use gasoline or natural gas, allowing for more flexibility in fuel choice.

2.1.3 Natural Gas Processing

The natural gas purchased by consumers consists almost entirely of methane, the simplest hydrocarbon. In gas reservoirs, however, methane is typically found with heavier hydrocarbons such as ethane, propane, butane and pentane. The raw gas also contains water vapor, hydrogen sulphide, carbon dioxide, nitrogen and other gases that are removed from the gas stream at processing plants.

In gas processing plants, hydrocarbons are separated through fractionation based on the different boiling points of the hydrocarbons in the natural gas liquids (NGL) stream. The liquids are cooled to temperatures around -50 °C and the various fractions are separated as they boil off as the liquids temperature is increased in stages in various heat exchangers. This cryogenic distillation, separating ethane and heavier hydrocarbons from sales gas (methane) occurs within cold boxes, typically made from aluminium (Coade and Coldham, 2006). An example of such a coldbox is shown in Figure 2.3.

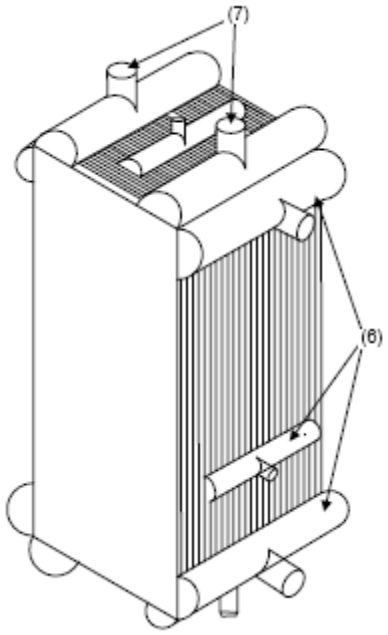

Figure 2.3: Schematic view of cryogenic heat exchanger showing the manifolds (6) and nozzles (7) (Coade and Coldham, 2006).

2.1.4 Carbon Dioxide Removal from Natural Gas

Fossil fuels will likely remain the mainstay of energy supply well into the 21st century. Availability of these fuels to provide clean, affordable energy is essential for the prosperity and the security of the world. However, increased CO_2 concentration in the atmosphere due to emissions of CO_2 from fossil fuel combustion has caused concerns about global warming. Improving the efficiency of energy utilization and increasing the use of low-carbon energy sources are considered to be potential ways to reduce CO_2 emissions. Recently, CO_2 capture and sequestration are receiving significant attention and being recognized as a third option for reduction in the global CO_2 emission (Khatri *et al*., 2005; Kaggerud *et al*., 2006). Furthermore, enriched CO_2 streams can be an important starting material for synthetic clean fuels and chemicals. For carbon

sequestration, the cost for CO_2 capture is expected to comprise about 75% of the total costs for geological or oceanic sequestration, with the other 25% costs attribute to transportation and injection. Therefore, the development of techniques for the cost-effective separation and capture of CO_2 is considered to be one of the highest priorities in the field of carbon sequestration (Xu *et* al., 2002; Xu *et* al., 2005).

2.1.4.1 Adsorption as a Method for CO_2 Removal

Adsorption is one of the promising methods that could be applicable for separating CO_2 from gas mixtures, and numerous studies have been conducted on separation of CO_2 by adsorption in the last two decades. Various adsorbents, such as activated carbons, pillared clays, metal oxides, and zeolites have been investigated. At lower temperatures (room temperature), the zeolite-based adsorbents have generally been found to show higher adsorption capacity. CO_2 adsorption capacity of zeolite 13X, zeolite 4A, and activated carbon was about 160, 135, and 110 mg/g-adsorbent, respectively, at 25 °C and 1 atm CO_2 partial pressure. However, their adsorption capacities rapidly decline with increasing temperature (Zheng *et al*., 2005). Moreover, since all the gases are physically adsorbed into/onto these adsorbents, the separation factors (such as CO_2/N_2 ratio) are low. To operate at relatively high temperature and reach a high separation factor, chemical adsorption was adopted. Investigation of the adsorption performance of hydrotalcite showed a CO_2 adsorption capacity of 22 mg/ g-adsorbent at 400 °C and 0.2 atm CO_2 partial pressure. Meanwhile, MgO showed an adsorption capacity of 8.8 mg/g-adsorbent at 400 °C. Both types of adsorbents need high temperature operation and have a low adsorption capacity, thus they are not suitable for practical use for CO_2 separation (Desideri and Paolucci, 1999; Xu *et* al., 2002; Xu *et* al., 2005).

For practical applications, selective adsorbents with high capacity are desired. Many of the separations should preferably be operated at relatively higher temperature, for example, higher than room temperature and up to ~150 °C which is a typical value of power plant stack temperature (Pedersen *et al*., 1995; Kaggerud *et al*., 2006). Developing an adsorbent with high CO_2 selectivity and high CO_2 adsorption capacity, which can also be operated at relatively high temperature, is desired for more efficient CO_2 separation by an adsorption method.

2.1.4.2 Adsorbent for CO_2 Removal

A new concept called "molecular basket" is being discovered to develop a high capacity, highly selective CO_2 adsorbent (Xu *et al*., 2002). A novel type of solid adsorbent has been discovered, which can serve as a "molecular basket" for "packing" CO_2 in condensed form in the nanoporous channels. To capture a large amount of CO_2 gas, the adsorbent needs to have large pore channels filled with a CO_2 capturing substance as the "basket". To cause the "basket" to be a CO_2 "molecular basket", a substance with numerous CO_2 affinity sites should be loaded into the pores of the support to increase the affinity between the adsorbent and CO_2 and as a result, the CO_2 adsorption selectivity and CO_2 adsorption capacity can be increased. In addition, the adsorption affinity to CO_2 by the CO_2 –philic substance increased in the confined mesoporous environment and therefore the mesoporous molecular sieve can have a synergetic effect on the adsorption of CO_2 by CO_2 –philic substance (Xu *et al*., 2003; Xu *et al*., 2005).

2.1.4.3 Amine Solutions as Carbon Dioxide Removal System

Several techniques to remove CO_2 from gas mixtures have been studied since 1970, but most of them were applied to produce technical CO_2 as process gas, mainly for the food and chemical industry. In the following decade, some of the CO_2 capture systems were considered for application in power plants and separation of natural gas. With the discovery of increased number of natural gas fields, more power plants are converting to the use of natural gas.

Among the alternative for CO_2 capture, chemical absorption with amine aqueous solutions was demonstrated as one of the most mature and less expensive technologies to be applied to power plants. The absorption stripping system is particularly interesting because of its possibility to regenerate the solution continuously, thereby in an almost closed cycle (Desideri and Paolucci, 1999; Xu *et* al., 2005). The plant for removing CO_2 from flue gases has two main elements, which are the absorption and stripping packed columns. This will allows a continuous regeneration of the amine solution, which saves considerable amounts of solvent. Amines in the water solution react with CO_2 in the absorption column, forming chemical compounds that separate CO_2 from the gas mixtures at a higher rate than the natural CO_2 absorption in pure water (Desideri and Paolucci, 1999).

To date, all commercial CO_2 capture plants use processes based on chemical absorption with alkanolamine such as monoethanolamine (MEA) solvent. An example is the Fluor Econamine process. However, the liquid amine-based processes suffer from high regeneration energy, large equipment size, solvent degradation and equipment corrosion. To overcome these disadvantages, several other separation technologies, such as, adsorption, membrane and cryogenic separation have been studied. Because of the low energy requirement, cost advantage, and ease of applicability over a relatively wide

range of temperatures and pressures, adsorption separation attracts much interest. The main target for adsorption separation is to develop an adsorbent with high CO_2 adsorption capacity and high CO_2 selectivity (Desideri and Paolucci, 1999; Xu *et* al., 2003; Xu *et* al., 2005).

2.2 Adsorption Process

Most of the physical, chemical and biological processes take place at the boundary between two phases, while others are initiated at that interface. The change in concentration of a given substance at the interface as compared with the neighboring phases is referred to as adsorption (Sing, 1998; Dabrowski, 2001). Depending on the type of phases in contact, adsorption process can be divided into following systems:

- Liquid-gas
- Liquid-liquid
- Solid-liquid
- Solid-gas

The major development of adsorption processes on a large, industrial scale deals mainly with the solid-gas and solid-liquid interfaces, but in various laboratory separation techniques all types of interfaces are applied. The term ‘fluid’ is commonly used to denote gas or liquid in contact with the boundary surface of solids.

2.2.1 Adsorption Concept

A basic concept in adsorption occurring at every interface is the real adsorption system. By considering this concept in terms of solid-gas interface, the real adsorption system can be defined as an equilibrium including the adsorbent being in contact with the bulk phase and the interfacial layer. This layer consists of two regions which are the part of gas residing in the force field of the solid surface and the surface layer of the solid. The term ‘adsorption’ deals with the process in which molecules accumulate in the interfacial layer, but desorption denotes the converse process.

Adsorption hysteresis is said to occur when the adsorption and desorption curves deviate from one another. In such a case the isotherm possesses a hysteresis loop, the shape of which varies from one adsorption system to another. Hysteresis loops are mostly with mesoporous solids, where the so-called capillary condensation occurs. The material in the adsorbed state is defined as the ‘adsorbate’, but that in the bulk gas or vapor phase prior to being adsorbed is called the ‘adsorptive’. The penetration by the adsorbate molecules into the bulk solid phase is determined as ‘absorption’. The term ‘sorption’ together with the terms ‘sorbent’, ‘sorbate’ and ‘sorptive’ is also used to denote both adsorption and absorption, when both occur simultaneously or cannot be distinguished (Sing, 2004; Sing, 1998; Dabrowski, 2001).

The fundamental concept in adsorption science is that named as the adsorption isotherm. It is the equilibrium relation between the quantity of the adsorbed material and the pressure or concentration in the bulk fluid phase at constant temperature. Apart from the results of the calorimetric measurements, the adsorption isotherm is the primary source of information on the adsorption process.

A complete statistical description is especially complicated by the heterogeneity of the solid materials which include porous adsorbents, as for the majority of industrial adsorbents. Assuming thermodynamic equilibrium between the surface and bulk phases, various adsorption isotherms can be derived by utilizing the equality of the chemical potentials of a given component in coexisting phases. The analytical forms of these equations depend on the assumed models for the surface and bulk phases. The surface phase may be considered as a monolayer or multilayer, and as localized, mobile or partially mobile. The analytical forms of adsorption isotherms are complex due to structural and energetic heterogeneity of the solid surfaces, which is characteristic of a great number of adsorbents used in practice (Sing, 1998; Choma *et* al., 2003; Dabrowski, 2001)..

2.2.2 Types of Adsorption

2.2.2.1 Ion Exchange

The equilibrium between a bulk phase and the surface layer may be established with regard to neutral or ionic particles. If the adsorption process of one or several ionic species is accompanied by the simultaneous desorption of an equivalent amount of ionic species, this process is considered as an ion exchange.

2.2.2.2 Physisorption

Adsorption can result either from the universal van der Waals interactions (physical adsorption, physisorption) or it can have the character of a chemical process (chemical adsorption or chemisorption). Physical adsorption can be compared to the condensation process of the adsorptive. As a rule, it is a reversible process that occurs at a temperature lower or close to the critical temperature of an adsorbed substance. Therefore, physical adsorption is very effective particularly at a temperature close to the critical temperature of a given gas.

2.2.2.3 Chemisorption

Contrary to physisorption, chemisorption occurs only as a monolayer (Adamson, 1996). Chemisorption occurs usually at temperatures much higher than the critical temperature and by contrast to physisorption is a specific process which can only take place on some solid surfaces for a given gas. Under favourable conditions, both processes can occur simultaneously or alternately. Physical adsorption is accompanied by a decrease in free energy and entropy of the adsorption system and, thereby, this process is exothermic (Sing, 1998; Dabrowski, 2001).

2.2.3 Adsorption Isotherms

Porous materials are defined in terms of their adsorption properties. The term adsorption originally denoted the condensation of gas on a free surface as opposed to its entry into the bulk, as in absorption. Today, however, this distinction is frequently not observed, and the uptake of a gas by porous materials is often referred to as adsorption or simply sorption, regardless of the physical mechanism involved. Adsorption of a gas by a porous material is described quantitatively by an adsorption isotherm, the amount of gas adsorbed by the material at a fixed temperature as a function of pressure. The uptake of fluids into a porous material could be intuitively viewed simply as the filling of an existing vacuum, but adsorption has long been recognized as a far more subtle phenomenon (Sing, 2004; Barton *et al*., 1999; Dabrowski, 2001).

J. W. Gibbs expressed the concept of adsorption on a general thermodynamic basis as follows. For the system of a fluid in contact with an adsorbent, he defined the amount adsorbed as the quantity of fluid that is in excess of that which would be present if the adsorbent had no influence on the behavior of the fluid. The concept of adsorption as related to an area of exposed surface was developed by Irving Langmuir in his work on the condensation of gases on surfaces. From these studies emerged the concept of adsorption as a dynamic equilibrium between a gas and a solid surface resulting in a surface layer that is only one molecule thick, a concept that quite naturally led to the Brunauer, Emmett, and Teller (BET) treatment of multilayer adsorption. The BET equation is still commonly used for the determination of surface areas of porous solids (Dabrowski, 2001; Barton *et al*., 1999; Zhao *et al*., 2001).

Porous materials are most frequently characterized in terms of pore sizes derived from gas sorption data, and IUPAC conventions have been proposed for classifying pore sizes and gas sorption isotherms that reflect the relationship between porosity and

sorption. In terms of the experience of adsorption science, total porosity is usually classified into three groups. According to the IUPAC recommendation (Everett, 1998), the micropores are defined as pores of a width not exceeding 2 nm, mesopores are pores of a width between 2 and 50 nm, and macropores represent pores of a width greater than 50 nm. The above classification is widely accepted in the adsorption literature. Nowadays, the expression nanopore is used to represent both micropores and mesopores. Adsorption by mesopores is dominated by capillary condensation, whereas filling of micropores is controlled by stronger interactions between the adsorbate molecules and pore walls. It is important that this nomenclature addresses pore width but not pore shape. Pore shape can be important in some circumstances, such as when dealing with shape selective molecular sieve behavior.

The IUPAC classification of adsorption isotherms is illustrated in Figure 2.4 The six types of isotherm are characteristic of adsorbents that are microporous (type I), nonporous or macroporous (types II, III, and VI) or mesoporous (types IV and V). The differences between types II and III isotherms and between types IV and V isotherms arise from the relative strengths of the fluid-solid and fluid-fluid attractive interactions: types II and IV are associated with stronger fluid-solid interactions and types III and V are associated with weaker fluid-solid interactions. The hysteresis loops usually exhibited by types IV and V isotherms are associated with capillary condensation in the mesopores. The type VI isotherm represents adsorption on nonporous or macroporous solids where stepwise multilayer adsorption occurs (Kruk *et al.*, 1999; Sing, 2001; Barton *et al*., 1999; Ustinov *et al*., 2005).

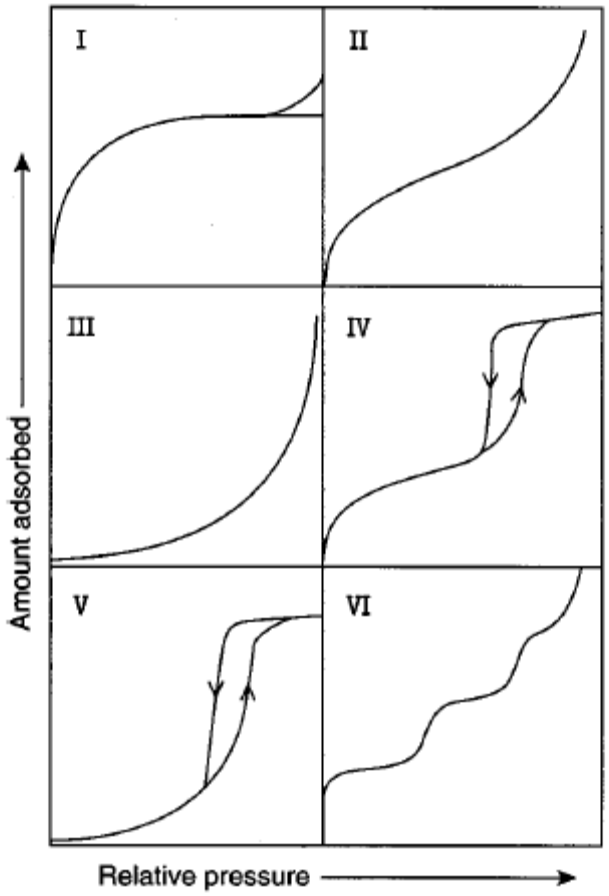

Figure 2.4: IUPAC classifications of adsorption isotherms (Barton *et* al., 1999).

Most of the solid adsorbents of great industrial applications possess a complex porous structure that consists of pores of different sizes and shapes. If the pores are slit shaped measurement used are in term of width but for the pores with a cylindrical shape the term diameter is frequently used.

The significance of pores in the adsorption processes largely depends on their sizes. Because sizes of micropores are comparable to those of adsorbate molecules, all atoms or molecules of the adsorbent can interact with the adsorbate species. That is the fundamental difference between adsorption in micropores and larger pores like mesopores and macropores. Consequently, the adsorption in micropores is essentially a

pore-filling process in which their volume is the main controlling factor (Everett, 1998; Dabrowski, 2001). Thus, as the essential parameter characterizing micropores is their volume usually referred to a unit mass of the solid and characteristics of their sizes. This characteristic is expressed by the micropore distribution function evaluated mainly from the low concentration adsorption data.

In the case of mesopores whose walls are formed by a great number of adsorbent atoms or molecules, the boundary of interphases has a distinct physical meaning. That means that the adsorbent surface area has also a physical meaning. In macropores the action of adsorption forces does not occur throughout their void volume but at a close distance from their walls. Therefore, the monolayer and multilayer adsorption takes place successively on the surface of mesopores, and their final fill proceeds according to the mechanism of capillary adsorbate condensation. Therefore, the basic parameters characterizing mesopores are:

- Specific surface area
- Pore volume
- Pore size or pore volume distribution.

Mesopores, like macropores, play an essential role in the transport of adsorbate molecules inside the micropore volume. The mechanism of adsorption on the surface of macropores does not differ from that on flat surfaces. The specific surface area of macroporous solids is very small, that is why adsorption on this surface is usually neglected. The capillary adsorbate condensation does not occur in macropores (Sing, 1998; Jaroniec *et al*., 2001; Dabrowski, 2001).

2.2.4 Adsorption Mechanism by Porous Adsorbents

2.2.4.1 Physisorption by Microporous Adsorbents

In the IUPAC classification of pore size, the upper limit of the micropore width was placed at approximately 2 nm. It turns out that this limiting width is somewhat arbitrary since the mechanism of pore filling is not determined by pore width alone.

The high p/p^0 plateau of a well-defined Type I isotherm always extends over a wide multilayer range. The great majority of Type I isotherms can be attributed to micropore filling, but there are a few systems like butanol on alumina with which a form of 'gas phase autophobicity' inhibits the development of the multilayer. This behavior is not possible with simple adsorptive molecules such as Ar, Kr, N , O and etc. Or even with alkanes and other larger molecules of low polarity. With these adsorptives, the low multilayer slope is a direct consequence of a small external area (Dabrowski, 2001; Sing, 1998).

It is now apparent that Type I isotherms can be broadly divided into two groups. Ultramicroporous carbons and molecular sieve zeolites exhibit high adsorption affinity, their isotherms generally having a high degree of rectangularity with the plateau approached at very low p/p^0. The second group of Type I isotherms are 'supermicroporous' activated carbons and oxide xerogels which have wider pores. In this case, the initial part of the isotherm is less steep and the approach to the plateau more gradual. However, this difference in isotherm shape is not really controlled by the absolute pore width, but it is dependent on the pore width and geometry in relation to the size, shape and electronic character of the adsorptive molecules (Barton *et* al., 1999; Dabrowski, 2001; Sing, 1998).

The micropores in activated carbons tend to be slit-shaped. In the ultramicropores of this shape there is a significant overlap of adsorption forces provided that the pore widths are not much larger than two molecular diameters. This is manifested in the form of enhanced adsorption energies, which are responsible for the steepness of the isotherm at low p/p^0. This process has been termed 'primary micropore filling'. Supermicropores in the range of approximately 2 to 5 molecular diameters are filled by a combination of surface coverage at low p/p^0 and a cooperative process or quasi-multilayer adsorption at higher p/p^0 (up to 0.2). Since it involves two overlapping stages, supermicropore filling is not a first order transition, as in the case of capillary condensation (Kruk *et al*., 1999; Sing, 1998).

2.2.4.2 Physisorption by Mesoporous Adsorbents

The characteristic shape of a Type IV isotherm is the result of surface coverage of the mesopore walls followed by pore filling. The onset of capillary condensation (the pore filling process) is indicated by an upward departure of the isotherm from the multilayer Type II isotherm for the same gas-solid system. The plateau at higher p/p^0 is attained when the mesopore filling is complete (Barton *et al*., 1999; Sing, 1998).

If the Kelvin equation is used to evaluate the mesopore size, it is necessarily assumed that a simple relationship relates the meniscus curvature to the pore shape and size. Thus, if the pores are cylindrical, the meniscus shape is hemispherical; but if the pores are slit-shaped, the meniscus becomes hemicylindrical. Other assumptions involved in the computation of the mesopore size distribution are that the pores are rigid and that a standard multilayer correction curve can be applied. To obtain the mesopore volume from the amount adsorbed at the plateau, the condensate is assumed to have the

same density as the liquid adsorptive at the operational temperature (Kruk *et al*., 1999; Sing, 1998).

A long-standing problem in mesopore analysis is the interpretation of the various hysteresis loops associated with most Type IV isotherms. For many years it was thought that the desorption branch of the loop represented thermodynamic equilibrium and therefore should be adopted for the pore size analysis. This practice is now questionable since the path of the desorption branch is often dependent on network-percolation effects. On the other hand, it is known that on the adsorption branch delayed condensation is the result of the persistence of a metastable multilayer, this effect being especially pronounced in slit-shaped pores (Kruk *et al*., 1999; Sing, 1998; Mercuri *et al*., 2006).

It is of great advantage to have independent information on the pore shape and connectivity, but the size and shape of the loop itself can also give a useful indication of the predominant pore filling or emptying mechanisms. Thus, a narrow Type H1 loop, with almost vertical and parallel branches, is generally associated with delayed condensation and very little percolation hold-up, whereas a much broader Type H2 loop (with a very steep desorption branch) has the typical features associated with network-percolation.

Recent work on MCM-41, a model mesoporous adsorbent, has revealed that it is possible to obtain well-defined reversible Type IV isotherms. The pore structure of MCM-41 is in the form of hexagonal arrays of uniform tubular channels of controlled width. Most attention has been given so far to a form of MCM-41 with 4 nm pores. With samples of this grade of MCM-41 the reversible capillary condensation/ evaporation of nitrogen at 77 K occurs over the narrow range of p/p^0 = 0.41- 0.46. By applying the Kelvin equation and correcting for multilayer thickness, pore diameters of 3.3- 4.3 nm

can be obtain, which agrees well with a mean value of approximately 4 nm derived from the volume/ surface ratio (Kruk *et al*., 1999; Mercuri *et al*., 2006; Sing, 1998). A number of other adsorptives such as argon, oxygen, carbon dioxide, sulfur dioxide and various alcohols have been found to give Type H1 hysteresis loops with the 4 nm MCM-41. In another investigation, it was found that the carbon tetrachloride isotherms determined at temperatures between 273 and 303 K on a 3.4 nm pure silica form of MCM-41 exhibited steep and very narrow hysteresis loops, whereas the corresponding isotherm at 323 K was completely reversible (Beck and Vartuli, 1996; Sing, 1998).

According to Sing, 1998, when they are confined to very narrow ranges of p/p^0, the reversible pore-filling steps appear to be equivalent to first order phase transformations, the p/p^0 being dependent on the adsorptive and the temperature. It seems significant that for a given adsorptive the characteristic p/p^0 is remarkably close to the lower limit of closure of the hysteresis loop (the limiting chemical potential controlling the stability of the capillary condensate). As a conclusion, the reversible stepwise filling of the mesopores in MCM-41 is due to:

(i) The absence of pore blocking effects.
(ii) The tubular pore shape.
(iii) The particular range of its narrow pore size distribution in relation to the temperature and properties of the adsorptive.

2.2.5 Adsorption Controlling Parameters

Since the discovery of porous materials, the adsorption study between solid and gas has advanced to a new level. There had been numerous studies on adsorption controlling parameters and can be concluded to the following factors:

(i) Nature of adsorbent and adsorbate.
(ii) Surface area of the adsorbent.
(iii) Pressure.
(iv) Temperature.

The nature of adsorbent and adsorbate show significant effect on the amount of gas (adsorbate) adsorbed into/ onto adsorbent. Easily liquefy gases such as SO_2, NH_3, HCl and CO_2 adsorbed more readily than permanent gases like H_2, N_2 and O_2 which do not liquefy easily. This is the result of Van der Waals or molecular forces of the easily liquefy gases which is much greater than permanent gases. Different type of adsorbents adsorbed different amounts of gas. Vice versa, different type of gases (adsorbate) adsorbed onto adsorbent in a different amounts depends on the nature of the adsorbates such as molecular weight, polarity, molecule size, shape and other physical and chemical properties (Dabrowski, 2001; Chhatwal and Mehra, 1974).

Adsorption refers to the condensation of gases on free surfaces as opposed to absorption where molecules penetrate into the mass of the absorbent. This shows how much important of high surface area in adsorption. A large specific surface area is preferable for providing large adsorption capacity. However, the creation of high internal surface area in a specific volume gives rise to a much larger numbers of small sized pores between adsorption surfaces. The size of the micropores determines the accessibility of adsorbate molecules to the internal adsorption surface, therefore the pore size distribution of micropores is another important property for characterizing

adsorptivity of adsorbents. Porous materials such as zeolite, mesoporous molecular sieves and carbon molecular sieves can be specifically synthesis with precise pore size distribution and hence can be tailored for a particular separation (Barton *et al.*, 1999; Beck and Vartuli, 1996).

Adsorption capacity also depends on the pressure of the gas in a certain confinement in the adsorption process. Adsorption of gas basically follow Le Chatelier's principle which stated that with the decrease of pressure, the magnitude of adsorption also decrease and vice versa. Besides that, Le Chatelier's principle can also be apply for temperature effects on adsorption. However, the principle is a bit different whereas, the decrease in temperature will result in increase of adsorption magnitude and vice versa. Physical adsorption (physisorption) is very effective particularly at a temperature close to the critical temperature of a given gas. Meanwhile, chemical adsorption (chemisorption) occurs usually at temperatures much higher than the critical temperature (Dabrowski, 2001; Sing, 1998; Chhatwal and Mehra, 1974).

2.3 Adsorbents

Most solid adsorbents for industrial applications possess a complex porous structure that consists of different sizes and shapes. If the pores are slit shaped, their width is consider as the size. However, for pores with cylindrical shape the term diameter is frequently used.

Adsorbents or porous materials are characterized in terms of pore sizes derived from gas sorption data. Through IUPAC conventions, classification of pore sizes and

gas sorption isotherms reflect the relationship between porosity and sorption (Dabrowski, 2001; Barton *et al*., 1999). Pores are classified according to pore diameter as follows:

- Micropores diameters less than 2 nm;
- Mesoporous diameters between 2 and 50 nm;
- Macroporous diameters more than 50 nm.

2.3.1 Microporous Materials

In the IUPAC classification of pore size, the upper limit of the micropore width was placed at approximately 2 nm. Any structure below 2 nm in pore size are considered microporous materials such as zeolite A, zeolite Y, ZSM-5, AlPO4-11, AlPO4-5, VPI-5, cloverite and others which mostly are from zeolite type of framework materials. Zeolites occur in nature and have been known for almost 250 years as aluminosilicate minerals. Examples are faujasite, mordenite, offretite, ferrierite, erionite and chabazite. Today, these and other zeolite structures are of great interest in catalysis and other applications, yet their naturally occurring forms are of limited value, because:

i) they almost always contain undesired impurity phases,
ii) their chemical composition varies from one deposit to another and even from one stratum to another in the same deposit,
iii) nature did not optimize their properties for catalytic applications.

Zeolite was originally discovered in the 18^{th} century (1756) by a Swedish mineralogist, Cronstedt, who describes the zeolite behavior under fast heating

conditions, when the zeolite minerals seem to boil because of the fast water loss. The word derives from two Greek words *zeo* and *lithos*, which means “stone that boils”. Typically, zeolites are hydrated, porous crystalline aluminosilicates. The framework is an assemblage of SiO_4 and AlO_4 tetrahedral joined together by sharing oxygen atoms (Ghobarkar *et al*., 1999; Weitkamp, 2000).

2.3.1.1 Classification of Zeolites

The term "molecular sieve" is used to describe a class of materials that exhibit selective sorption properties, for instance that are able to separate components of a mixture on the basis of molecular size and shape. The term molecular sieve is used to describe microporous crystalline materials such as aluminosilicates (zeolites), silica molecular sieves, aluminoposphates and related materials.

The extraordinary properties of zeolites are caused by their crystal lattice. Therefore, a proper classification starts from the 3-dimensional bonding of the tetrahedrally coordinated framework cations. Today about 800 different zeolites are known which can be classified by 119 different zeolite structure types. These structure types are described by a three letter code. Only about l/4 of them are naturally occurring, the others are synthetic. Instead of using the unit cell of the respective zeolite for description, which is only specific for the zeolite type, secondary building units (SBU’s) consisting of different arrangements of tetrahedra (primary building units) are used. The SBUs are, however, only building elements of the zeolite unit cell. Different SBUs can be used for the classification of a zeolite (Ghobarkar *et al*., 1999; Weitkamp, 2000).

The topology of the zeolite framework is given by a unique three-letter code which is not related to the composition of the material. Thus, ZSM-5 and silicalite-1 are materials with MFI topology. Silicalite-1 is a pure silica analogue of ZSM-5 (generally, an MFI type material is regarded as ZSM-5 when there is more than one aluminum per unit cell, for example a SiO_2/Al_2O_3 ratio less than 190) and strictly it cannot be considered as a zeolite but rather as a silica molecular sieve. The MFI structure is built up by 5-1 secondary building units (SBU; the smallest number of TO_4 units, where T is Si or Al, from which zeolite topology is built) which are link together to form chains as shown in Figure 2.5 and the interconnection of these chains leads to the formation of the channel system in the structure. The MFI structure has a three dimensional pore system consisting of sinusoidal 10-ring channels (5.1 x 5.5 Å) and intersecting straight 10-ring channels (5.3 x 5.6 Å) (Weitkamp, 2000; Han *et al*., 2005)

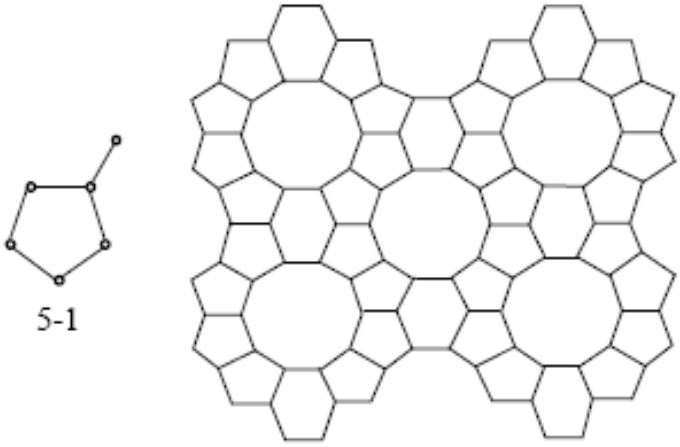

Figure 2.5: A 5-1 secondary building unit and the MFI structure (Weitkamp, 2000).

2.3.1.2 Structure and Framework of Zeolites

The elementary building units of zeolites are SiO and AlO tetrahedra. Adjacent tetrahedra are linked at their corners via a common oxygen atom, and this result in an inorganic macromolecule with a structurally distinct three-dimensional framework. It is evident from this building principle that the net formula of the tetrahedra is SiO and AlO_2^- . The framework of a zeolite contains channels, and channel interintersections and/or cages with dimensions from 0.2 to 1 nm. Inside these voids are water molecules and small cations which compensate the negative framework charge.

Figure 2.6 shows the structures of four selected zeolites along with their respective void systems and pore dimensions. In these commonly used representations, the T-atoms are located at the vertices, and the lines connecting them stand for T–O–T bonds. For example, if 24 tetrahedra are linked together as shown in the top line of Figure 2.6, the cubo-octahedron, also referred to as a sodalite unit or β-cage, results. It is an important secondary building unit from which various zeolite structures derive. If sodalite units are connected via their hexagonal faces as shown in Figure 2.6, the structure of the mineral faujasite results. Zeolite Y is of utmost importance in heterogeneous catalysis, for example it is the active component in catalysts for fluid catalytic cracking. Its pore system is relatively spacious and consists of spherical cages, referred to as supercages, with a diameter of 1.3 nm connected tetrahedrally with four neighboring cages through windows with a diameter of 0.74 nm formed by 12 TO_4-tetrahedra. Zeolite Y is therefore classified to possess a three-dimensional, 12-membered-ring pore system (Han *et al*., 2005; Derouane, 1998; Weitkamp, 2000; Astala and Auerbach, 2004).

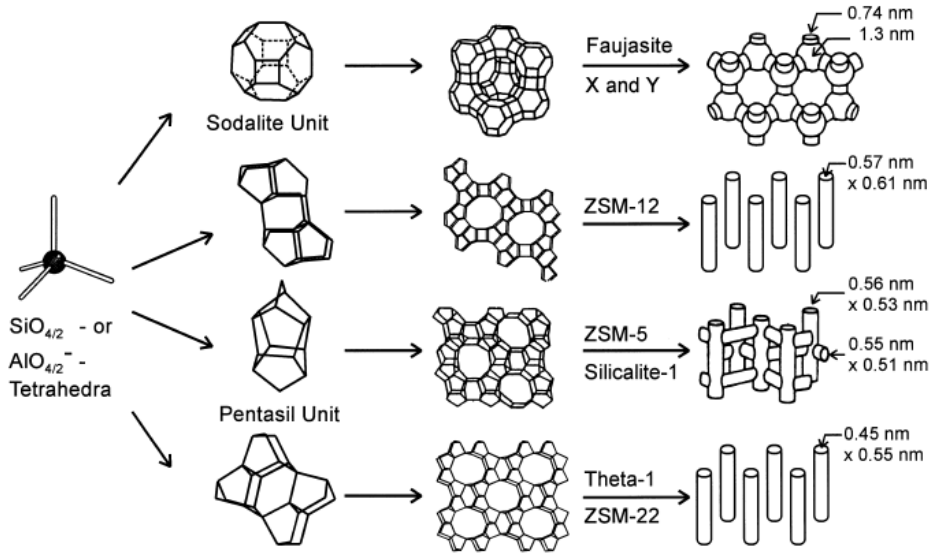

Figure 2.6: Structures of four selected zeolites (from top to bottom: faujasite or zeolites X, Y; zeolite ZSM-12; zeolite ZSM-5 or silicalite-1; zeolite Theta-1 or ZSM-22) and their micropore systems and dimensions (Weitkamp, 2000).

2.3.2 Mesoporous Materials

Porous materials have attracted the attention of chemists and materials scientists due to commercial interest in their application in chemical separations and heterogeneous catalysis as well as scientific interest in the challenges posed by their synthesis, processing, and characterization. Application of basic scientific principles to the key technological issues involved has been difficult, however, and much more progress has been achieved in tailoring porous materials through manipulation of processing parameters than through understanding of the chemical and physical mechanisms that influence porosity. As a result, the tailoring of porous materials has proceeded largely in an empirical fashion rather than by design (Barton *et al.*, 1999).

The discovery of the first ordered (where the pores are ordered periodically), mesoporous molecular sieves has sparked interest throughout the scientific community. These materials, possessing pore sizes in the ~2-50 nm range, have a wide range of potential applications including shape-selective catalysis and sorption of large organic molecules, chromatographic separations, and uses as hosts to confine guest molecules and atomic arrays. Several reviews on the general classification, properties, synthesis, and potential applications of mesoporous materials have already been studied.

The rational design of structured, complex inorganic frameworks with pores large enough to be used in the various applications awaited a viable synthetic approach. Several years ago, such an approach was discovered, resulting in the synthesis of the first members of an extensive family of silicate/aluminosilicate mesoporous molecular sieves designated as M41S. An unusual mechanism for the formation of these materials, known as liquid crystal templating, in which supramolecular assemblies of cationic alkyhrimethylammonium surfactants serve as components of the template for the formation of these materials, was proposed to account for their formation (Zhao *et al*., 1996; Mercuri *et al*., 2006; Barton *et al*., 1999; Beck and Vartuli, 1996; Kruk *et al*., 1999).

The discovery of these new materials led to an extension of the structure directing or templating concepts. That is, traditional zeolite synthesis typically involves the crystallization of a silicate around a single molecule. These new materials extended this single molecule concept making it possible to use a group of molecules like micelles. In the formation of these mesoporous materials a highly unusual combination of supramolecular cationic surfactant aggregates and anionic silicate species make up the functional templating agents. The ability to tailor these surfactant assemblies so that they can be used to design novel molecular sieve materials with engineered structure, pore diameter, and composition has provided an excellent opportunity for further advances in this area (Zhao *et al.*, 1996; Beck and Vartuli, 1996; Barton *et al.*, 1999).

2.3.2.1 Formation Mechanism of Mesoporous Materials

A new class of mesoporous molecular sieves, M41S, has been discovered by extending the concept of zeolite templating with small organic molecules to longer chain surfactant molecules. Rather than individual molecular directing agents participating in the ordering of the reagents to form the porous material, assemblies of molecules, dictated by solution energetics, are responsible for the formation of these pore systems. This supramolecular directing concept is illustrated in Figure 2.7 has led to a family of materials whose structure, composition, and pore size can be tailored during synthesis by variation of the reactant stoichiometry, nature of the surfactant molecule, or by postsynthesis functionalization techniques (Zhao *et al*., 1996; Boger *et al*., 1997; Barton *et al*., 1999; Beck and Vartuli, 1996).

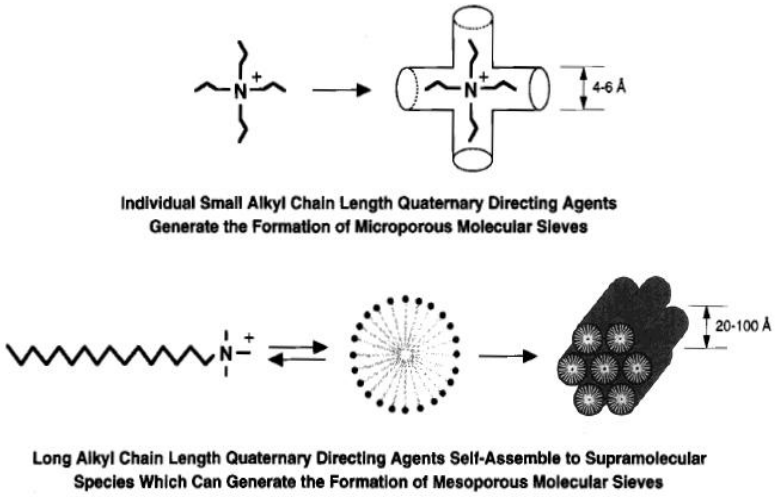

Figure 2.7: The formation of microporous molecular sieves using individual small alkyl chain length quaternary directing agents (top) and the formation of mesoporous molecular sieves using long alkyl chain length quaternary directing agents (bottom) (Barton *et al*., 1999).

The formation mechanism of this mesoporous family of molecular sieves is dictated by two features. The first is the dynamics of surfactant molecules to form molecular assemblies which lead to micelle and, ultimately, liquid crystal formation. The second is the ability of the inorganic oxide to undergo condensation reactions to form extended thermally stable structures. The initial discovery involved the formation of silicates using alkyltrimethylammonium cationic surfactants in a basic medium. Subsequent efforts have shown these structures can also be formed in acid media and by using neutral normal amines, nonionic surfactants, and dialkyldimethylammonium cationic surfactants. In addition, several mechanistic studies have expanded the initial pathway studies to a more generalized view of an organic/inorganic charge balance driving force for the formation of these structures (Zhao *et* al., 1996; Zhao *et* al., 2000; Barton *et al*., 1999).

Initial speculation on the mechanistic pathway shown in Figure 2.8, leading to the formation of these mesoporous materials considered two possibilities. The first was that the surfactant molecules organize independently of the inorganic silicate crystallization, and that the siliceous framework polymerizes around these preformed surfactant aggregates. The second was that silicate anions in solution, by virtue of their charge balance with the cationic surfactants, play an intimate role in directing the formation of the supramolecular surfactant arrays. In either ease a liquid crystal template is implicated.

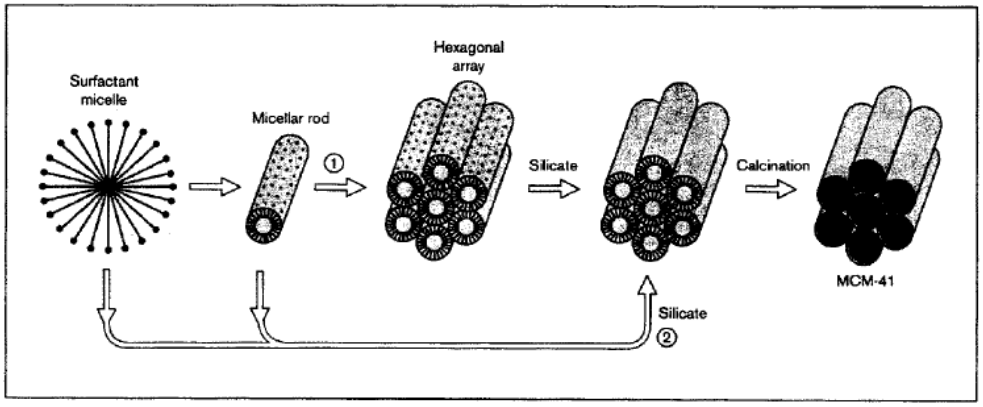

Figure 2.8: Possible mechanistic pathways for the formation of MCM-41: (1) liquid crystal initiated and (2) silicate anion initiated (Beck and Vartuli, 1996).

2.3.2.2 Types of Mesoporous Materials

The initial members of the M41S family consisted of MCM-41 (hexagonal phase), MCM-48 (cubic *Ia*3*d* phase), and MCM-50 (a stabilized lamellar phase). MCM-41 exhibits an X-ray diffraction pattern containing three or more low angle (below 10° 2θ) peaks that can be indexed to a hexagonal *hk*0 lattice. The structure is proposed to have an hexagonal stacking of uniform diameter porous tubes whose size can be varied from about 15 to more than 100 Å. An example of the characteristic X-ray diffraction pattern and proposed structure are shown in Figure 2.9.

MCM-48, the cubic material, exhibits an X-ray diffraction pattern, shown in Figure 2.9, consisting of several peaks that can be assigned to the *Ia*3*d* space group. The structure of MCM-48 has been proposed to be bicontinuous with a simplified representation of two infinite three-dimensional, mutually intertwined, unconnected network of rods. A more sophisticated and perhaps more realistic model would be based

on the concept of an infinite periodic minimal surface of the gyroid form, Q, proposed for water surfactant systems. A proposed structure is also shown in Figure 2.9.

MCM-50, the stabilized lamellar structure, exhibits an X-ray diffraction pattern consisting of several low angle peaks that can be indexed to *h*00 reflections. This material could be a pillared layered material with inorganic oxide pillars separating a two dimensional sheet similar to that of layered silicates such as magadiite or kenyaite as illustrated in Figure 2.9. Alternatively, the lamellar phase could be represented by a variation in the stacking of surfactant rods such that the pores of the inorganic oxide product would be arranged in a layered form (Zhao *et* al., 1996; Beck and Vartuli, 1996; Barton *et al*., 1999; Choma *et al.*, 2002; Zhao *et al*., 2000).

Other M41S type mesoporous materials are SBA-1 (cubic *Pm*3*n* phase) and SBA-2 (cubic *p*63/*mmc* phase). Further materials have been synthesized that are not as readily classified. These materials generally exhibit limited X-ray diffraction information (one peak) and may contain a random array of pores as shown in transmission electron micrographs of Figure 2.10. All of these mesoporous materials are characterized by having narrow pore size distributions comparable to microporous materials and extraordinary hydrocarbon sorption capacities which are up to or equal to their weight.

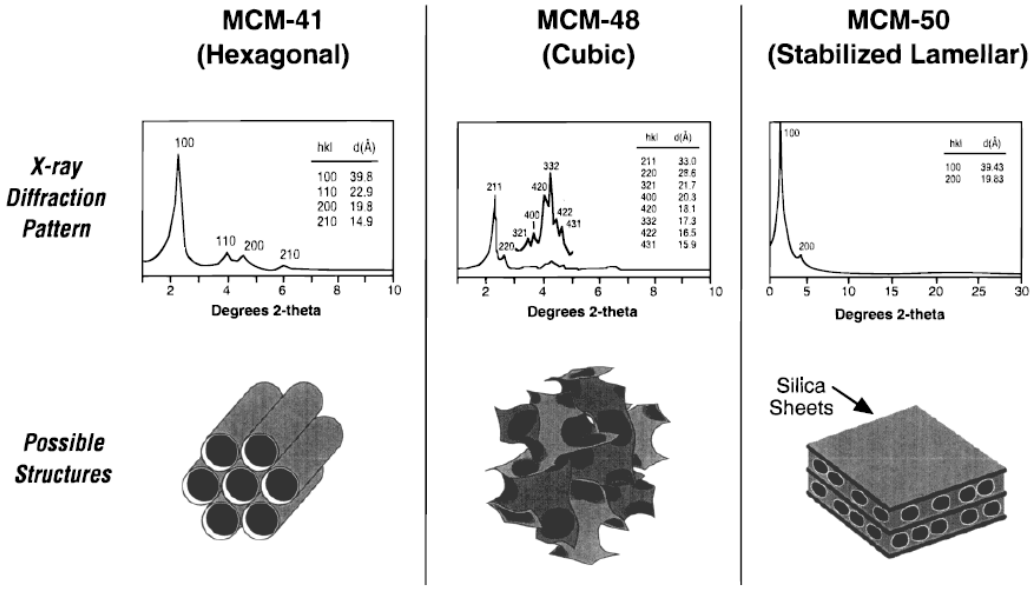

Figure 2.9: The X-ray diffraction patterns and proposed structures of MCM-41, MCM-48, and MCM-50 (Barton *et al.*, 1999).

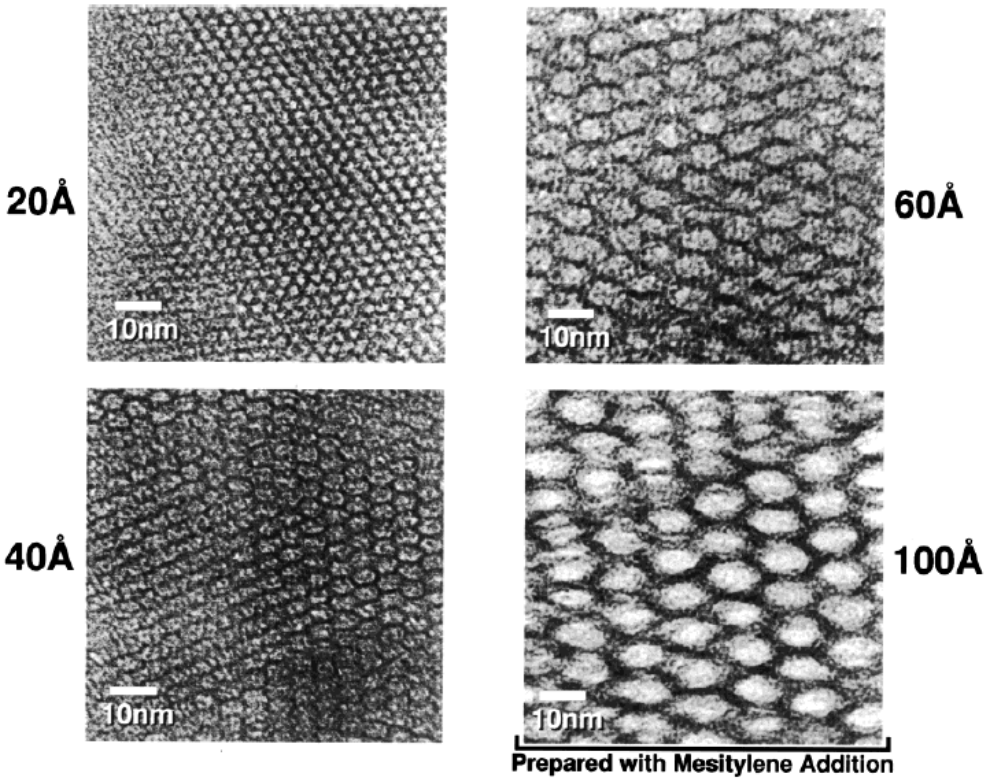

Figure 2.10: Transmission electron micrographs of MCM-41 materials with pore sizes of 20, 40, 60, and 100 Å (Barton *et al.*, 1999).

The initial forms of the M41S family were synthesized as silicates and aluminosilicates. Subsequent synthesis efforts have produced materials having heteroatom substitution as well as nonsiliceous products. The initial nonsiliceous materials included oxides of W, Fe, Pb, Mo and Sb. Many of these materials exhibited very poor thermal stability and upon the removal of the template, the structures collapsed. Mesoporous zirconia and titania materials have been prepared but only exhibit satisfactory thermal stability and thus are believed to be composed of extended and complete oxide nets of the elements (Zhao *et* al., 1996; Barton *et al*., 1999; Zhao *et al*., 2000).

2.3.2.3 Application of Mesoporous Materials

Potential applications of these mesoporous molecular sieves are as exciting as their discovery. In earlier years, mesoporous materials were examined for applications relating to their large pore volumes. Such applications including the use of mesoporous adsorbents for removal of volatile organic compound (VOC) in the industrial setting. In pursuit of such goals, the behavior of a variety of adsorbates has now been comprehensive. Almost all reported data agree that mesoporous materials have large accessible internal pore volumes which can be filled at pressures appropriate with the pore size (Zhao *et al*., 2001; Beck and Vartuli, 1996).

The sorptive properties of MCM-41, the hexagonal member of the M41S family of mesoporous silicates, have been extensively characterized using a variety of adsorbates. Some recent highlights include careful comparison of adsorption of a series of gases in a single sample of MCM-41. This work showed that the type of isotherm observed is highly dependent upon a number of factors including the material

composition, pore size, and nature of the adsorbent. Current study of adsorption isotherms on gases like argon, nitrogen and oxygen using well characterized MCM-41 sample confirm that MCM-41 has a narrow pore size distribution and exhibits extraordinary pore volume compared to classical microporous materials (Zhao *et* al., 1996; Dabrowski, 2001; Barton *et al*., 1999; Beck and Vartuli, 1996).

Despite the impressive adsorption capacities of these materials, their type IV isotherm behavior requires the adsorbate, in the gas phase, to be at high partial pressure. However, by contrast in most industrial application, for example VOC uptake, where adsorption at low partial pressures (type I isotherms) is required and poses constraint to the mesoporous materials application. Industrial applications which utilize mesoporous materials are catalytic processes, mini-reactors for electron transfer reaction, as a host for quantum confinement, molecular wires and shape-selective polymerization (Beck and Vartuli, 1996).

2.3.3 Modification of Porous Materials

One of the unique features of the M41S family materials is the ability to tailor pore size. The pore size can be varied from about 15 Å to more than 100 Å by varying the length of the alkyl chain of the template molecule or by the use of supporting solubilized molecules. A series of transmission electron micrographs of MCM-41 materials having pore diameters from 20 to 100 Å is shown in Figure 2.8. The approach taken to varying mesopore size in a regular, systematic fashion shows the contrast to the inability to accomplish such goals for traditional microporous zeolitic materials (Zhao *et* al., 1996; Barton *et al*., 1999; Kumar *et al*., 2001; Zhao *et al*., 2001).

Mobil catalytic materials of number 41 or MCM-41 belongs to the family of mesoporous molecular sieves discovered in the 1990s. These highly ordered pore systems with tunable pore sizes, large specific surface areas and pore volumes, and high density of surface silanols provide excellent opportunities for inclusion chemistry. A large number of functionalizing entities including both organic and inorganic components have been introduced into the channels to generate catalysts, adsorbents, and to improve the hydrothermal and mechanical stabilities.

All these modifications/ functionalizations can be achieved either by post-modification or by in situ synthesis. By post-modification, it is possible to sophisticatedly design and synthesize custom-tailored materials. For example, post-silylation can drastically improve the hydrothermal stability and mechanical stability of MCM-41 materials due to enhanced surface hydrophobicity. Meanwhile, thiol-functionalized MCM-41 adsorbents show a high adsorption efficiency of heavy metal ions from water. Although the detailed chemical reaction mechanism of post-modification has not been fully understood, it is believed that surface silanols serve as reactive sites and can be replaced by other components which act as modifiers. In such a way, a monolayer of a given modifier is attached to the surfaces of MCM-41, resulting in the changes of not only structural properties such as pore size, pore volume, and surface area, but also surface properties such as hydrophobicity/ hydrophilicity, polarity, acidity, afinity, etc (Zhao *et* al., 1996; Zhao *et al*., 2000; Zhao *et* al., 2001; Barton *et al*., 1999; Beck and Vartuli, 1996; Choma *et al*., 2002).

Another method which is considered new but has become useful, versatile, simple and efficient method recently known as freeze drying method. This method has been used widely to obtain porous ceramic materials or granules. Through this method, it is possible to control the porosity by varying a number of parameters and to improve the sinterability of the materials, reducing the temperature of sintering and decreasing the shrinkage and defects. The freeze drying method consists of a rapid freezing in small

droplets of salt solution which contain the desired cation or cations, maintaining the chemical homogeneity. Subsequent sublimation of ice under vacuum conditions leads to porous spheres of the anhydrous salt with a high surface area, which consolidates during the calcination process needed to remove the anion and grow the oxide nanoparticles. Freeze drying method is preferred for this study as the amines used for modification have moderate boiling temperatures. This method also allows the synthesis of a variety of powders with accurate control of the composition while evidently maintain the structure of support materials (Tallon *et al*., 2006a; Tallon *et al*., 2006b; Lee *et al*., 2006).

2.4 Summary

Porous materials such as microporous and mesoporous materials have high potential in a wide range of application including catalytic, adsorption processes, encapsulation technology, gas storage, separation and nanoparticles technology. The unique properties of these materials such as highly ordered pore structure, high surface area, tunable pore size or the ability to tailor framework, high hydrothermal and mechanical stabilities, large pore volumes and high density of surface silanol have make these materials superior compare to other materials. All these advantages lead to research and development interest in improving these materials by modifying using various types of components organic and inorganic. The importances of amine modified supporting materials are outlined in the review as well as the modification method and applications. Attentions of the literature have been made for the separation of carbon dioxide from natural gas using solid adsorbent through adsorption process.

Through literature study, the removal of carbon dioxide from crude natural gas is accomplished by gas-liquid absorption processes using aqueous solutions of alkanolamines. However, this gas absorption process is highly energy intensive for regeneration of the solvents and is also plagued by corrosion problems. The development of regenerable solid sorbents with high selectivities for carbon dioxide and high adsorption capacities is a potential alternative for natural gas purification because such materials are more environmentally benign and easier to handle in solid form as well as able to regenerate under mild condition thus more energy efficient. Silica and ordered mesoporous silica are ideal solid supports for active functions because of their large surface area and well defined pore structures. More importantly, the hydroxyl groups on their surfaces are important for many surface phenomena, such as gas adsorption, surface modification and wetting. Because of the high concentrations of surface silanol groups (SiOH), silica and ordered mesoporous silicas such as MCM-41 and SBA-15 are widely used for surface modification for instance, grafting of functional groups like amines onto the pore walls of the silica via silylation reactions between the surface silanol groups and the grafting material.

CHAPTER 3

MATERIALS AND METHODS

3.1 Materials

3.1.1 Chemicals

The general chemicals needed for the synthesis of mesoporous adsorbents are shown in Table 3.1. All chemicals which required dilution and glassware required rinsing were from freshly deionised water from Purite Select AN HP40 (Purite Ltd, England) with resistivity ~15 – 16 MΩ cm. Amines used were monoethanolamine (Merck), diethanolamine (Merck), triethanolamine (BDH), methyl diethanolamine (Merck) and polyethylenimine (Fluka) for modification of support materials. High purity commercial chemical such as cetyltrimethylammonium bromide (BDH), tetraethyl orthosilicate (Merck), ammonium hydroxide (Merck), hydrochloric acid (Merck) and Pluronic P123 (BASF) were used to synthesis mesoporous supports.

Table 3.1: General chemicals for the synthesis of mesoporous adsorbents.

Chemicals	MCM-41	SBA-15
Surfactant	Cetyltrimethylammonium Bromide (CTAB)	Pluronic P123 ($PEO_{20}PPO_{70}PEO_{20}$)
Solvent	Deionised water	Deionised water
Silica precursor	Tetraethyl Orthosilicate (TEOS)	Tetraethyl Orthosilicate (TEOS)
Mineralizing agents	Ammonium Hydroxide (NH_4OH)	Hydrochloric Acid (HCl)

3.1.2 Zeolites

Commercial synthetic zeolite Na-Y and 13X were selected and used as support or parent material for the modification by amines. The products were purchased from Zeolyst International Corporation (CBV 100, Lot number 10003101171) and Aldrich respectively.

3.1.3 Metal nitrates

High purity commercial powder metal nitrates, $Co(NO_3)_2.6H_2O$ (>98%, Fluka), $Ni(NO_3)_2.6H_2O$ (99%, Acros Organics) and $Cu(NO_3)_2.3H_2O$ (>98%, Fluka) were employed as metal oxide precursors to modify MCM-41.

3.1.4 Gases

Linde Gas Singapore PTE LTD supplied all gases used in this study. The specifications of the gases are as follow: Carbon dioxide (high purity grade, 99.995%), nitrogen (high purity grade, 99.995%) and purified argon (high purity grade, 99.999%).

3.2 Experimental Procedures

3.2.1 Preparation of Adsorbents

Many preparation methods have been developed by researchers for the synthesis of MCM-41 and SBA-15 (Xu *et al*., 2003; Vartuli *et al*., 2001; Klimova *et al*., 2006; Fulvio *et al*., 2005). General flow sheet of the procedures adopted is shown in Figure 3.1.

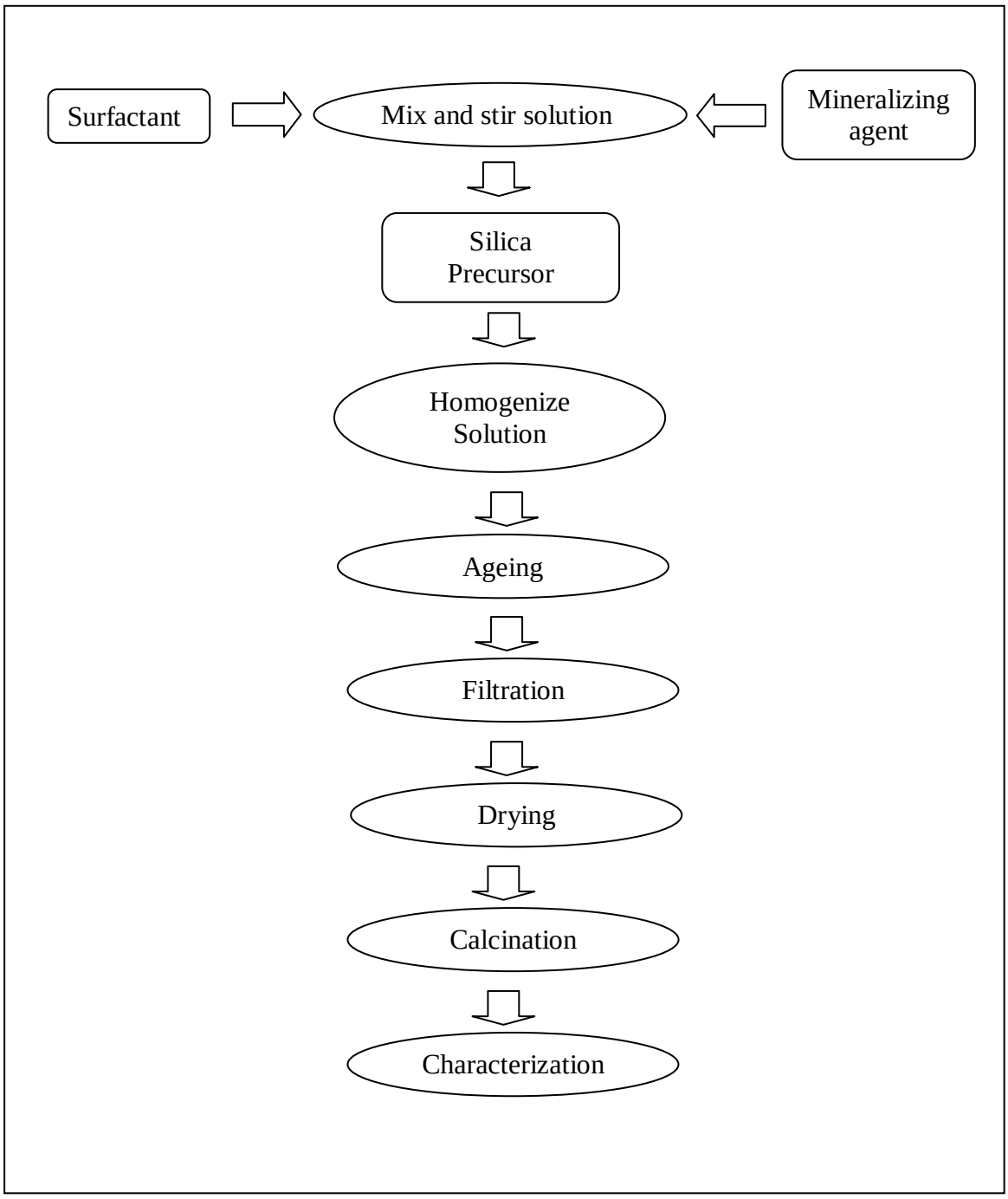

Figure 3.1: General experimental flow sheet.

3.2.1.1 MCM-41 Preparation

MCM-41 was synthesized according to standard methods in literatures (Kumar *et al*., 2001; Xu *et al*., 2003; Hadi Nur *et al*., 2004; Vartuli *et al*., 2001; Zhao *et al*., 1996). Synthesizing of MCM-41 began by dissolving 2.4g CTAB in 120g deionised water and the solution is stirred to form homogeneous and clear solution. Then, 8ml ammonium hydroxide was added into the solution and stirred for 5 min after which 10ml of TEOS was added into the solution. The solution was stirred overnight. Then, the solution was transfer into a container and put in oven at 100ºC for 2 days. After that, pH control was done at 10.2 each day until stable (2-3 days). The final product was filtered and washed with deionised water. Then, the sample was spread onto a plate and dried in oven at 100ºC for 24 hours. Calcination was performed at 550 ^{0}C for 5 hours

3.2.1.2 SBA-15 Preparation

Method for synthesizing of SBA-15 was in accordance to literatures reviewed (Klimova *et al*., 2006; Fulvio *et al*., 2005; Mirji *et al*., 2006; Luan *et al*., 2005; Srivastava *et al*., 2006; Andreza and Edesia, 2005). 4.0 g of Pluronic P123 was dissolved in 30ml of deionised water. Then, 120ml of 2.0 M HCl was added into the solution and stirred at room temperature for 2 hours. The resulting solution was then transferred into a container and stirred at 40ºC. After that, 8.5g of TEOS was added drop by drop into the solution while stirring for 30 minutes. Then, slowing down the stirring rate to around 120 rpm and stirred for another 20 hours at the same temperature. After that, ageing of the solution was done in an oven at 100ºC for 48 hours without stirring.

The final product was filtered, washed with deionised water and dried for 24 hours at 80ºC. Finally, the calcination was done at 550ºC for 5 hours under flowing air.

3.2.1.3 Metal modified MCM-41

Basically the preparation of metal modified MCM-41 is the same of preparing pure MCM-41. Initially 2.4 grams of CTAB was mixed with 120 grams of deionized water and the mixture was stirred until homogenous and clear solution was formed. After about 2 hours, 8 mL of ammonium hydroxide was added and the mixture was stirred for 5 minutes. Then 10 mL of TEOS and x grams (0.5 wt%) of respective metal source (Copper Nitrate, Cobalt Nitrate or Nickel Nitrate) were added and the mixture was stirred overnight. The mixture was then transferred into a teflon autoclave and aged at 100^0C for 2 to 3 days in the oven. pH control is done at 10.2 everyday by using acetic acid until no significant changes in the pH value. The final product was then filtered and washed thoroughly with deionised water. The filtered sample was transfered onto a plate and dried in oven at 100ºC for 24 hours. Finally, the sample was calcined at 550ºC at a rate of 1ºC /min for 5 hours.

3.2.2 Preparation of Modified Adsorbents

From previous study, modifying MCM-41 and SBA-15 using amines as functional groups utilize the same conventional method which is known as wet impregnation method (Xu *et al*., 2002; Xu *et al*., 2005). For MCM-41, methanol was used as solvent to allow amine solution dissolved in the mixture before adding to the calcined MCM-41. Then, the resultant slurry was stirred and dried at 70°C for 16 hours under 700 mmHg vacuum. The same method was applied for SBA-15 with the only different is that, the solvent used was toluene and the impregnated sample was heated at 150°C for 20 hours in a vacuum oven (Khatri *et al*., 2005; Gray *et al*., 2005). Meanwhile, amine modified zeolites were prepared by reaction of raw zeolite with amine at 200°C in an autoclave for 48 hours and some required calcination at high temperature of up to 500°C for 2 hours (Han *et al*., 2005; Guo *et al*., 2006).

Through literature study, it can be observed that by using wet impregnation and autoclave method, temperature of up to 200°C must be applied. This proves to be inappropriate since the boiling point of most amine solutions are in a range of moderate temperature. Therefore, this study attempts to introduce a new modification method which is freeze drying method. In a typical preparation, the desired amount of amine was mixed together with calculated amount of adsorbent and stirred for 2 hours. The mixture was then solidified in a freezer for 24 hours and the crystal ice mixture finally went through freeze drying process utilizing Freeze Dryer (Heto FD 4.0) to remove water and obtained powder form product.

3.2.3 Characterization

3.2.3.1 Structural Characterization

The structural properties of modified adsorbents were characterized by powder X-Ray Diffraction (XRD) using diffractometer (Bruker) with CuKα radiation at a wave length 1.5418 Å. XRD patterns were obtained with 40 kV and 40mA in the range of 2θ = 0.6° - 10° for SBA-15 and 2θ = 1.5° - 10° for MCM-41 with a scan speed of 0.02° per second. (Gaydhankar *et al*., 2005; Klimova *et al*., 2006). Other than X-Ray Diffractometer, Fourier Transform Infrared Spectrometer (FTIR) Perkin Elmer Model 2000 was used for identifying types of chemical bonds (functional groups) in the amine modified adsorbents samples.

3.2.3.2 Physical Properties Characterization

Nitrogen adsorption and desorption isotherms were measured at 77K using Quantachrome Autosorb to determine the physical properties such as pore diameter, pore volume and surface area. Specific surface areas were calculated by conventional Brunauer, Emmett, Teller (BET) method, pore volumes determined by nitrogen adsorption at a relative pressure of 0.98 and pore size distributions from the desorption isotherms by Barrett-Joyner-Halenda (BJH) method (Klimova *et al*., 2006; Kumar *et al*., 2001; Zhao *et al*., 2000; Thommes *et al*., 2002; Gaydhankar *et al*., 2005; Fajula *et al*., 2005).

3.2.4 Gas Adsorption Measurement

3.2.4.1 Thermal Gravimetric Analyzer (TGA)

The adsorption performance of the adsorbent was measured using thermal gravimetric analyzer, Perkin Elmer Pyris 1 TGA. This instrument was used to measure weight changes in sample as a function of either time or temperature. In a typical adsorption measurement process, about 20 mg of the sample was used. Initially, heat was supplied to the sample through furnace and the system was vacuum at the same time for 24 hours to remove unwanted impurities and water vapor. The temperatures used were varied from as low as 25˚C (without heating) up to 200˚C. Then, the temperature was lowered and at the same time the target gas (carbon dioxide) will be introduce for gas adsorption process. The temperature of adsorption process was set at 50˚C, however for further study the adsorption temperatures were differed from 25˚C (room temperature) to as high as 75˚C. The temperature was held isotherm for approximately 24 hours until equilibrium state was achieved. The carbon dioxide gas used was 99.995% high purity grade and flowing through silica gel to further remove moisture. The heating rate was set to 10˚C/min and cooling rate at 5˚C/min in order to allow considerable time of adsorption. The adsorption capacity was evaluated from weight changes of the samples in mg adsorbate/ g adsorbent. (Xu *et al*., 2003; Xu *et al*., 2002; Zheng *et al*., 2005; Zhao *et al*., 2001).

3.2.4.2 Fourier Transform Infrared Spectroscopy (FTIR)

Fourier Transform Infrared Spectroscopy (FTIR) was used to study the microscope behavior of molecules adsorbed on the adsorbents. Infrared studies had been successfully used in studying the configuration and orientation of physisorbed and chemisorbed species on an adsorbent surface (Rajesh *et al*., 2005; Zheng *et al*., 2005; Rege and Yang, 2001).

A laboratory-made FTIR cell unit used in this study is illustrated in Figure 3.2. The apparatus for FTIR measurement is made up of stainless steel equipped with a CaF_2 window 25 mm in diameter in order to be used at 423.15 K under the pressure up to 276 kPa. CaF_2 with 77, 000 – 900 cm^{-1} useful range has been chosen as window material due to the high resistance to most acids and bases; does not fog; insoluble in water and useful for high pressure work (Philippe *et al*., 2004a; Philippe *et al*., 2004b). The diameters of external and internal FTIR cell are 31 mm and 25 mm, respectively.

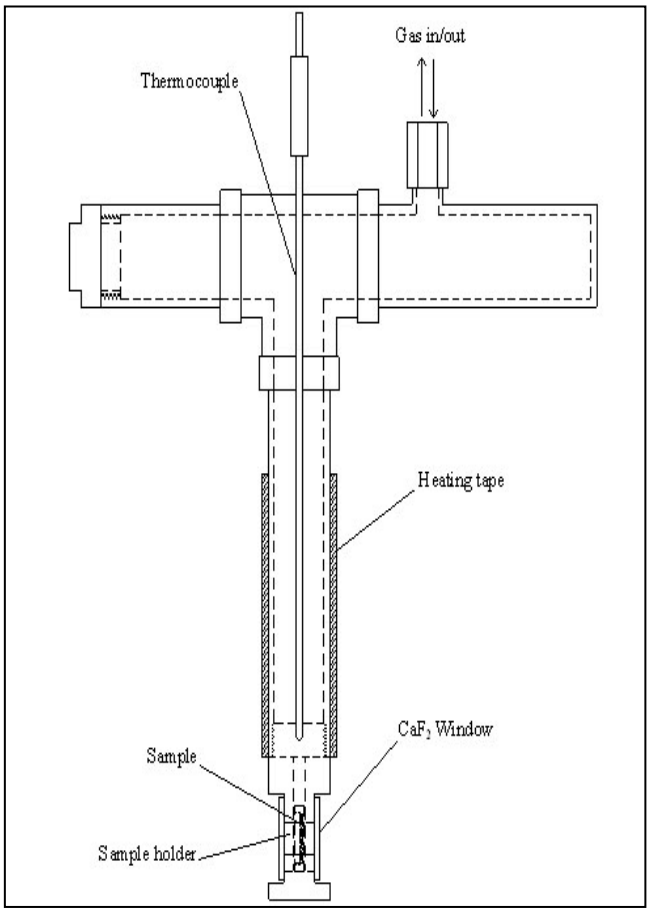

Figure 3.2: The schematic diagram of in situ FTIR cell.

For the purpose of studying gas adsorption on some adsorbents that had been selected after the analytical characterizations, the adsorbent powders were pressed into thin circular pellet using a hydraulic press (Carver Hydraulic Unit Model 3912) under a pressure of 5 metric tons. The pellet weighed about 20 mg with a diameter of 13 mm was carefully put into the O ring shape sample holder with a 10 mm hole diameter in the center and external diameter of 20 mm and 5 mm thick which was made up of brass.

Before activating the sample pellet, the whole system was vacuumed with a vacuum-adsorption apparatus at a pressure below 10^{-3} mbar for 1 hour. Then, the adsorbent pellet was activated by heating to 100˚C for 2 hours in situ, which was simultaneously vacuumed with vacuum pump under pressure below 10^{-3} mbar. The pellet was heated using a Cole-Parmer heating tapes (2 feet × ½ inches dimensions) connected to a Han Young DX 3 Temperature Controller Model TC 300P. The temperature of the FTIR cell was determined using an in situ thermocouple in contact with the wall of FTIR cell. After the heat treatment for removing impurities, the FTIR cell with sample pellet was further cooled down to room temperature for FTIR measurement.

All the spectrums were recorded on a FTIR, Perkin Elmer 2000 with a resolution of 4 cm^{-1}. Each sample will be scan for a total of 10 scans and using automatic smooth when necessary. The sample was vacuumed for 30 minutes, before introducing the target gas into the FTIR cell at room temperature (298 K) and at a variation of pressure. The FTIR cell was allowed to stay in equilibrium for 1 hour before scanning using FTIR, Perkin Elmer 2000. The areas under the peak corresponding to the physically adsorbed adsorbate species were then determined and correlated with the corresponding adsorbed amounts.

3.3 Summary

The materials chosen were of high purity and quality in conjunction with well designed methods using appropriate equipments in order to achieve the objectives and scopes underlined. Standard synthesis method for synthesizing MCM-41 and SBA-15 were used while freeze drying technique was employed to incorporate amine solution

into/onto silica support materials. All methods used were highly efficient procedures for amine modified adsorbents sample preparation. The selected analytical procedures utilizing effective instrumentations enable accurate characterization of modified adsorbents physicochemical properties and gases adsorptive characteristics being carried out and investigated.

CHAPTER 4

RESULTS AND DISCUSSIONS

4.1 Introduction

Adsorption is one of the promising methods that is applicable for separating CO_2 from gas mixtures, and numerous studies have been conducted on separation of CO_2 by adsorption using porous materials in the last two decades (Khatri *et al*., 2005; Xu *et* al., 2005). Various adsorbents consist of porous materials, such as MCM-41, activated carbons, zeolites, pillared clays and metal oxides have been investigated (Zheng *et al*., 2005). Amine functional groups are useful for CO_2 removal because of their ability to form ammonium carbamates and carbonates reversibly at moderate temperature (Desideri and Paolucci, 1999; Xu *et* al., 2005). The incorporation of organic amines into a porous support is another promising approach for CO_2 adsorption combining good capacity and selectivity at moderate temperature. Modifications of porous materials using amines will greatly influence the physicochemical properties of the porous materials and directly affects gases adsorption characteristics of the modified adsorbents (Zhao *et* al., 1996; Barton *et al*., 1999; Beck and Vartuli, 1996; Choma *et al*., 2002). The understanding of structural characteristics and properties before and after the

modification, as well as the function of various amines incorporated on the adsorbents play a vital part in CO_2 adsorption performance. In this regard, this chapter will discuss the characterization of amine modified adsorbents in conjunction to their CO_2 adsorption properties. In order to further understand the adsorbate-adsorbent interaction between CO_2 and modified adsorbents, gas-solid interaction using FTIR spectroscopy has also been included in the discussions.

4.2 Structural Characteristics and Properties

4.2.1 Effects of Various Amines

Powder X-Ray Diffraction has been used to characterize the structure of the materials used in this study. The X-Ray Diffraction (XRD) patterns of synthesized MCM-41 and amine modified MCM-41 are shown in Figures 4.1 and 4.2. As can be seen, XRD pattern exhibit one intense diffraction peak (100) at about 2˚ and three minor peaks indexed as 110, 200 and 210 in the region of 4˚ - 6˚, which are typical of MCM-41 mesoporous phase. From Figure 4.1, 4 peaks were observed, one main peak at 2θ= 2.176˚ corresponding to the 100 plane of MCM-41 which give a value of d_{100} of 4.05nm and 3 smaller peaks at 2θ= 3.747˚, 4.324˚ and 5.708˚ which correspond to the 110, 200 and 210 planes of MCM-41 respectively. The presence of these smaller peaks confirms that long range order was present in the samples (Xu *et al*., 2002; Zhao *et al.*, 2000; Xu *et al.*, 2003; Kumar *et al.*, 2001).

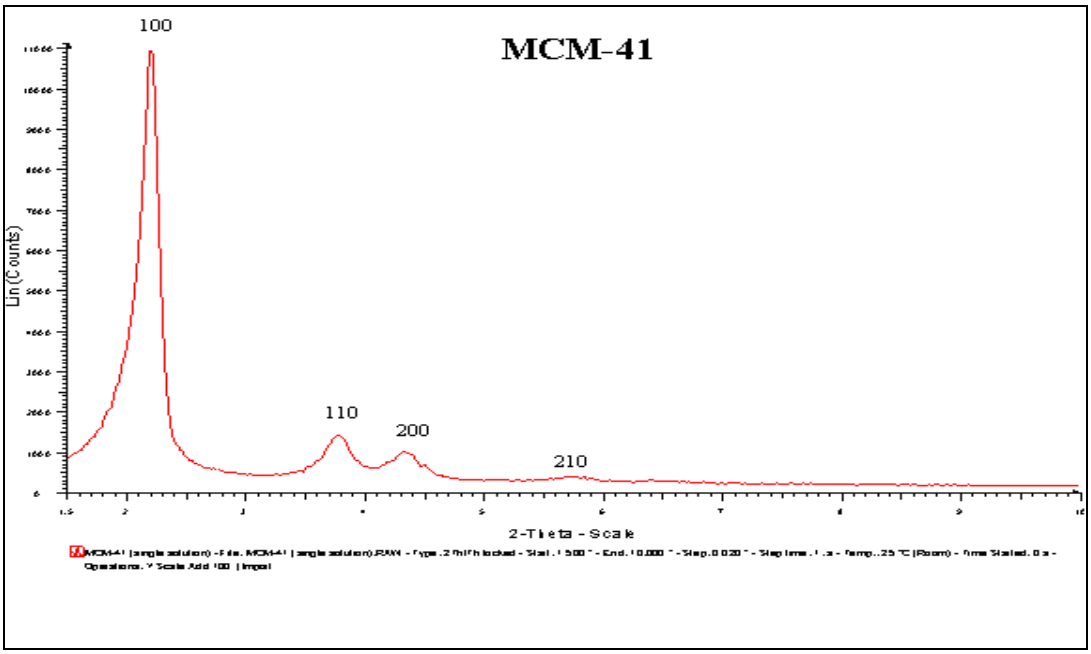

Figure 4.1: XRD pattern of as-synthesized MCM-41.

XRD patterns of MCM-41 before and after loading of various types of amines are compared in Figure 4.2. The diffraction patterns of MCM-41 did not change much after different amines were loaded. However, the intensity of the diffraction patterns of MCM-41 changed. Through this study, the diffraction intensity of MCM-41 decreased substantially after modification using different amines. The decreased intensity was caused by pore filling effect and indicated that amine was loaded into the pores of MCM-41.

Furthermore, the degrees of Bragg diffraction angles were nearly identical indicating that the structure of MCM-41 was preserved after loading of various amines. The degree of Bragg diffraction angle of the (100) plane slightly increased from 2.176˚ for MCM-41 to 2.185˚ - 2.212˚ for various amines modified MCM-41. These changes were caused by pore filling effect of MCM-41 channels and amines coating on the outer surface of MCM-41 crystals (Xu *et al.*, 2002; Zhao *et al.*, 2000; Xu *et al.*, 2005).

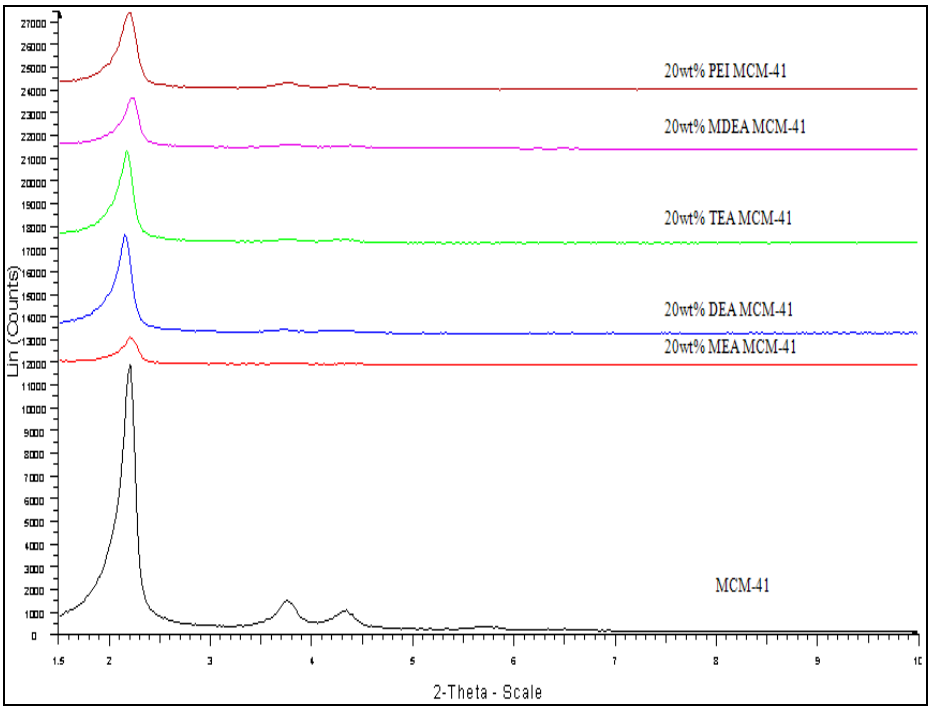

Figure 4.2: XRD patterns of different amines grafted on MCM-41. (PEI= polyethylenimine, MDEA= methyl diethanolamine, TEA= triethanolamine, DEA= diethanolamine, and MEA= monoethanolamine).

From Figure 4.2, the diffraction intensity of 20 wt% MEA/MCM-41 is especially low compare to others. There can be two possibilities that caused the lower intensity which are the effect of pore filling and the coating of outer surface of MCM-41 crystals. Xu et al. (2002) reported that amine coated on the outer surface of MCM-41 crystals hardly influenced the diffraction intensity of MCM-41 support. Therefore, the low diffraction intensity of 20 wt% MEA/MCM-41 is mainly caused by pore filling effect. Moreover, the size of MEA molecule is smaller than other amines molecule which further verifies that it is easier for MEA molecules to fill the pores of MCM-41 compare to other amines and resulted in lower diffraction intensity.

The nitrogen adsorption isotherms of MCM-41 and 20 wt% MEA/MCM-41 are shown in Figure 4.3, which further confirm the MEA was loaded into the pore channels

of the MCM-41 support. Completely degassed MCM-41 shows type IV isotherm (Figure 4.3). The surface area, pore volume and average pore diameter were 1035 m^2/g, 0.93 cm^3/g and 2.73 nm respectively. After loading of 20 wt% MEA, the mesoporous pores were partially filled with MEA, resulting in a type II isotherm (Figure 4.3), further restricting the access of nitrogen into the pores at liquid nitrogen temperature. The residual pore volume of 20 wt% MEA/MCM-41 is only 0.21 cm^3/g, the surface area is estimated to be 49.98 m^2/g and the average pore diameter was smaller than 1.69 nm. These results correlate with the pore filling effect of MEA as well as other amines which was also reflected by XRD characterization (Burleigh *et al.*, 2001; Murcia *et al.*, 2003; Xu *et al.*, 2002; Zhao *et al.*, 2000).

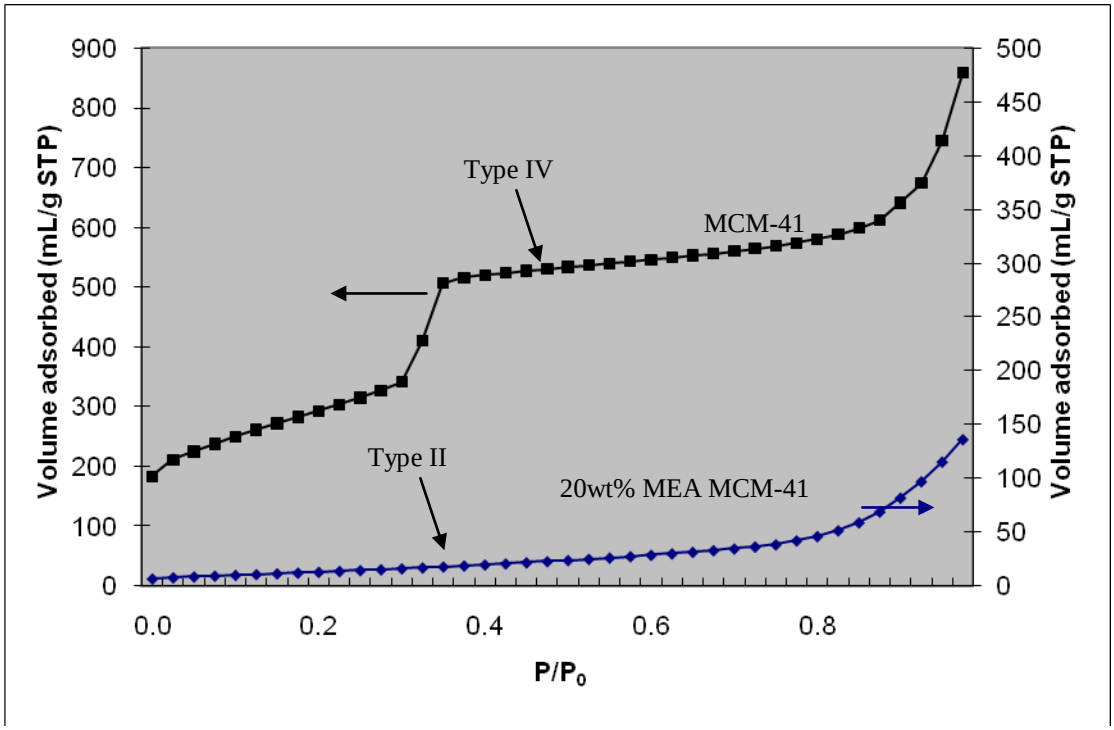

Figure 4.3: Nitrogen adsorption isotherm of MCM-41 and 20 wt% MEA/MCM-41.

In the physical properties characterization, the surface area and pore structure of MCM-41 before and after modification by amines were characterized using N_2 adsorption at 77 K. The nitrogen adsorption isotherms over the whole relative pressure

range for MCM-41 and 20 wt% MEA/MCM-41 are shown in Figure 4.3. Generally, the adsorption isotherm before amine modification are of type IV in the Brunauer, Deming, Deming and Teller (BDDT) classification indicating that they are mesoporous solids. The abrupt increase of N_2 adsorption at relative pressure ($P/P_0 \sim 0.3$) occurs because N_2 molecules are able to penetrate freely into the pores of MCM-41 without steric factor which capillary condensation and multilayer adsorption starting to occurs. As for 20 wt% MEA/MCM-41, the low adsorption was due to primary micropore filling effect since the amine modified MCM-41 had reduced pore diameter (1.69 nm) which fall into the region of micropore (< 2 nm). However, since the fluid-solid interaction of nitrogen and 20 wt% MEA MCM-41 is strong, the adsorption isotherm tends to be type II rather than type I of microporous (Xu *et al.,* 2002; Xu *et al.*, 2003). Table 4.1 lists complete physical properties for the rest of modified MCM-41 including pore volume and pore diameter.

Table 4.1: Summary of N_2 adsorption properties for MCM-41 and amine modified MCM-41.

Samples	BET Surface Area (m^2/g)	Pore Volume (cm^3/g)	Pore Diameter (nm)
MCM-41	1035.00	0.93	2.73
20wt% PEI/MCM-41	992.30	0.96	3.88
20wt% MEA/MCM	49.98	0.21	1.69
20wt% DEA/MCM	535.70	0.52	3.92
20wt% TEA/MCM	834.50	0.63	3.02
20wt% MDEA/MCM	723.30	0.42	3.56

Figure 4.4 presents the FTIR spectra for the as-synthesized MCM-41. The pure silica shows bands at around 3400, 1640, 1100, 962, 800 and 464 cm^{-1} region. The peak at 3447 cm^{-1} represents stretching vibrations of adsorbed water or structural –OH groups. Another peak at 1637 cm^{-1} is assigned to OH bending vibrations of the adsorbed water molecules. Typical antisymmetric and symmetric Si-O-Si stretching vibrations are

centered at 1087 and 798 cm^{-1}, respectively. The band at 968 cm^{-1} corresponds to Si-OH vibrations of the surface silanols, which is the characteristics of mesoporous silica (Cheng *et al*., 2006a; Luan *et al*., 2005; Rege and Yang, 2001)

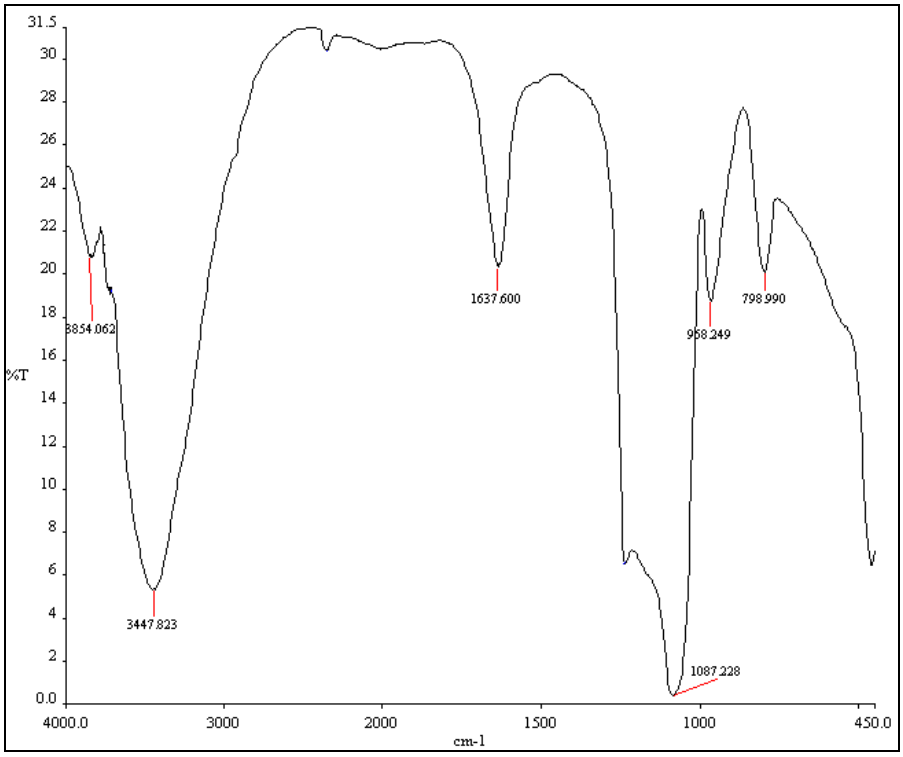

Figure 4.4: FTIR spectra of MCM-41.

The amine modified MCM-41 differs from the pure MCM-41 in several ways. Beside the peaks characteristic of MCM-41, amines molecules vibrations also reflect on the trace as shown in Figure 4.5. The intensity of the peak at 3440 cm^{-1} region is smaller than that of MCM-41 due to the formation of amine in the channels. The weak absorption band at 1550 cm^{-1} region is associated with C-C stretching vibrations, the peak at 1455 cm^{-1} region represents C-N stretching vibrations, while the absorption bands at 785 and 672 cm^{-1} correspond to C-H outerbending vibrations. All these adsorption bands are clearly visible as shown in Figure 4.5 with slightly shifted adsorption band for different type of amines. Absorption bands at 3430, 3280 and 1592

cm^{-1} region are assigned to asymmetric NH_2 stretch (ν_{as} NH_2), symmetric NH_2 stretch (ν_s NH_2) and NH_2 deformation (δNH_2) of hydrogen bonded amino group, respectively (Cheng *et al*., 2006a; Zhao *et al*., 1996; Wakabayashi *et al*., 1997; Hiyoshi *et al*., 2005). Besides these, absorption bands due to (Si-)OH stretch is visible at 3400 cm^{-1} region, overtone of Si-O-Si lattice weak vibration at 1980 and 1850 cm^{-1} region, CH_2 stretch at 2850 and 2930 cm^{-1} region and CH_2 deformation at 1460 cm^{-1} region were also observed in the spectrum which overlaps with C-N stretching vibrations. In addition, the peak at 1090 cm^{-1} region is assigned to the in-plane deformation vibrations of N^+H_2 formed on the amine chains by protonation, which is overlapped by the peak of the antisymmetric Si-O-Si stretching vibrations of MCM-41 (Zheng *et al.*, 2005; Cheng *et al.*, 2006a; Hiyoshi *et al.*, 2005). As for secondary amine (DEA), the absorption peak of NH stretch (ν NH) would overlap with symmetric NH_2 stretch (ν_s NH_2) at around 3300 cm^{-1}. Meanwhile, as for tertiary amine (TEA) the peak at 1456 cm^{-1} will be the dominant absorption band represents C-N stretching vibrations as can be seen in Figure 4.5 for the spectrum of 20 wt% TEA/MCM-41.

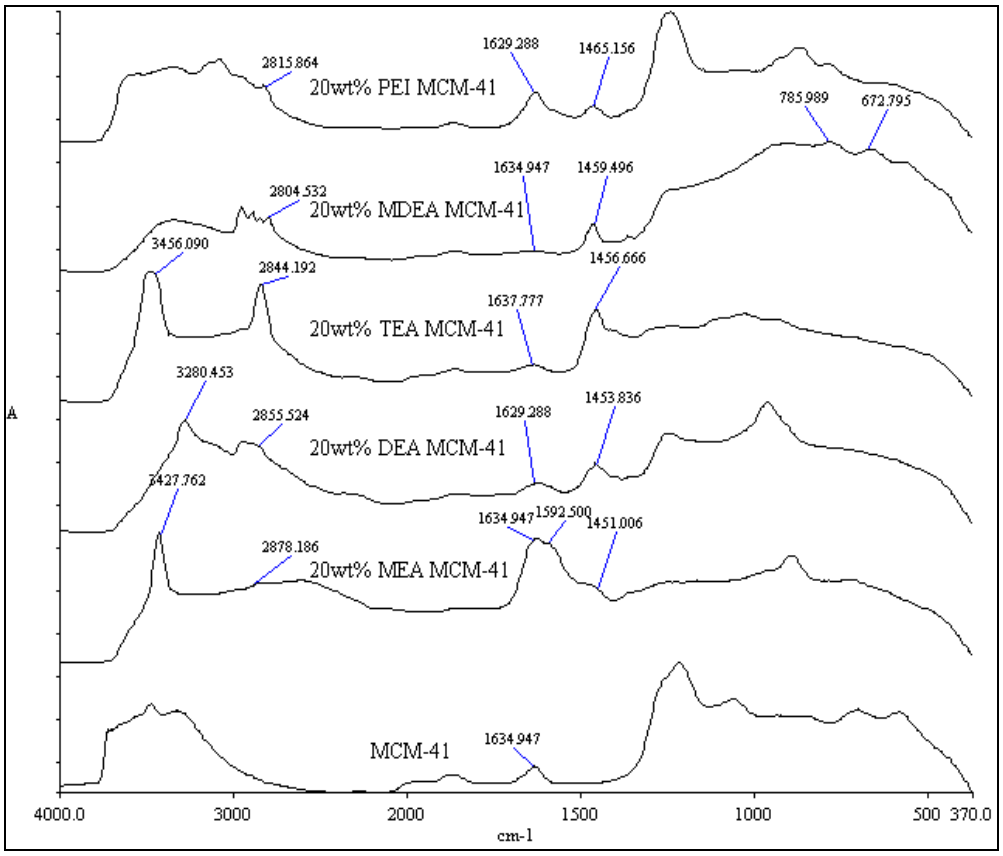

Figure 4.5: FTIR spectra of amines modified MCM-41.

Thus, the FTIR spectra of amine modified MCM-41 confirm the incorporation of amine inside the pore channels of MCM-41. Small shifts between the absorption peaks of amine molecules in the nanocomposite and bulk amine suggest that chain growth of amine in the mesopores is limited by diffusional restriction (Cheng *et al*., 2006a; Cheng *et al*., 2006b; Luan and Fournier, 2005).

4.2.2 Effects of Metals Loading

XRD patterns of different metals loading on MCM-41 are shown in Figure 4.6. There is no obvious decrease in peak intensity observed which indicates that ordered hexagonal mesoporous structure is well developed for each metal modified MCM-41. Furthermore, the presence of 3 smaller peaks (d_{110}, d_{200} and d_{210} peaks) confirms that long range order was present in the samples.

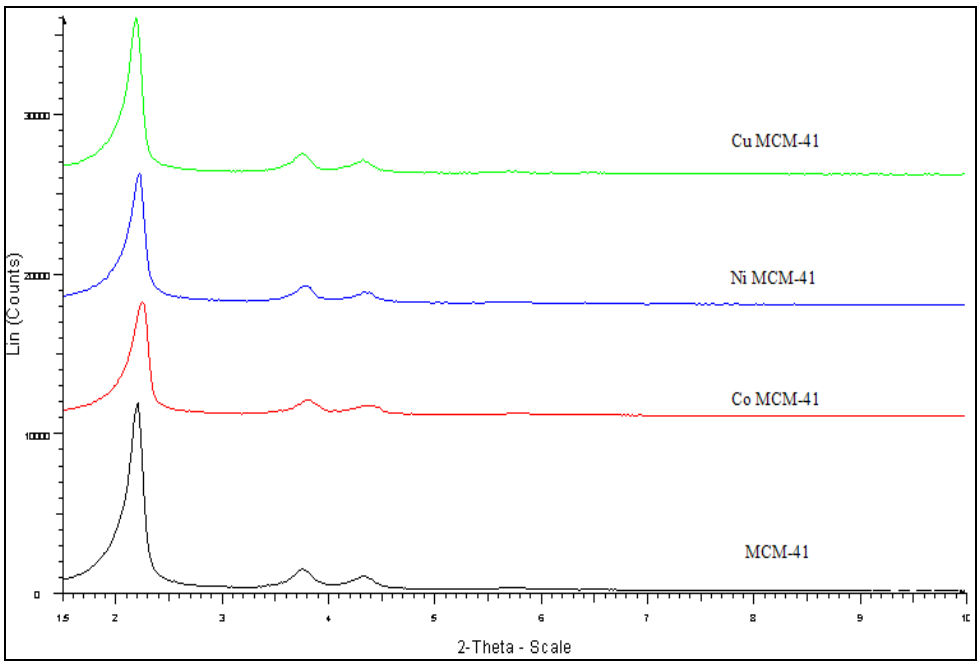

Figure 4.6: XRD patterns of MCM-41 and 0.5wt% 0f different metals loading on MCM-41. (Cu= copper, Ni= nickel, Co= cobalt).

The calcination process in the direct synthesis of metal modified MCM-41 method used high temperature at 550˚C. This may results in oxidation of metal nitrate which is used in the synthesis to form bulk metal oxide ($CuNO_3 \rightarrow CuO$, $NiNO_3 \rightarrow NiO$ and $CoNO_3 \rightarrow Co_3O_4$). Moreover, the high calcination temperature may also transport some of metal oxide species out of the pore system and remove some of their deposition

at the external surface of MCM-41, to form larger size crystallites. When all the useable vacant sites are occupied, a close-packed capping O^{2-} layer is formed and transformed them into the most stable form of oxide (Evans *et al.*, 2000; Parvulescu and Su, 2001; Xu *et al*., 2003).

The factors such as the pore size of MCM-41, the dynamic diameter of the metal oxides (particle size) and their physicochemical properties highly influence the incorporation of metal on MCM-41 either into the pore channel or onto the external surface of MCM-41. The particle size of metal oxides and their bond length between metal cation and oxygen molecule are listed in Table 4.2. It is reasonable that the incorporation of metal oxides into MCM-41 only occurs under the condition, when the dynamic diameter of metal oxides is smaller or similar to the pore size of MCM-41.

Table 4.2: Physical properties of metal oxides (Náray-Szabo, 1969).

Samples	Particle Size (nm)	Bond Length (Å)
CuO	25.51	1.84
Co_3O_4	99.13	2.10
NiO	69.91	2.03

Figure 4.7 shows the XRD patterns of MEA grafted on metals modified MCM-41. The decrease of the corresponding first peak (d_{100} peak) intensity (especially for MEA/CuMCM-41 and MEA/CoMCM-41) and the lack of the fourth peak (d_{210} peak) compared to parent MCM-41, reflects a less ordered hexagonal mesoporous structure for the amine grafted metal modified MCM-41. However, the metal modified MCM-41, after calcination, maintained its typical hexagonal structure, with no obvious decrease in peak intensity is observed as shown in Figure 4.6. This indicates that the decrease in the peak intensity is mainly related to the introduction of amine species instead of the thermal instability of the support (Xu *et al.*, 2002; Evans *et al.*, 2000; Xu *et al*., 2003).

Thus, it is confirm that the decreased intensity was caused by the amine coating on the outer surface of metal modified MCM-41 crystals as well as pore filling effect which further indicates that amine was loaded into the pores of modified MCM-41.

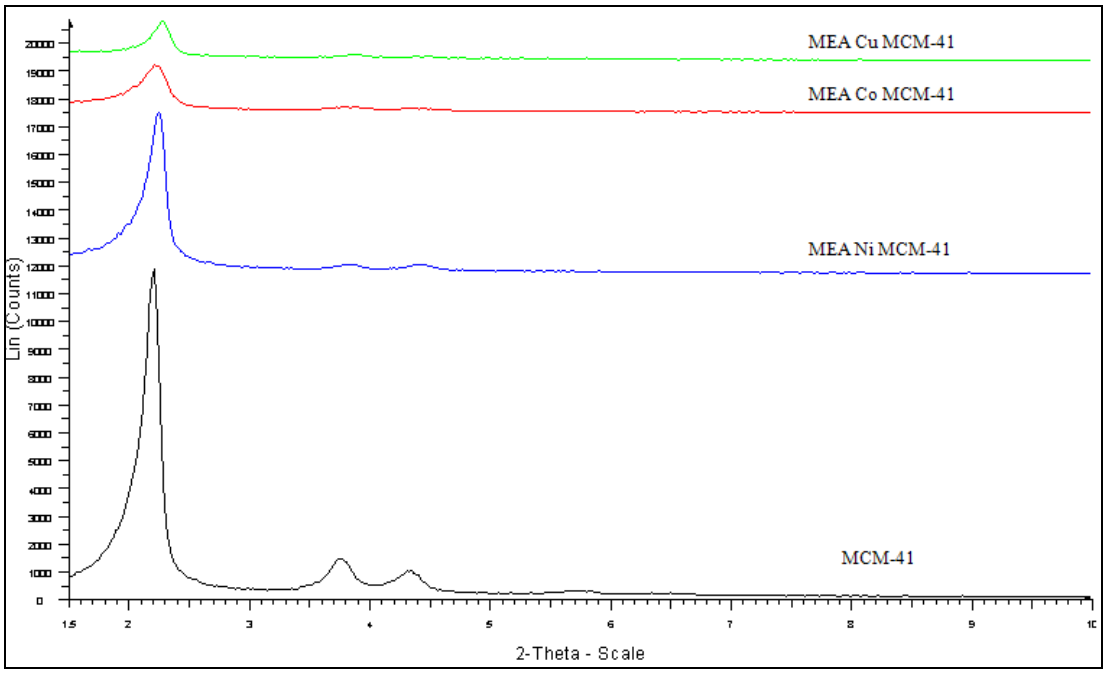

Figure 4.7: XRD patterns of 20wt% MEA grafted on different metals modified MCM-41.

4.2.3 Effects of Amine on Microporous Materials

Powder X-Ray Diffraction has also been used to characterize the crystallinity and structure of microporous materials used in this study which are NaY and 13X. The flat baselines of the X-ray diffraction pattern as shown in Figures 4.8 and 4.9 indicated a good crystallinity of all the samples. It was observed that the peak intensities of the XRD reflections for MEA modified NaY and 13X decreased as compared to unmodified commercial NaY and 13X. This is due to the presence of MEA particles within the

framework of the zeolite NaY and 13X. This result shows similarity as to MEA modified MCM-41. Therefore, regardless of the size of pores, the peak intensities of the XRD patterns decreased after incorporation of amines.

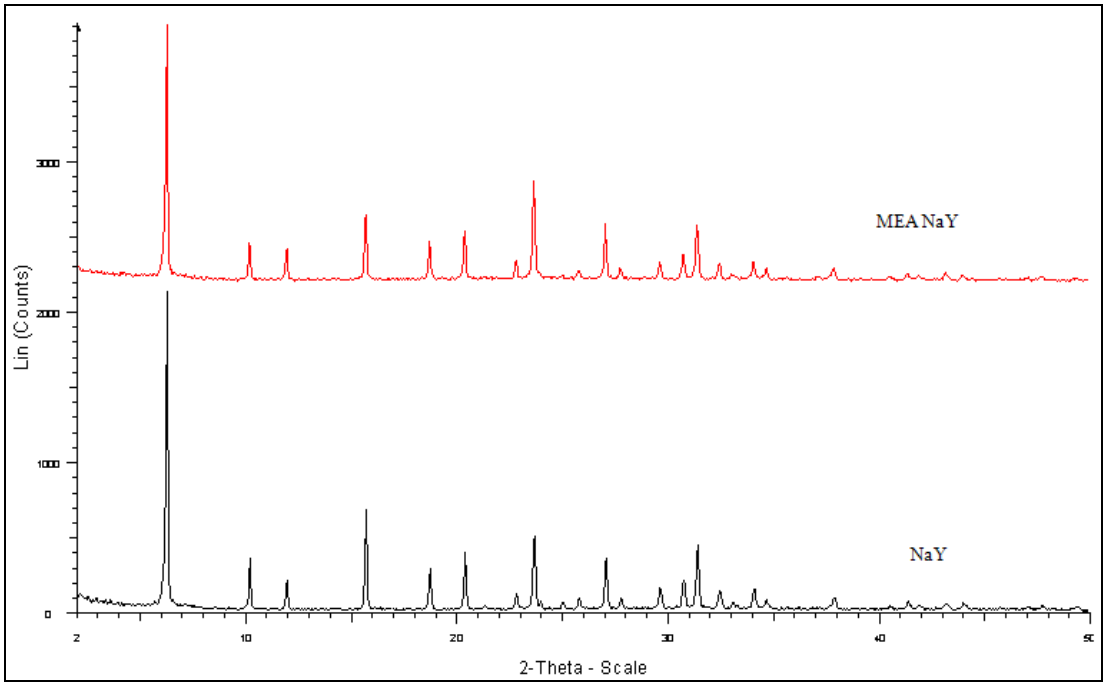

Figure 4.8: XRD patterns of zeolite NaY and MEA modified NaY.

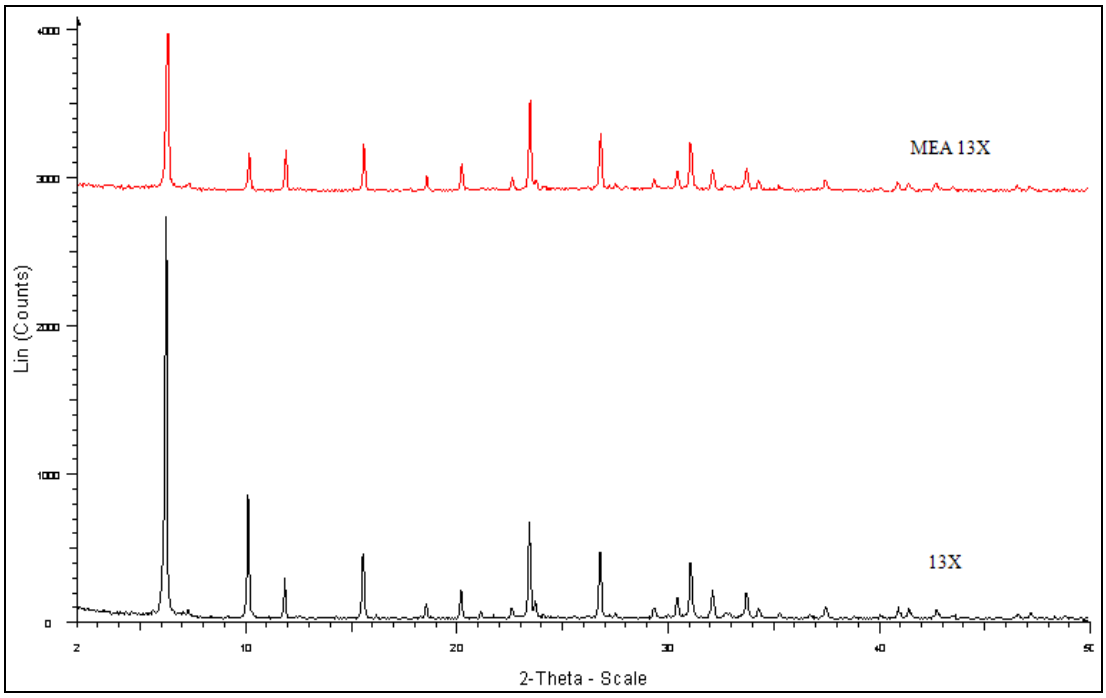

Figure 4.9: XRD patterns of zeolite 13X and MEA modified 13X.

The crystallinity of samples, which were denoted as relative intensity (I_{rel}) is determined by comparing the sum of the six reflection peaks (ASTM D3906) namely {331}, {511}, {440}, {533}, {642} and {555} of the modified samples with those of the NaY and 13X zeolite taken as reference (100% crystalline at ambient temperature) respectively. The relative crystallinity was calculated to determine the effects of MEA modification procedure employed on phase crystallinity of the parent zeolite. The crystalline phase of MEA modified samples decreased moderately for MEA/NaY sample while MEA/13X crystalline phase decrease further more as calculated in Table 4.3 but the support has remained unchanged. The relative intensity for MEA/NaY sample is 78.74 which is about 10% higher than MEA/13X sample at 68.93. The higher relative intensity for MEA/NaY indicated that the sample has better crystalline phase than MEA/13X. These results give further explanation for the introduction of MEA into zeolites framework and the phase crystallinity itself proves no significant alteration of the zeolites framework even after MEA modification procedure.

Table 4.3: Structural characterization of metal oxide modified Na-Y zeolites.

Samples	Relative Intensity (I_{rel})
NaY	100.00
MEA/NaY	78.74
13X	100.00
MEA/13X	68.93

4.2.4 Effects of Amine Concentrations

MEA MCM-41 samples with different MEA loadings were prepared and characterized by XRD and TGA. From XRD results, comparing the diffraction patterns of MCM-41 with those of MEA MCM-41 modified samples with different MEA loadings, shows that the degree of Bragg diffraction angles were nearly identical, indicating that the structure of MCM-41 was preserved after loading of MEA. However, the intensity of the diffraction patterns of MCM-41 decreased significantly after the MEA was loaded as shown in Figure 4.10.

By using MEA to modified the parent MCM-41, it is expected that the diffraction intensity of the (100) plane of MCM-41 will decreased because of pore filling effect since amine was loaded into the pores of MCM-41. However, when the concentration of MEA is increased it seems that the diffraction intensity of the (100) plane of MCM-41 is decreased as well until certain limit that further concentration increment would not affect the diffraction intensity anymore.

Figure 4.10 shows the diffraction intensity of (100) plane MEA/MCM-41 samples with different MEA loadings (0 wt%, 10 wt%, 20 wt%, 50 wt% and 75wt %). By increasing the MEA concentrations, the intensity of the diffraction peaks will decrease as well. The intensity of the diffraction peak of 50 wt% MEA/MCM-41 and 75 wt% MEA/MCM-41 was reduced to about 10.8% of the original intensity of MCM-41 support.

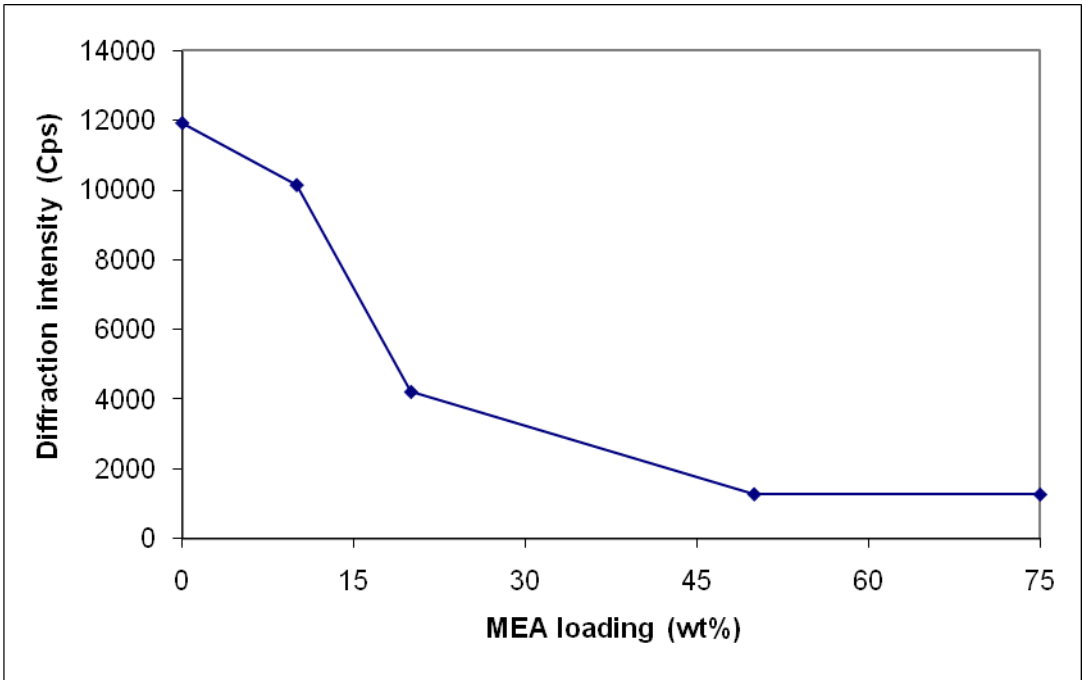

Figure 4.10: The effect of MEA loadings on the diffraction intensity of the (100) plane of MCM-41.

Since the pore volume of MCM-41 support is 0.93 cm^3/g and the density of MEA is about 1.0 g/cm^3, therefore the maximum MEA loading in the pores of MCM-41 is 48.2 wt%. The rest of the MEA should be coated on the outer surface of MCM-41 crystals. As for 75 wt% MEA/MCM-41, there should be more MEA coated on the outer surface of MCM-41 support compare to 50 wt% MEA/MCM-41 since the MEA concentration used is 50% more. However, the diffraction intensity of the (100) plane for 50 wt% MEA/MCM-41 and 75 wt% MEA/MCM-41 was nearly the same. The result indicated that the MEA coating on the outer surface of the crystals hardly influenced the

diffraction intensity of the MCM-41 support. Therefore, the decrease in the diffraction intensity of the (100) plane can be ascribed mainly to the loading of MEA into the MCM-41's pore channels (Xu *et al*., 2002; Xu *et al*., 2003).

4.3 Carbon Dioxide Adsorption Characteristics

Gas CO_2 adsorption capacity of amine modified mesoporous and microporous materials were studied and presented in the following section. Based upon the results obtained from the equilibrium adsorption capacity, the effects of amine modification on the CO_2 adsorption could be evaluated and characterized. The procedures for evaluation of gas CO_2 adsorption capacity by amine modified mesoporous and microporous materials were investigated in single adsorbate adsorption atmosphere at equilibrium pressure of 138 kPa and 50˚C as a standard operating temperature. All amines use for modification is standardized at 20 wt%. Adsorbate uptake capacity was measured until equilibrium reached.

4.3.1 Effects of Various Amines

Before amine was loaded, MCM-41 support alone shows CO_2 adsorption capacity of 18.58 mg/g sorbent. The low adsorption capacity was due to weak interaction between CO_2 and MCM-41 at relatively high temperature. In order to strengthen the interaction between CO_2 and MCM-41, different types of amines with numerous CO_2-capturing sites were incorporated into/onto MCM-41.

CO_2 adsorption capacity increased considerably after modification of MCM-41 using different types of alkanoamines. Delaney et al. (2002) reported that the ratio of CO_2 molecular per available N atom in the presence of hydroxyl group is approximately twice that without hydroxyl group. It is suggested that the CO_2 chemical adsorption mechanism of amine changed in the presence of hydroxyl group. Without the hydroxyl group, the formation of carbamate is favored in the manner of following Equation (4.1 - 4.4):

$$CO_2 + 2NH_3 \Leftrightarrow NH_4^+ + H_2NCOO^- \quad (4.1)$$

$$CO_2 + 2RNH_2 \Leftrightarrow NH_4^+ + R_2NCOO^- \quad (4.2)$$

$$CO_2 + 2R_2NH \Leftrightarrow R_2NH_2^+ + R_2NCOO^- \quad (4.3)$$

$$CO_2 + 2R_3N \Leftrightarrow R_4N^+ + R_2NCOO^- \quad (4.4)$$

With the absence of hydroxyl group, 2 moles of amine groups are required to react with 1 mole of CO_2 molecule. However, when hydroxyl groups are present, the reaction is two times as much leading to the formation of another type of carbamate. The formation of carbamate type zwitterions is stabilized in a manner depicted in Equation 4.5. In the presence of hydroxyl groups, 1 mole of amine groups reacts with 1 mole of CO_2 molecule. Therefore, the adsorption capacity of alkanoamine modified MCM-41 increased since the hydroxyl groups of the amines able to promote the formation of carbamate type zwitterions and more CO_2 molecules can be adsorbed (Xu *et al*., 2002; Zhang *et al.*, 2005; Xu *et al.*, 2003; Evans *et al.*, 2000).

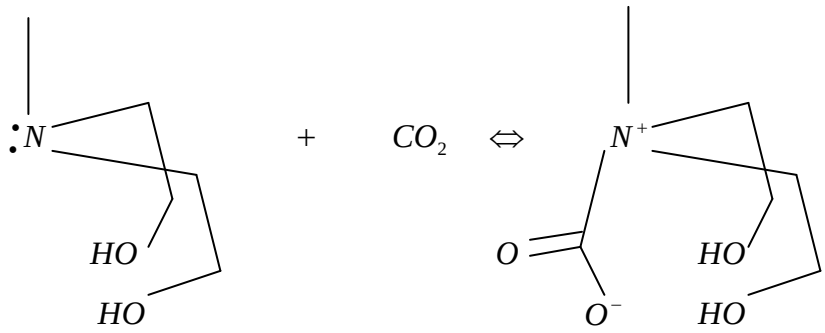

(4.5)

To further understand the reaction theory, let's discuss on the interaction between the basic surface of adsorbents and acidic CO_2 molecules. There are two conditions which affect the interaction between the amine modified silanol surface and CO_2 molecules. First, under anhydrous conditions, the reaction tends toward the formation of surface ammonium carbamates. Second, the reaction tends toward the formation of ammonium bicarbonate and carbonate species in the presence of water (Xiao *et al*., 2002; Knowles *et al*., 2005). Thus, in dry CO_2 which is in my case, adsorption capacities are limited to 1 mol of CO_2 for every 2 mol surface-bound amine groups. However, adsorption capacities may increase up to 2 mol of CO_2 with every 2 mol of surface-bound amine groups when water is presence. Therefore, it is desirable to develop adsorbents with the highest possible concentration of basic nitrogen groups accessible to CO_2 (Knowles *et al*., 2005; Xu *et al*., 2003; Guli *et al*., 2007). Figure 4.11 further demonstrate the reaction between amine groups on the silanol surface and CO_2.

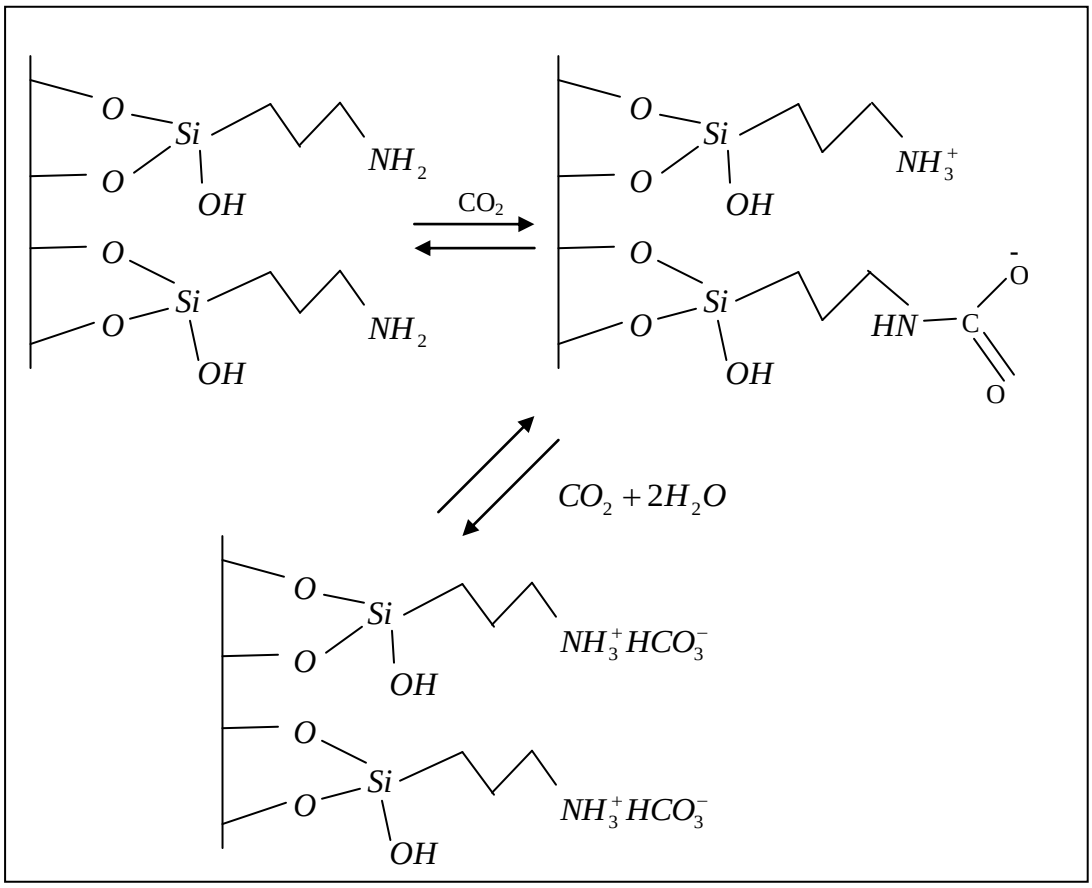

Figure 4.11: Surface reactions of amine groups with CO_2.

Figure 4.12 shows gas CO_2 adsorption capacity for MCM-41 support and amine modified MCM-41. MEA modified MCM-41 indicated the highest CO_2 adsorption capacity at 40.91 mg/g sorbent which is 2.2 times higher than MCM-41 support itself. As for tertiary amine modified MCM-41 such as TEA/MCM-41 and MDEA/MCM-41, the CO_2 adsorption capacity is rather low at 12.04 and 17.26 mg/g sorbent respectively which is lower than MCM-41 support. Meanwhile, DEA modified MCM-41 also shows high adsorption capacity at 38.18 mg/g sorbent. Although PEI is considered as a mixture of primary, secondary and tertiary amine, the adsorption capacity is quite high at 27.55 mg/g sorbent. This is due to the long chain of numerous alkyl chains within PEI structure (Xu *et al.*, 2002; Zhang *et al.*, 2005; Xu *et al.*, 2003).

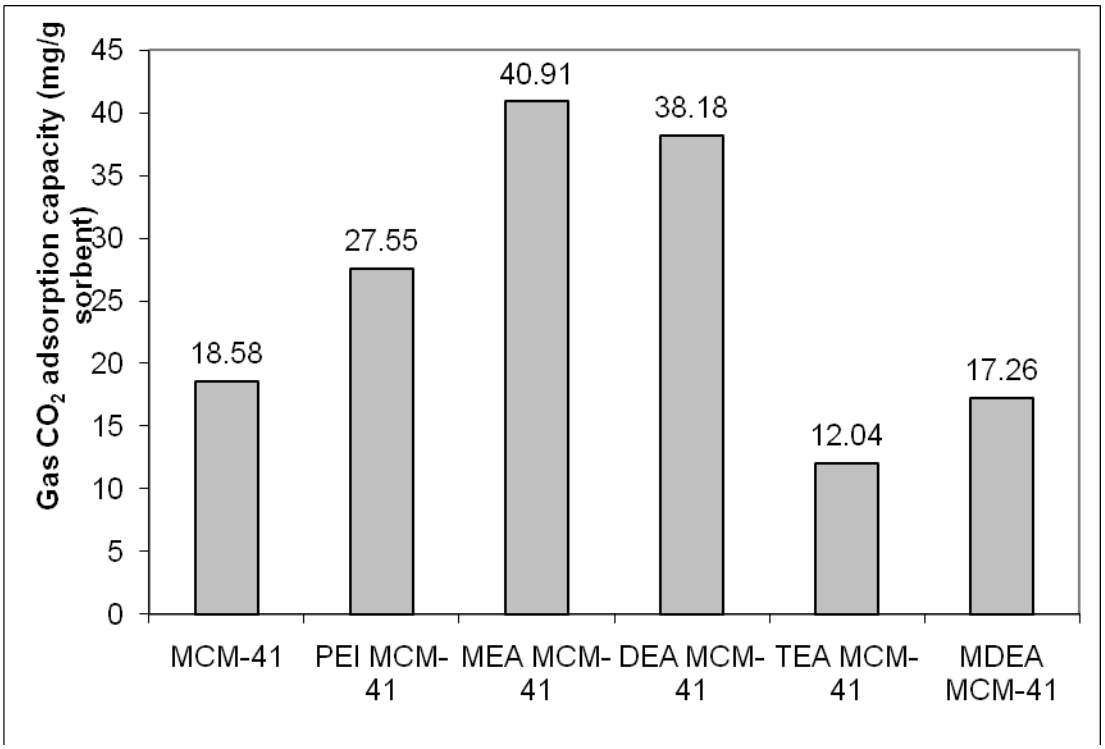

Figure 4.12: Gas CO_2 adsorption capacity for MCM-41 support and amines modified MCM-41.

There are two possible reasons for synergetic effect of MCM-41, one is the high surface area of MCM-41 and another is the uniform mesoporous channel of MCM-41. When amine was loaded onto the materials with high surface area, there will be more CO_2 affinity sites exposed to the adsorbate and thus increasing the adsorption capacity. When the channels of MCM-41 are filled by amine, the apparent pore size of the parent MCM-41 will be decreased as discussed. Hence, reducing the pore volume and decreasing the maximum CO_2 adsorption capacity. However, at the same time more CO_2 affinity sites are introduced into the pore channel of MCM-41. Both these contradicting effects occurred simultaneously and directly affected the adsorption capacity.

The amount of CO_2 adsorbed increases with increasing of the straight alkyl chain in the amines. PEI is one example of this case which consists of numerous long alkyl

chains which explain the higher CO_2 adsorption capacity compare to the parent MCM-41. However, amines with larger molecular size will results in lower adsorption due to steric hindrance which explain the low adsorption capacity of TEA/MCM-41 and MDEA/MCM-41 as both are tertiary amine with large molecular size. Furthermore, this also explains why the adsorption capacity of PEI/MCM-41 did not exceed the adsorption capacity of MEA/MCM-41 since PEI consists of longer alkyl chains but with larger molecular size.

In order to further study the characteristic of CO_2 adsorption by amine modified MCM-41, CO_2 adsorption capacity is related to BET surface area as shown in Figure 4.13. MCM-41 support gives the highest surface area at 1035 m^2/g. However, upon modified with amines, the surface area decrease substantially. MEA modified MCM-41 shows the most significant decrease of surface area which was reduced to 49.98 m^2/g. This is as expected since the molecular size of MEA is the smallest compare to other amine in this study. Hence, making the inclusion of amine molecules into the pore channel of MCM-41 easier. Nevertheless, even at low surface area, MEA MCM-41 gives the highest CO_2 adsorption capacity.

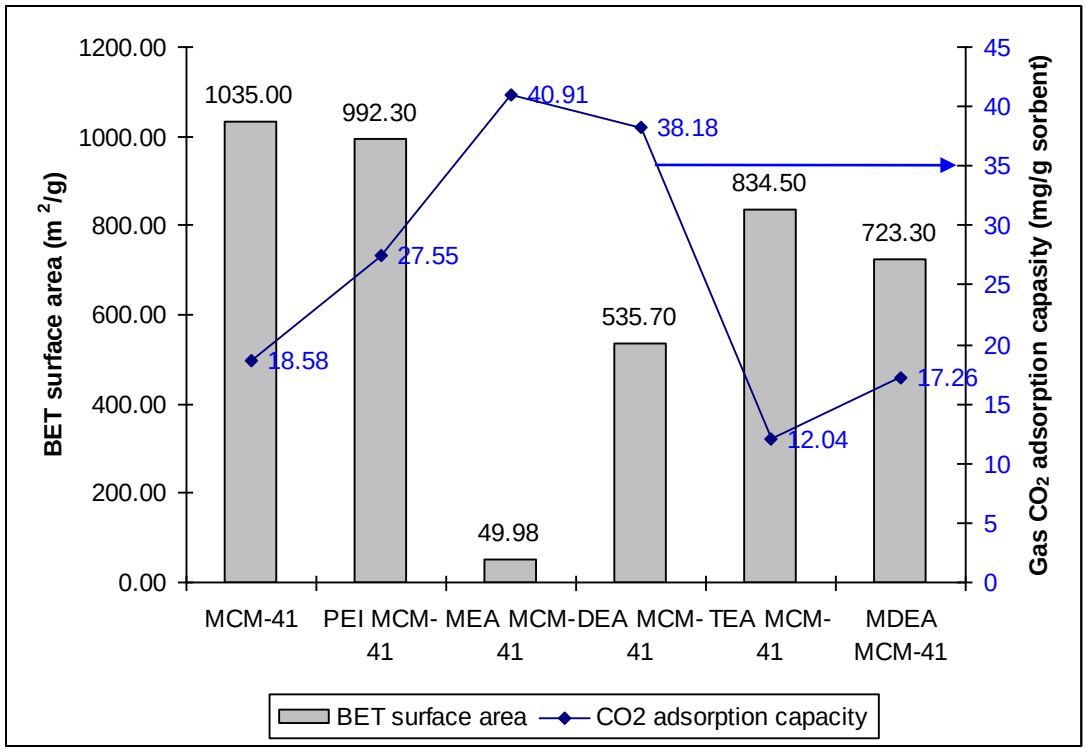

Figure 4.13: Comparison of BET surface area and gas CO_2 adsorption capacity for MCM-41 support and amines modified MCM-41.

The same phenomenon also reflect by other amines as in Figure 4.13 which confirm that higher surface area does not necessarily means higher adsorption capacity in this case. These results also further validate the theory of synergetic effect of MCM-41 (Zhang *et al.*, 2005; Xu *et al.*, 2003). As amine was loaded onto MCM-41, the pore channel of MCM-41 will be filled with amine hence increasing the steric hindrance for physisorption of CO_2 to occur. At the same time, more CO_2 affinity sites were exposed for chemisorption to take place. Therefore, it can be said that high adsorption capacity for amine modified MCM-41 is significantly due to chemisorption process.

TGA curves of initial CO_2 adsorption capacity along with slope of each graphs which represent the initial gas uptake rate for MCM-41 support and amine modified MCM-41 are presented in Figure 4.14. The adsorption of CO_2 gas by MCM-41 and

amine modified MCM-41 adsorbents have rapid uptake in the early period, but slows down at latter periods of the adsorption process. As illustrated in Figure 4.14, CO_2 gas adsorbed rapidly to around 70% - 85% of total CO_2 uptake in the first 50 minutes. This is true for MCM-41 support and all amine modified MCM-41 except for TEA/MCM-41 and MDEA/MCM-41. The larger molecular size of TEA and MDEA had resulted not only in lower adsorption capacity but also slower adsorption rate (0.129 mg/g sorbent/min and 0.248 mg/g sorbent/min respectively) due to steric hindrance. Meanwhile, DEA modified MCM-41 CO_2 gas uptake rate seem to be the next slowest. For the initial 50 minutes of adsorption, only 53% of total CO_2 uptake was obtained. The highest initial gas uptake rate is by PEI/MCM-41 with a rate of 0.662 mg/g sorbent/min followed by MEA/MCM-41 at 0.545 mg/g sorbent/min. These two adsorbents have the highest initial gas uptake rate because of numerous CO_2 active sites within the adsorbents especially for PEI modified MCM-41 which consists of longer alkyl chains. All CO_2 uptake rate for other amine modified MCM-41 are listed in Table 4.4.

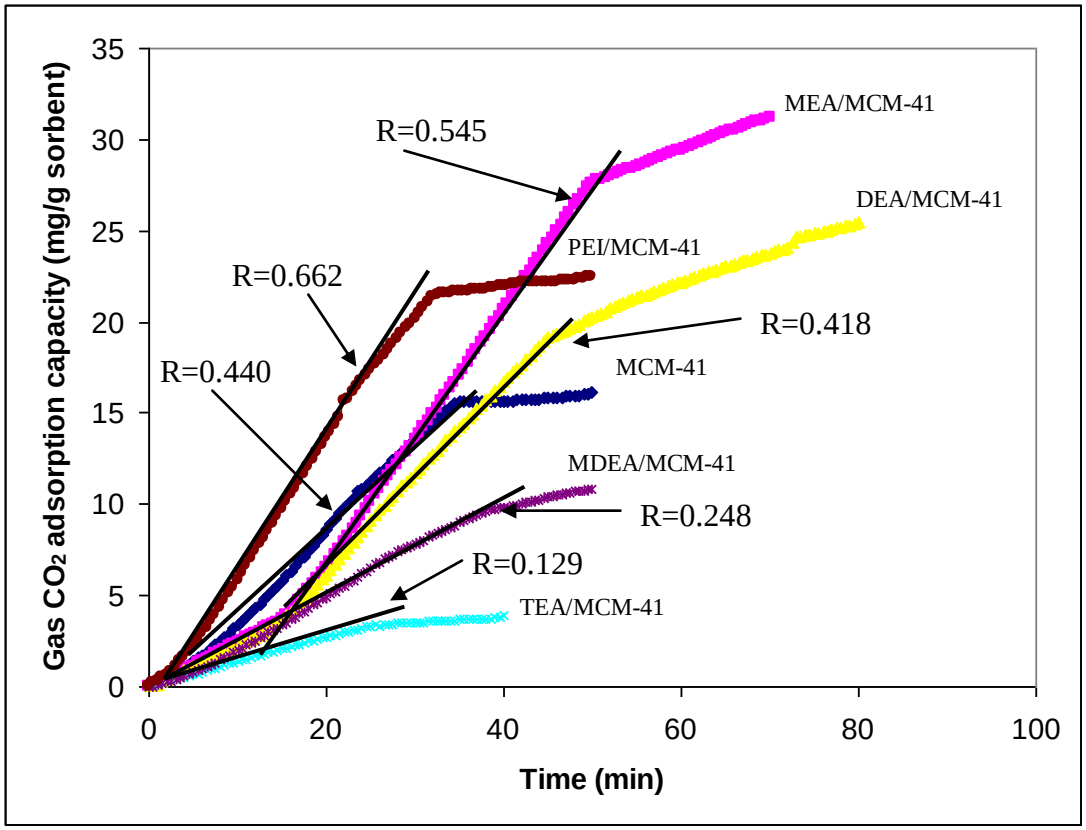

Figure 4.14: R represents the slope of CO_2 uptake for MCM-41 and amine modified MCM-41.

Different types of amine exhibited different equilibrium adsorption time requirement as well as adsorption capacity. The adsorption time that required for CO_2 adsorbate to reach equilibrium was shown in Figure 4.15 and listed in Table 4.4. Generally DEA/MCM-41 sample would take longer time to reach equilibrium compared to other samples. The fastest to reach equilibrium adsorption time would be the parent MCM-41 itself with just 250 minutes. However, the adsorption characteristic results shows that even though the CO_2 adsorption process for several types of samples studied reached the saturation condition faster than others, does not mean that the adsorption capacity is higher as well. Lets observed PEI/MCM-41 sample as an example. The equilibrium adsorption time requirement for PEI/MCM-41 is 485 minutes which is less than the equilibrium adsorption time requirement for DEA/MCM-41 (975 minutes). However, the adsorption capacity of PEI/MCM-41 is 27.55 mg/g sorbent which is lower

than that of DEA/MCM-41(38.18 mg/g sorbent). These results clearly proved that the adsorption processes that reach equilibrium state faster would not necessary result in higher adsorption capacities. It depends on the structure and physical properties of adsorbate and adsorbent as well as the extent of interaction of adsorbate with adsorbent surfaces.

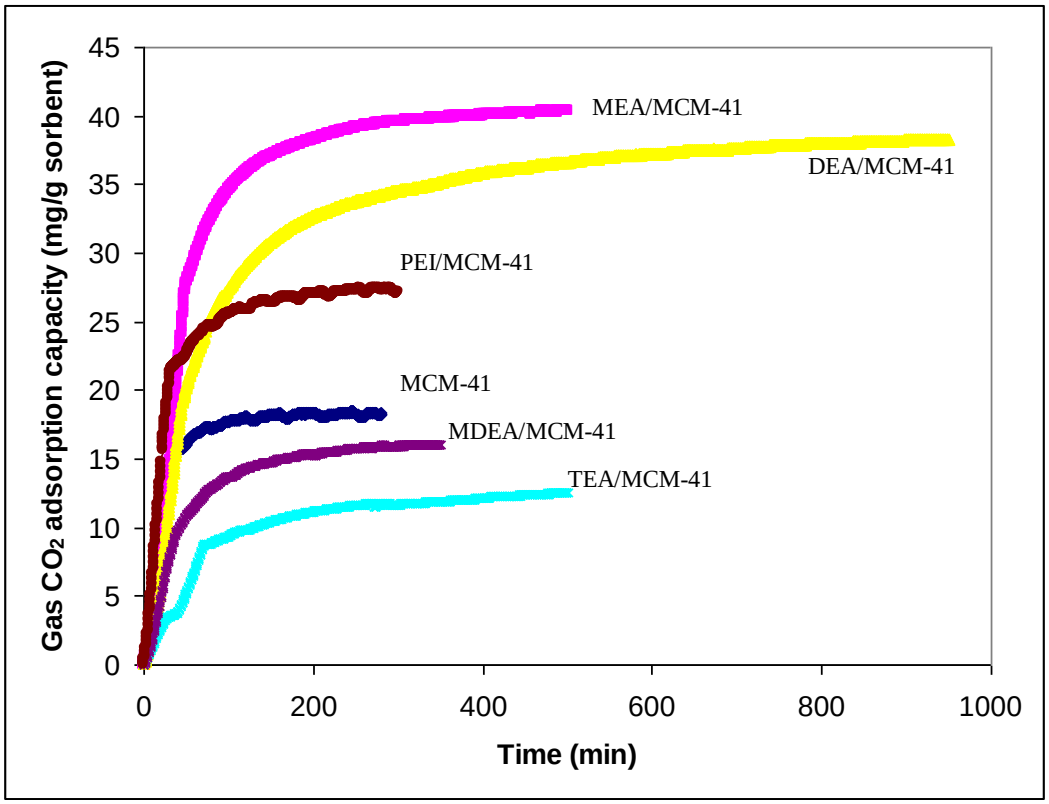

Figure 4.15: CO_2 adsorption capacity for MCM-41 and amine modified MCM-41.

Table 4.4: CO_2 uptake rate, R and equilibrium adsorption time requirement for different amines modified MCM-41.

Samples	Slope, R (mg/g sorbent/min)	CO_2 adsorption equilibrium time (min)
MCM-41	0.440	250
MEA MCM-41	0.545	500
DEA MCM-41	0.418	975
TEA MCM-41	0.662	505
MDEA MCM-41	0.248	585
PEI MCM-41	0.129	485

4.3.2 Effects of Amine Concentrations

To investigate the effects of amine concentration on the gas CO_2 adsorption capacity, MEA amine had been used to modified MCM-41 support at concentration of 10 wt%, 20 wt%, 50 wt% and 75 wt%. The results are shown in Figure 4.16. Generally, at low MEA loading, the MEA amine had little contribution on CO_2 adsorption capacity as can be observed in the case of 10 wt% MEA/MCM-41 sample. The adsorption capacity of 23.93 mg/g sorbent is only about 29% increase compare to the parent MCM-41 support. The highest adsorption capacity was reached at 20 wt% of MEA. The 20 wt% MEA/MCM-41 shows high adsorption capacity at 40.91 mg/g sobent which is 120% higher than the parent MCM-41 support.

The pore channels of MCM-41 play an important role on the increase of CO_2 adsorption capacity. When the channels of the MCM-41 are filled with MEA, the

apparent pore size of the MCM-41 will be decreased. At the same time, more CO_2 affinity sites are introduced into the channel. These two effects may combine together and result in further increment of the adsorption capacity. In the case of MEA modified MCM-41, physisorption and chemisorption take place at the same time. Physisorption on the MEA/MCM-41 sample occur mainly in the pore channels of MCM-41 support, while chemisorption involve the reaction of CO_2 and MEA in the channels of MCM-41 as well as on the external surface of MCM-41. When the channels of MCM-41 are fully filled with MEA, the highest adsorption capacity can be obtained. When MEA concentration was further increased and the MEA begin to coat on the external surface of MCM-41, the adsorption capacity starting to decrease (Xu *et al*., 2002; Xu *et al.*, 2003). Therefore, as can be observed from Figure 4.16, higher MEA concentration at 50 wt% and 75 wt% resulted in reduced adsorption capacity as more pore channel of MCM-41 being filled with MEA hence blocking the pore channels for physisorption to occur resulting in steric hindrance (McKittrick and Jones, 2003).

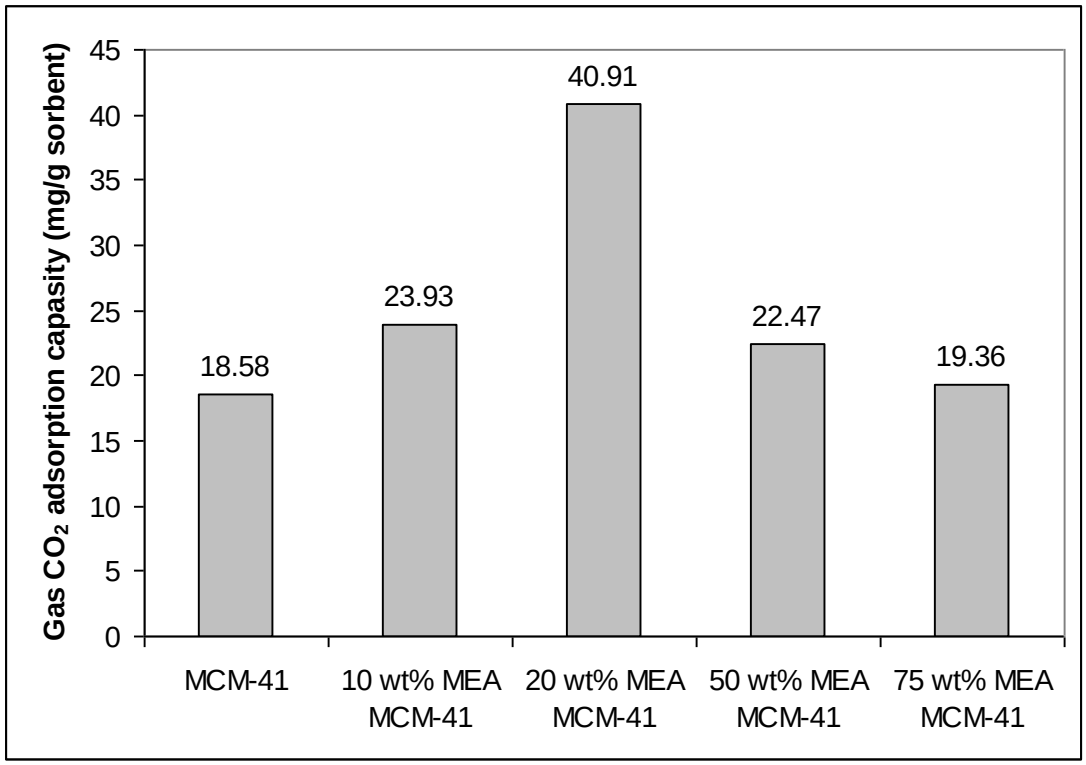

Figure 4.16: Gas CO_2 adsorption capacity for MEA modified MCM-41 at different concentrations.

Figure 4.17 presents the TGA curves of CO_2 adsorption capacity for MEA modified MCM-41 at MEA concentration of 10 wt%, 20 wt%, 50 wt% and 75 wt%. There is no specific trend in CO_2 equilibrium adsorption time requirement when increasing the MEA concentration. The fastest CO_2 equilibrium time reached is achieved by 50 wt% MEA/MCM-41 sample which took only 200 minutes to reach equilibrium. 50 wt% MEA/MCM-41 not only require less time to reach equilibrium but also has a high rate of CO_2 uptake which reached 90% of total CO_2 uptake in just 50 minutes at a rate of 0.535 mg/g sorbent/min. Sample 20 wt% MEA/MCM-41 still the slowest to reach equilibrium at 500 minutes but has the highest CO_2 uptake rate at 0.545 mg/g sorbent/min and was able to reach the highest adsorption capacity compare to other concentration. The results show that at 20 wt% of MEA concentration, physisorption and chemisorption were able to occur synergeticly. The MEA amine occupied the pore channels of MCM-41 but still leave some space adequate enough for CO_2 molecules to adsorb (physisorption) added by chemisorption on the external and internal surface of MCM-41 produced the highest adsorption capacity. The amine concentration higher than 50 wt% would cause blockage of the pore channels hence making the CO_2 penetration into the channels harder and consequently lower adsorption capacity. All CO_2 uptake rate and CO_2 adsorption equilibrium time for MEA modified MCM-41 at different concentrations are listed in Table 4.5.

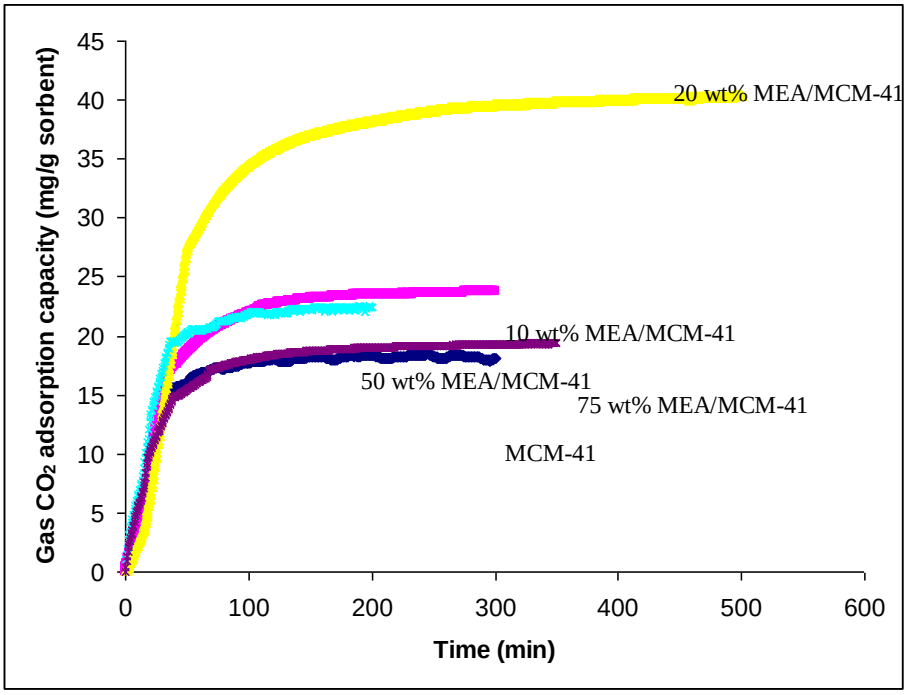

Figure 4.17: CO_2 adsorption capacity for MEA modified MCM-41 at different concentrations.

Table 4.5: CO_2 uptake rate and equilibrium adsorption time requirement for MEA modified MCM-41 at different concentrations.

Samples	CO_2 uptake rate (mg/g sorbent/min)	CO_2 adsorption equilibrium time (min)
MCM-41	0.440	250
10 wt% MEA/MCM-41	0.486	300
20 wt% MEA/MCM	0.545	500
50 wt% MEA/MCM	0.535	200
75 wt% MEA/MCM	0.384	350

4.3.3 Effects of Support Materials

In order to investigate the effects of different support materials on CO_2 adsorption characteristics, mesoporous and microporous supports were utilized in the study as well as amine and metal nitrates as the modify agents. Mesoporous supports synthesized in the study are MCM-41 and SBA-15, meanwhile microporous supports of NaY and 13X are obtained commercially. Three Metal nitrates was chosen namely copper nitrate, cobalt nitrate and nickel nitrate to incorporate into MCM-41 support during direct synthesis. Then, MEA was used as the standard modify agent for each of the supports. The CO_2 adsorption characterization of the adsorbents produced was done by thermal gravimetric analyzer at standard condition of 138 kPa CO_2 gas pressure and 50˚C of adsorption temperature.

At low loadings, materials with the strongest enthalpic interactions with sorbed molecules showed the highest level of adsorption. These tend to be materials with narrow pores, because small pores increase the interaction between gas and the framework. However, materials with narrow pores also have the highest framework densities and thus the lowest amount of free void space per gram of material. Therefore, at the highest pressure when the pores are nearly filled, the materials with the largest free volumes have more room for quest molecules and consequently show the highest uptake (Frost *et al*., 2006).

Three different adsorption regimes can be identified. At low pressure, the amount adsorbed correlates with the heat of adsorption. At intermediate pressure, the amount adsorbed correlates with the surface area. And at the highest pressure, the amount adsorbed correlates with the free volume. According to Frost et al., hydrogen molecules adsorbed less for zeolite Y than for zeolite X. As zeolite Y has fewer exchangeable cations (and consequently more void space) than zeolite X, these results

indicate that interaction of hydrogen molecules with exchangeable cations is important to adsorption process. For zeolite X and Y, hydrogen uptake relates closely to the BET surface area.

Figure 4.18 shows gas CO_2 adsorption capacity for various mesoporous and microporous supports as well as the 20 wt% MEA modified of each supports. From the figure, the adsorption capacity of microporous supports (NaY and 13X) shows significantly high level of CO_2 adsorption compare to mesoporous supports. The highest adsorption is achieved by NaY support at 183.57 mg/g sorbent which is about 9.9 times higher than MCM-41 support. This is due to the high level of interaction between CO_2 gas and the framework of NaY with such narrow pores at low pressure condition. This also applied to 13X support which shows slightly decreased adsorption capacity at 162.02 mg/g sorbent. However, after the modification using MEA was grafted onto these supports, the adsorption capacity significantly decreased by up to 60% of its original adsorption capacity. This phenomenon is due to pore blockage by the amine molecules since the pore size of microporous supports (cages ~ 0.74 nm, supercages ~ 1.3 nm) is smaller than the approximately larger radius of the amine (~1.4 nm) (Weitkamp, 2000; Inoue *et al*., 1991). When using MEA to modify microporous supports, the amine tends to disperse on the surface of the zeolite framework hence covering the pore of the support. Although MEA itself does provide additional CO_2 adsorption site, but adsorption in the pore of the zeolite framework seems to be the more significant role affecting the adsorption capacity. Furthermore, the crystalline phase of NaY and 13X decreased after modification by MEA as calculated in Table 4.3. The relative intensity for MEA/NaY sample is 78.74 which is higher than MEA/13X sample at 68.93. The higher relative intensity for MEA/NaY indicated that the sample has better crystalline phase than MEA/13X which explained the higher CO_2 adsorption capacity for MEA modified NaY. Besides, the decreased crystalline phase for both NaY and 13X after MEA modification clarify the decreased adsorption capacity of the MEA modified microporuos supports.

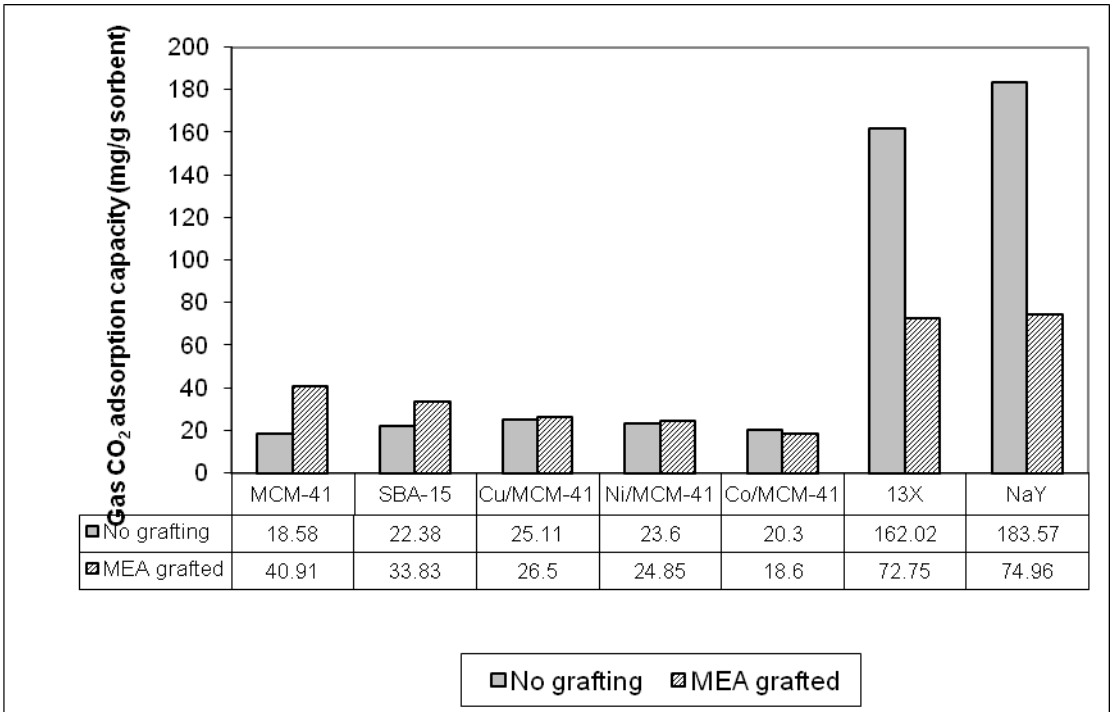

Figure 4.18: Gas CO_2 adsorption capacity for various mesoporous and microporous supports and MEA modified supports.

Meanwhile, as for mesoporous supports, all MEA grafted mesoporous supports show increment in CO_2 adsorption capacity except for MEA modified Co/MCM-41 sample. Based on Table 4.2, cobalt oxide has the largest particle size compare to the other two metal oxides. Co_3O_4 particle size is 1.4 times larger than NiO particle size and 3.9 times larger than CuO particle size. The large particle size of Co_3O_4 formed on the surface of the support after calcination proved to be the cause of low adsorption capacity by blocking the pores of the support. As for Cu/MCM-41 and Ni/MCM-41 supports, after grafting of MEA show only a small increase in adsorption capacity. The results show that MEA is not the appropriate modify agent to improve adsorption capacity for metal modified supports.

From Figure 4.18, the CO_2 adsorption capacity for SBA-15 is 1.2 times higher than MCM-41 support without MEA grafted. The slightly higher adsorption of SBA-15 is due to larger pore size poses by SBA-15 support. Besides, there were also micropores within the wall of SBA-15 structure contribute to the higher adsorption capacity. The existences of micropores in SBA-15 also provide higher total pore volume at 1.164 cm^3/g compare to 1.0 cm^3/g for MCM-41 (Klimova *et al*., 2006; Zhou *et al*., 2005; Fulvio *et al*., 2005). These interesting characteristics of SBA-15 proved to be advantageous towards increasing the adsorption capacity. However, after MEA had been grafted into both MCM-41 and SBA-15 supports, the MEA modified MCM-41 shows even higher adsorption capacity compares to MEA modified SBA-15. This is caused by the intrusion of MEA molecules into the pores of SBA-15 and blocked the micropores on the surface of the walls. The blocked micropores will result in reducing the total pore volume of SBA-15 support and apparently decreasing the adsorption capacity.

TGA curves of CO_2 adsorption capacity for MEA modified on different mesoporous and microporous supports are shown in Figure 4.19. Averagely, microporous supports show more rapid uptake in the early period compares to mesoporous supports. This is evidently shown in the Figure 4.18 especially for MEA grafted NaY and 13X which has the fastest CO_2 uptake rate at 1.398 mg/g sorbent/min and 1.280 mg/g sorbent/min respectively. MEA modified microporous supports do not only have the higher CO_2 uptake rate but also higher CO_2 adsorption capacity due to the high level of interaction between CO_2 gas and the framework of micropore supports as discussed previously.

The adsorption time required for CO_2 adsorbate to reach equilibrium and CO_2 uptake rate for MEA modified on different mesoporous and microporous supports is shown in Table 4.6. Generally, MEA/MCM-41 sample has the longest time to reach equilibrium compare to other samples. The fastest to reach equilibrium adsorption time would be MEA/13X in just 160 minutes at a rate of 1.280 mg/g sorbent/min. However,

the adsorption characteristic results show that even though the CO_2 adsorption process for several types of samples studied reached the saturation condition faster than others, does not necessarily mean higher adsorption capacity. This is evidently shown in Figure 4.18 as MEA/SBA-15 sample equilibrium adsorption time is about 180 minutes compare to 500 minutes for MEA/MCM-41 sample. However, the adsorption capacity of MEA/SBA-15 is 33.83 mg/g sorbent which is 17.3% less compare to adsorption capacity of MEA/MCM-41 at 40.91 mg/g sorbent.

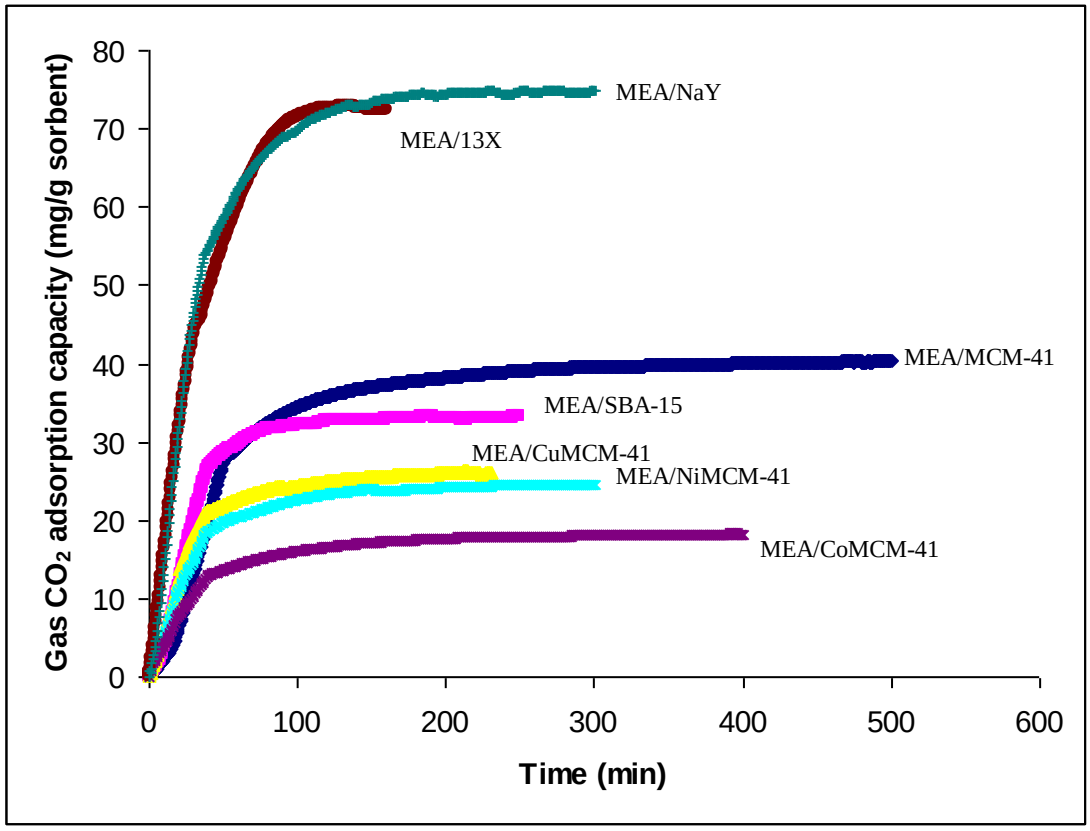

Figure 4.19: TGA curves of CO_2 adsorption capacity for MEA modified mesoporous and microporous supports.

Table 4.6: CO_2 uptake rate and equilibrium adsorption time requirement for MEA modified on different mesoporous and microporous supports.

Samples	CO_2 uptake rate (mg/g sorbent/min)	CO_2 adsorption equilibrium time (min)
MEA/MCM-41	0.545	500
MEA/SBA-15	0.640	180
MEA/CuMCM-41	0.535	230
MEA/NiMCM-41	0.465	305
MEA/CoMCM-41	0.296	400
MEA/13X	1.280	160
MEA/NaY	1.398	300

4.3.4 Influence of Operating Temperature

The procedure of operating the TGA equipment involved heating and cooling steps that may affects the CO_2 adsorption capacity results. Before CO_2 gas being introduce into the TGA for adsorption by the samples, heating step is required to remove water vapor and other impurities. By observing the results of adsorption capacity at a range of heating and adsorption temperatures, the influence of different operating temperatures of TGA on CO_2 adsorption capacity can be studied. The experiments run at standard 138 kPa of pure CO_2 pressure and temperatures ranges from as low as 25˚C up to 150˚C.

4.3.4.1 Influence of Adsorption Temperatures

The adsorption of CO_2 by porous materials or amines is an exothermic process. Accordingly, the adsorption capacity should decrease with the increase of temperature. However, study by Xu et al. (2002), shows otherwise that the CO_2 adsorption capacity increases with increasing temperature. In the end, it is stated that the adsorption capacity at low temperature will eventually be larger than at high temperature if the adsorption time is long enough to ensure that it reaches equilibrium state. As in this study, there is no such issue as contradicting the exothermic process theory as the adsorption time is long enough (24 hours) for the samples to reach equilibrium state with the CO_2 adsorbate. The results are evidently shown in Figure 4.20, as the adsorption capacity decreased when the temperature is increased.

The effects of different adsorption temperatures on CO_2 adsorption capacity for 20 wt% MEA modified MCM-41 are presented in Figure 4.20. As expected, the CO_2 adsorption capacity at adsorption temperature 25˚C (room temperature) shows the highest value at 82.30 mg/g sorbent. When the adsorption temperature increased to 50˚C, the adsorption capacity decreased to 40.91 mg/g sorbent which is 50.3% reduced in total amount CO_2 adsorbed. When the adsorption temperature is further increased to 75˚C, the adsorption capacity is the lowest at 17.00 mg/g sorbent which is about 58% decrease compare to amount adsorbed at 50˚C. These results indicated that for each 25˚C increment in adsorption temperature, about half of the adsorption capacity is reduced. At higher temperature the adsorbate CO_2 molecules tend to be in active energized form and are harder to adsorb compare to molecules at lower temperature which has lower activation energy to be adsorbed.

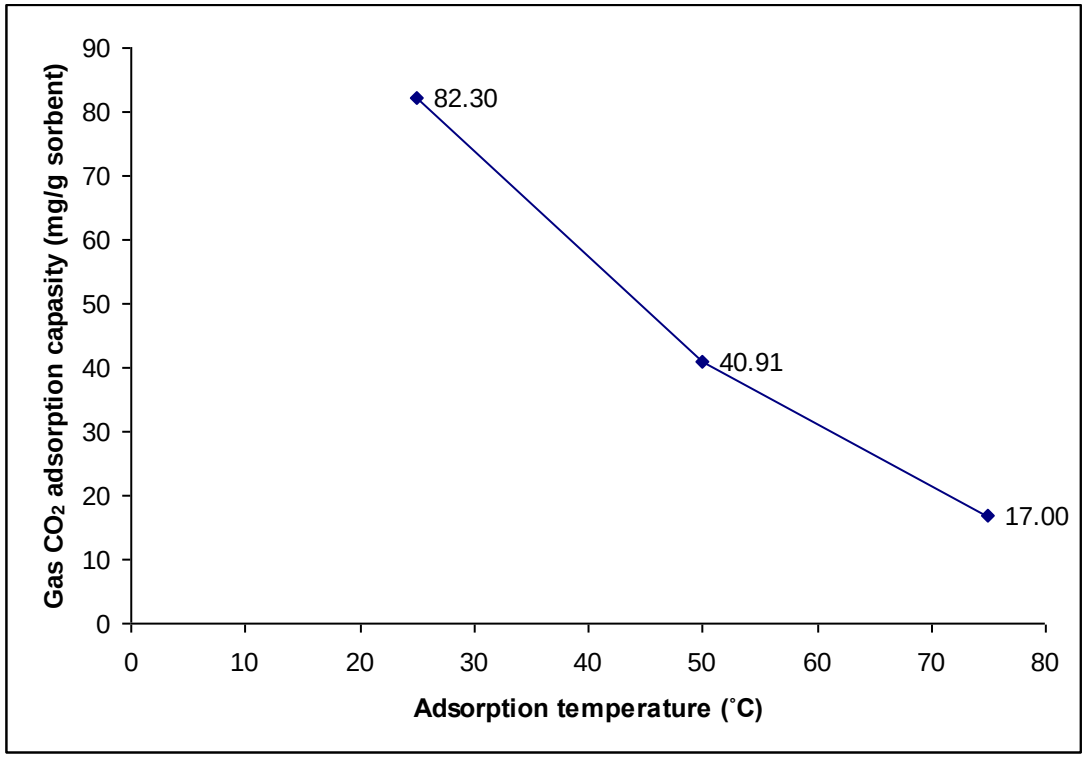

Figure 4.20: Gas CO_2 adsorption capacity for 20 wt% MEA modified MCM-41 at different adsorption temperatures.

The adsorption temperatures do not only affect the adsorption capacity but also the CO_2 gas uptake rate of 20 wt% MEA/MCM-41 sample. Figure 4.21 represents TGA curves of CO_2 adsorption capacity for 20 wt% MEA modified MCM-41 at adsorption temperatures of 25˚C, 50˚C and 75˚C as well as the slope, R which represent the rate of CO_2 uptake in mg/g sorbent/min. The adsorption at 25˚C gives the highest adsorption capacity and the fastest CO_2 uptake rate at 82.30 mg/g sorbent and 0.668 mg/g sorbent/min respectively. On the other hand, adsorption at 75˚C shows the lowest adsorption capacity and uptake rate of 17.00 mg/g sorbent and 0.367 mg/g sorbent/min respectively since at 75˚C CO_2 molecules tend to be in active energized form and are harder to adsorb.

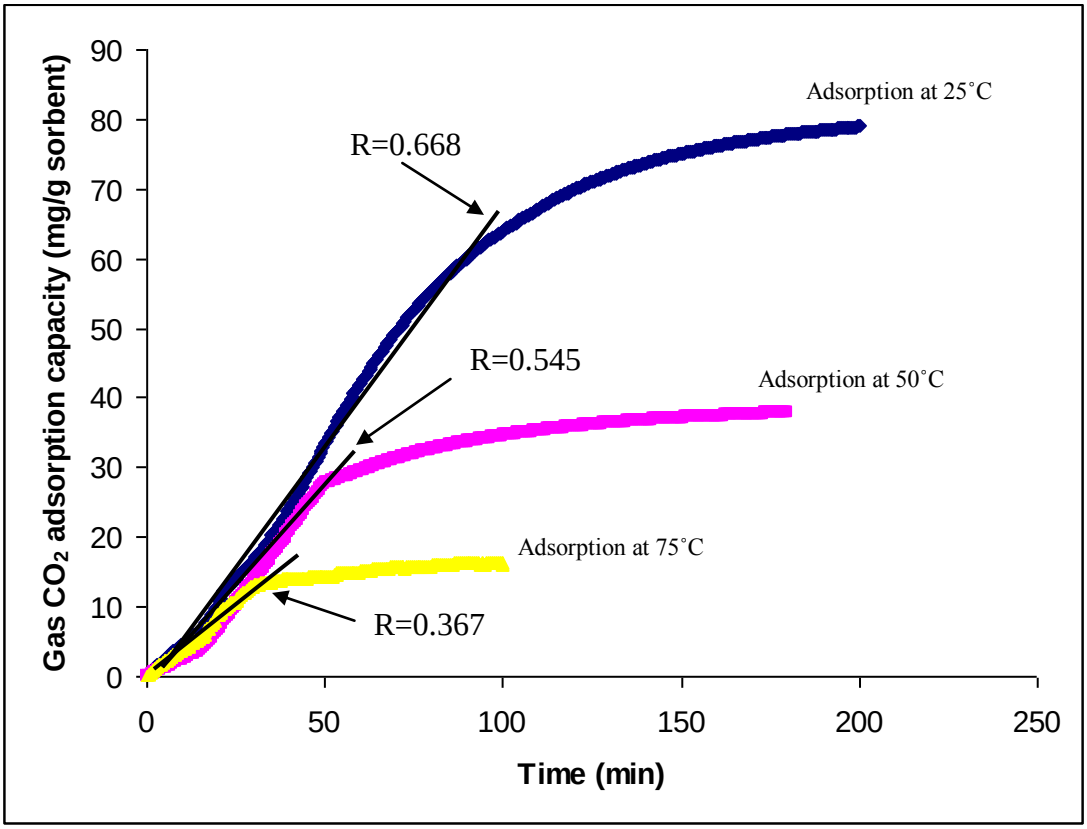

Figure 4.21: Slope, R represent rate of CO_2 uptake for 20 wt% MEA modified MCM-41 at different adsorption temperatures.

4.3.4.2 Influence of Heating Temperatures

The water vapor content in natural gas mixtures can vary from less than 1% to more than 10%. On the other hand, water also plays an important role of proton transfer agent in the reaction of acidic gas and amine solutions (conventional method of removing acidic gas from natural gas). Therefore, it is important to study the effects of water on acidic gas adsorption (Kaggerud *et al*., 2006; Huang and Yang, 2003).

Huang and Yang (2003) indicated that water vapor actually enhanced CO_2 adsorption on the amine modified samples. Quantitative analysis of the CO_2 desorption amount according to the peak area indicates that the amount of CO_2 desorbed is twice when the water was present during the adsorption. Their result is consistent with the fact that the mechanism for CO_2 removal using amines is dependence on the presence of water. Two moles of amine groups are required to remove every one mol of CO_2 molecules in order to form carbamate when water vapor is absent from the reaction. Whereas one mol of amine groups is effective enough in removing one mol of CO_2 to form bicarbonate in the presence of water. The study also suggests that the CO_2-amine bonding is enhanced when water vapor is presence during the adsorption (Gray *et al*., 2005; Zhou *et al.,* 2005; Khatri *et al.,* 2005; Huang and Yang, 2003).

Since the presence of water affects the CO_2 adsorption capacity, thus it is essential to study the effect of water vapor during gas-solid adsorption interaction. In this study, the main purpose of applying heat to the samples through TGA equipment is to remove impurities and water vapor in order to obtain clean adsorption on the adsorbents. However, since the presence of water proved to be affecting the adsorption capacity, the following experiment was designed to verify the theory. Four different heating temperatures were applied through TGA to investigate the adsorption capacity of 20 wt% MEA modified MCM-41 as shown in Figure 4.22.

The first heating temperature was 25˚C at room temperature. The result shows adsorption capacity of 21.71 mg/g sorbent which is lower than standard experiment temperature at 100˚C with high adsorption capacity of 40.91 mg/g sorbent. The same result is obtained when heating temperature is raised to 50˚C with only a slight increase of adsorption capacity of 23.47 mg/g sorbent. These findings clearly show that although the presence of water does improve adsorption, but without impurities being removed from the pore channels and surface of the adsorbents, it is impossible to achieve maximum CO_2 adsorption capacity. For the last experiment, heating temperature was

applied higher than water boiling point at 150˚C since even at 100˚C there still is a small trace of water vapor trapped. This is to ensure all water vapor is removed from the system, hence the adsorption of CO_2 without the presence of water vapor is able to be confirmed. The CO_2 adsorption capacity at heating temperature of 150˚C is 33.11 mg/g sorbent which is about 19% lower than standard at 100˚C. The result further confirm that the presence of water vapor does contribute to CO_2 adsorption capacity by amine modified MCM-41.

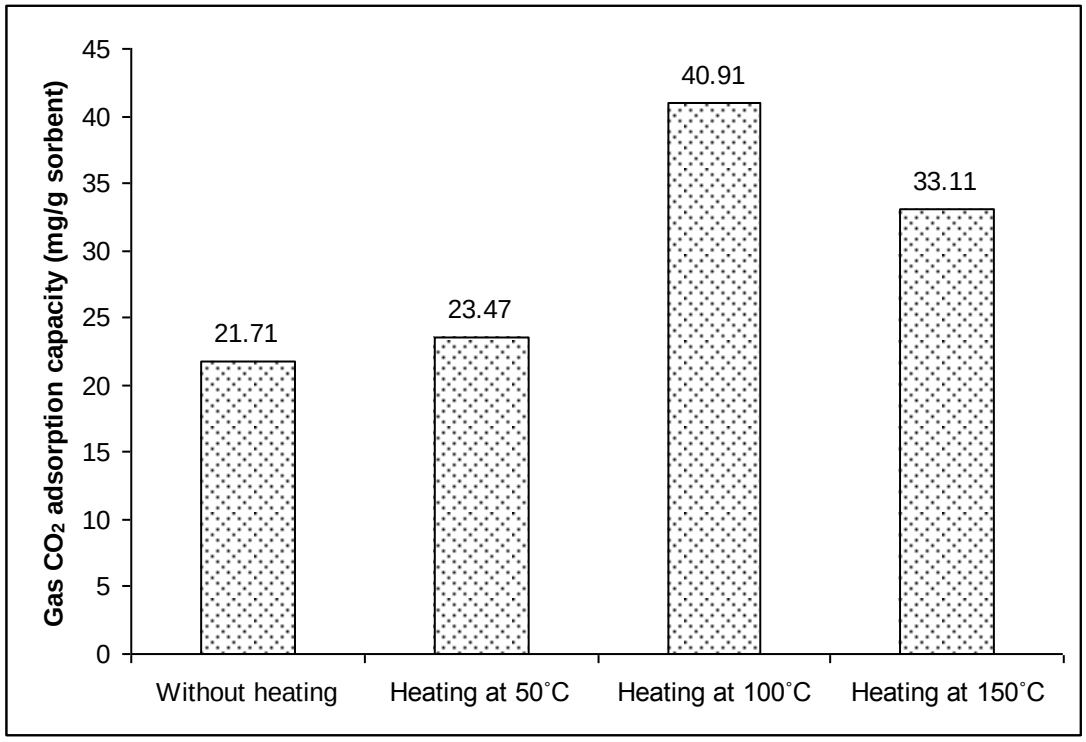

Figure 4.22: Gas CO_2 adsorption capacity for 20 wt% MEA modified MCM-41 at different heating temperatures.

In order to study the effect of heating temperatures on CO_2 uptake rate of 20 wt% MEA modified MCM-41, Figure 4.23 is presented. Surprisingly, although without heating gives the lowest adsorption capacity, the rate of CO_2 adsorption is extremely fast (1.424 mg/g sorbent/min) compare to others. For the first 20 minutes, a total of 94%

CO_2 uptake is already adsorbed by the adsorbent and the equilibrium is reached in less than 80 minutes. As for heating temperature at 50˚C, the uptake rate is a bit slower at 0.958 mg/g sorbent/min with 83% of total uptake can be achieved for the first 20 minutes and the equilibrium time required is also quite fast at 110 minutes. Finally, the CO_2 uptake rate shows by 20 wt% MEA modified MCM-41 at heating temperature of 150˚C is the slowest (0.507 mg/g sorbent/min). The equilibrium adsorption time is also longer (350 minutes) but is still faster than standard heating temperature (100˚C).

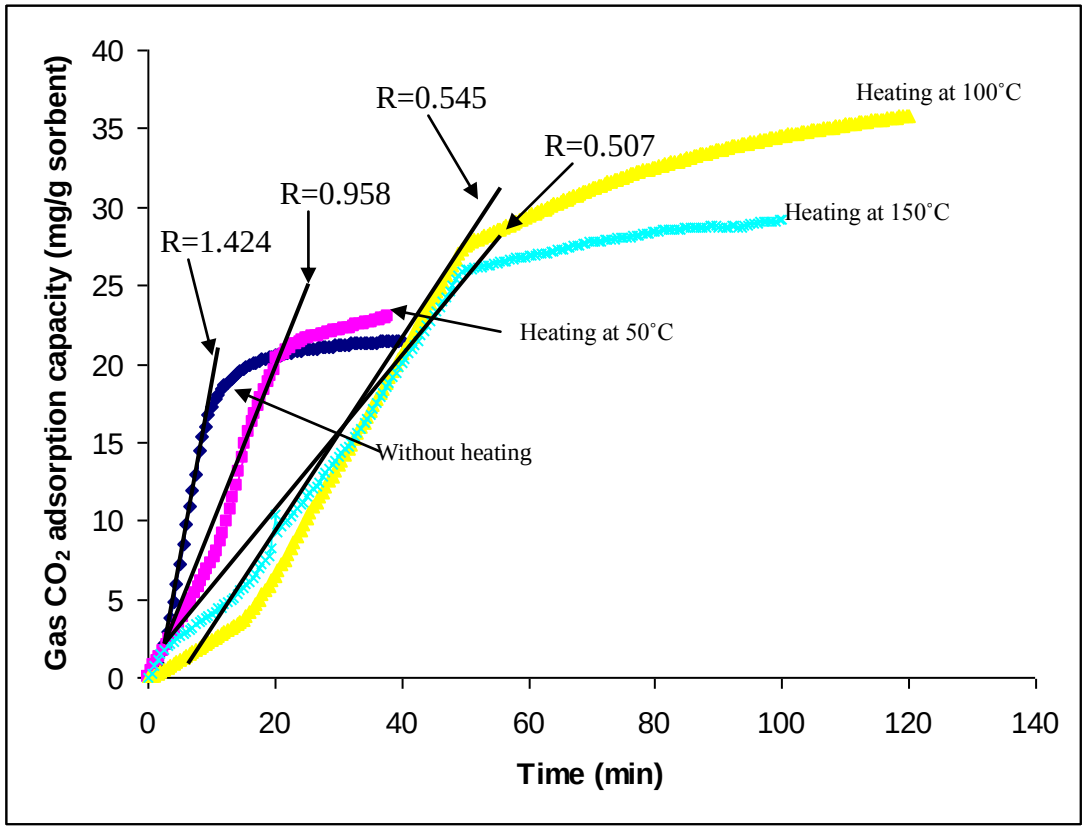

Figure 4.23: Slope, R represent rate of CO_2 uptake for 20 wt% MEA modified MCM-41 at different heating temperatures.

4.4 Gas-Solid Interaction

Interaction between gas asorbate and the solid adsorbent plays an important role in adsorption process. Therefore, it is essential to fully understand the characteristics of interaction between the adsorbed CO_2 gas molecules and the amine modified support materials. In situ FTIR spectroscopy has been utilized for studying the adsorbed species interaction with support materials surface directly and the transport of interacting molecules in pores of the support materials (Rajesh *et al*., 2005; Zheng *et al*., 2005). For this study, the amine modified samples were activated at 100˚C and vacuum at the same time for 2 hours before the introduction of CO_2 gas at various pressures. After the adsorption of CO_2 at room temperature for another 1 hour, the samples were studied by transmission FTIR spectroscopy. Thus, the FTIR spectra acquired were the result of solely the interaction of CO_2 gas with the support surface only.

Through the study of Yang *et al*. (2006) regarding the interaction between CO_2 molecules with silica surfaces, the fields of the minimum potential energy of a CO_2 molecule over the solid surfaces were evaluated. The study involved the evaluation of dispersion/repulsion and the electrostatic energies between the atoms in the CO_2 molecules with the surface atoms which evidently showed there are bonds between CO_2 molecules and the silica surface. However, the bonds do not show the obvious characteristic peak indicating any orientation of CO_2 molecules with respect to this surface is allowed. Since there is no certain appropriate interaction directly on silica surface, the discussion will focus on the interaction of CO_2 molecules on amine modified silica surface instead.

4.4.1 Interaction of CO_2 on Various Amines Modified MCM-41

Carbon dioxide is a linear molecule with four fundamental vibration modes at v_1 1340 cm^{-1}, v_3 2350 cm^{-1} and two bending modes at 666 cm^{-1}, only v_3 and one of the v_2 bending modes that in the plane position are infrared active (Hiyoshi *et al.*, 2005; Ingle and Crouch, 1988). The in situ FTIR cell used in this study consists of CaF_2 window which leads to the limitation of wavelength range at 77,000 – 900 cm^{-1}. Hence, the vibration of CO_2 molecules will only be detected at 2350 cm^{-1} region. FTIR spectra of various amines modified MCM-41 after CO_2 adsorption process is presented in Figure 4.24. The spectra are separated into two sections which are physisorption section in the region of 2600 – 2000 cm^{-1} and chemisorption section in the region of 1580 – 1350 cm^{-1}.

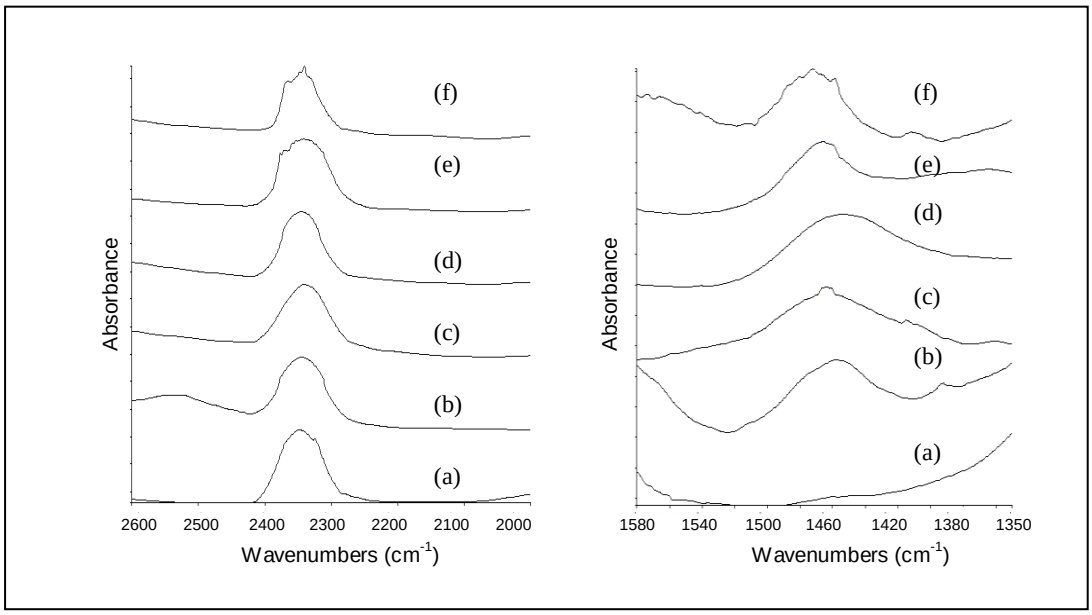

Figure 4.24 FTIR spectra of CO_2 adsorbed on: (a) MCM-41; (b) 20 wt% MEA/MCM-41; (c) 20 wt% DEA/MCM-41; (d) 20 wt% TEA/MCM-41; (e) 20 wt% MDEA/MCM-41; and (f) 20 wt% PEI/MCM-41 at equilibrium pressures of 138 kPa and 25˚C.

From Figure 4.24, the band with frequencies around 2350 cm^{-1} is attributed to the v_3 vibration of physisorbed CO_2. It was observed that the FTIR spectra of adsorbed CO_2 in amine modified MCM-41 is similar to the CO_2 band for the parent MCM-41 support. The 2350 cm^{-1} band in the spectra CO_2 appeared at the same location for the pure CO_2 gas phase and the adsorbed physisorbed phase which further confirmed the physisorption of CO_2 molecules on the amine modified MCM-41. Meanwhile, another broader band in the 1580 – 1350 cm^{-1} region was observed for all the amine modified MCM-41 except the MCM-41 support. The peak broad band at around 1455 cm^{-1} represents the C-N stretching vibrations in other word the chemisorbed CO_2 band. The parent MCM-41 spectrum does not exhibit the band at 1455 cm^{-1} region since no amine was detected. This clarify the 1455 cm^{-1} band is attributed to chemisorption of CO_2 reacted with amine of the amine modified MCM-41 to form carbonates and bicarbonates in certain circumstance (Zhao *et al*., 1996; Wakabayashi *et al*., 1997; Khatri *et al*., 2005; Hiyoshi *et al*., 2005).

All amine modified MCM-41 and parent MCM-41 show absorption band at 2350 cm^{-1} region which represent physisorption of CO_2 on the adsorbents as shown in Figure 4.24. All the bands can be observed at around the same region of 2350 cm^{-1}. However, the opposite happen on the chemisorption section which shows inconsistent band and with different absorbance value. The 20 wt% TEA/MCM-41 spectrum shows the absorption band at 1456.46 cm^{-1} which is slightly shifted to the lower wavelength compares to others which are more consistent. On the other hand, the parent MCM-41 spectrum does not shows any peak at 1455 cm^{-1} region since there is no amine being modified on the adsorbent. The main difference of CO_2 absorption bands for different types of amine modified MCM-41 is the peak areas corresponding to the adsorbed species. The areas of the FTIR absorption peaks are proportional to the adsorbed amount of CO_2 as revealed in Figure 4.25. The amount of gas adsorbed for these adsorbate–adsorbent systems were measured using gravimetric experimental technique while the absorbance areas were measured by FTIR.

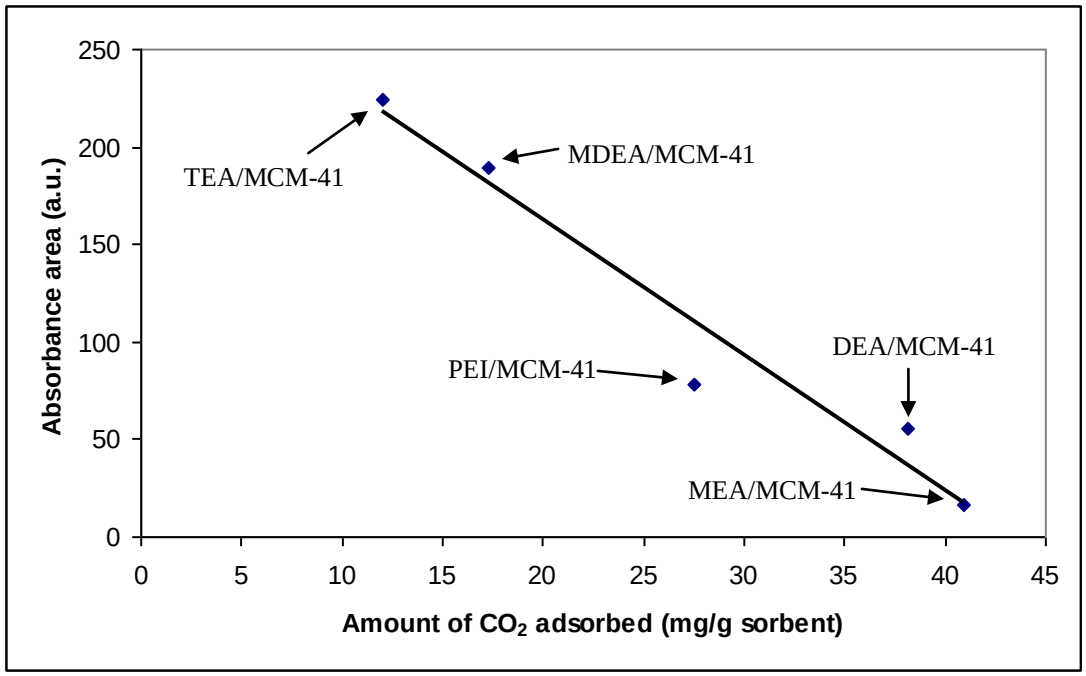

Figure 4.25: The corresponding areas of the FTIR spectrum peak at (1520 – 1420 cm^{-1} region) versus the amount of CO_2 adsorbed on amine modified MCM-41.

The sketch of CO_2 adsorption mechanism on amine modified MCM-41 is illustrated in Figure 4.26 to further explain the interaction between CO_2 and amine modified MCM-41 surface. Since the grafted amine group RNH_2 is weak alkali, and the atom N has a pair of lone electrons, it can easily attack the C atom in acid gas CO_2. As a result, carbamates are formed and the active H atom in carboxyl may then form a hydrogen bond with the nearby amine group. Thus, stabilize the chemisorption of CO_2 (Srivastava *et al.*, 2006; Zhao *et al.*, 2007).

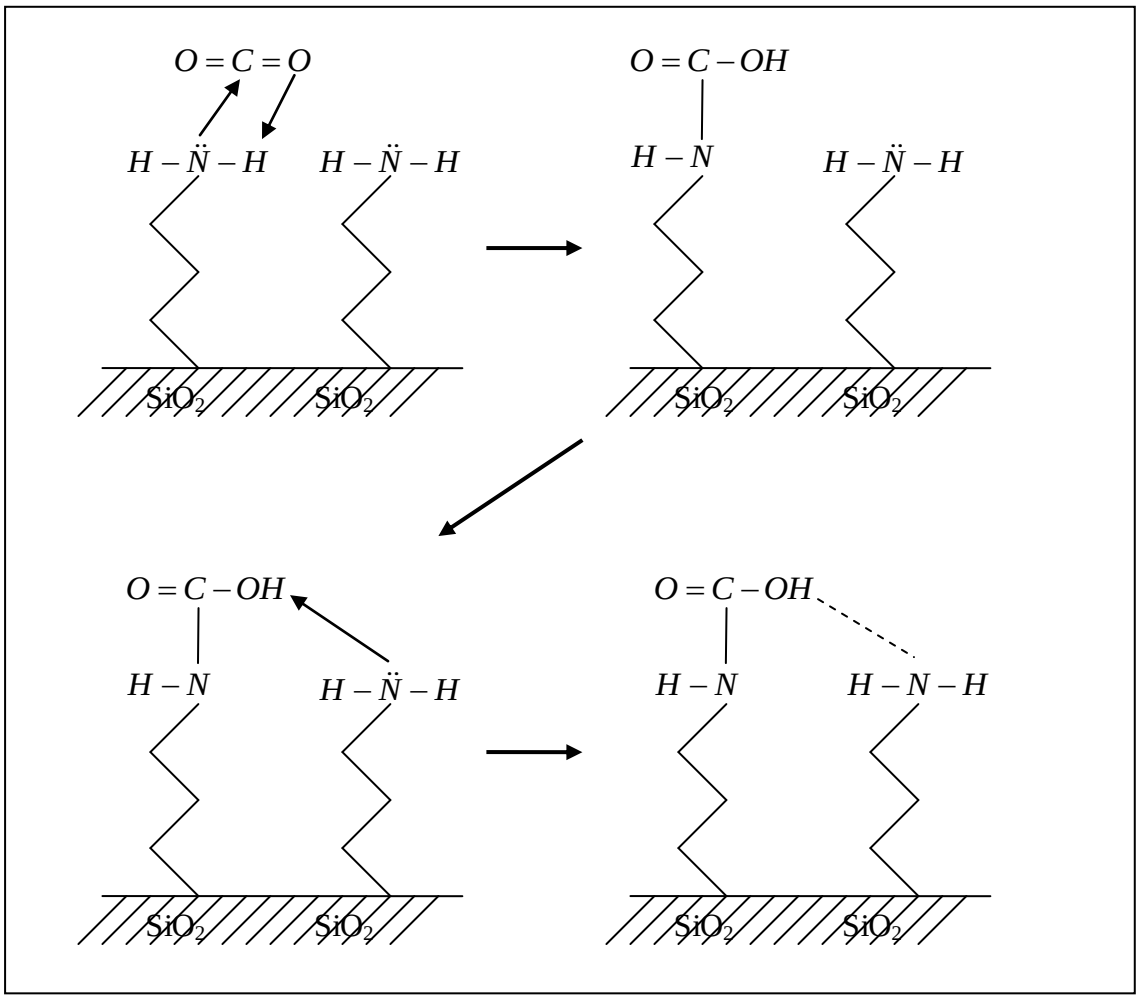

Figure 4.26: Schematic diagram of CO_2 adsorption on amine modified mesoporous silica.

4.4.2 Interaction of CO_2 on MEA Modified MCM-41 at Various Pressures

In order to investigate the effect of equilibrium pressure to the mechanism of CO_2 gas interaction with MCM-41 surfaces, the adsorption of CO_2 molecules at room temperature (25˚C) with increasing pressure on amine modified MCM-41 was carried out and the results are shown in Figure 4.27. Although the absorbance of the stretching

bands changed with increasing pressure, but the band frequencies almost remain unchanged.

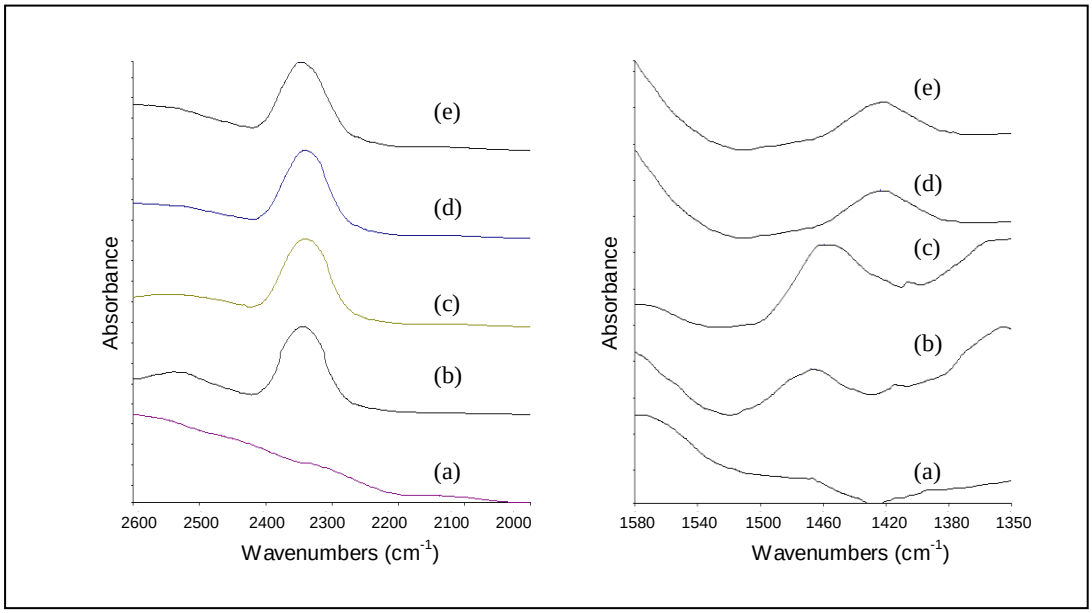

Figure 4.27: FTIR spectra of CO_2 adsorbed on MEA modified MCM-41 at 25˚C and equilibrium pressure: (a) without CO_2; (b) 138 kPa; (c) 276 kPa; (d) 414 kPa and (e) 552 kPa.

By observing the FTIR spectra, increased of the equilibrium pressure would result in an increase of the intensity of the 2350 cm^{-1} absorption band which is assigned to physisorbed CO_2 band. All the bands show consistent frequencies but increased in intensity. As for the chemisorbed band at 1455 cm^{-1} region, the absorption peaks are not consistent especially at high pressure of 414 kPa and 552 kPa. The bands clearly shift to lower frequencies at around 1420 cm^{-1}. Although the intensity peaks increase, the absorbance areas decrease after 276 kPa as shown in Figure 4.28. This result is consistent and well proven by Llewellyn and Maurin (2005) regarding on adsorbate-adsorbent interaction. Relatively, strong interaction between the adsorbing molecules and the surface occurs in the initial state of adsorption. The strength of these interactions

will then decrease (absorbance areas) as these specific sites are occupied or reached saturation capacity.

By increasing the CO_2 equilibrium pressures, the absorbance area for the physisorption peaks also increase up to 276 kPa as shown in Figure 4.28. However, further increase in pressure up to 414 kPa and 552 kPa shows decreasing in absorbance area. The peak area in the 2420 – 2380 cm^{-1} region starting to decrease at high pressure as the CO_2 adsorption achieved saturation condition in the case of physisorption as explained earlier. However, in the case of chemisorption, higher CO_2 equilibrium pressure applied, the more interaction between amine and CO_2 molecules resulting in more chemical reaction and higher chemisorption (Hiyoshi *et al.*, 2000; Zheng *et al.*, 2005; Xu *et al*., 2003; Cheng *et al.*, 2006a). This is evidently shown in Figure 4.29 as the peak area in the 1520 – 1380 cm^{-1} region kept increasing with pressure increasing.

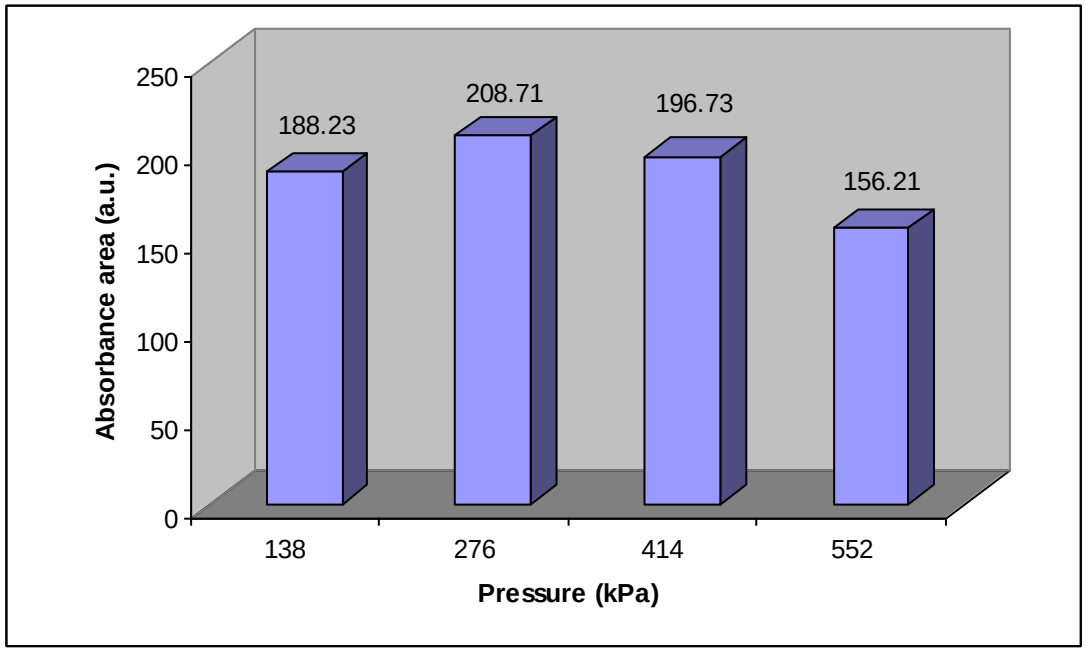

Figure 4.28: Effect of equilibrium CO_2 pressure on the FTIR absorbance areas (2420 – 2380 cm^{-1} region) for the physisorption peak.

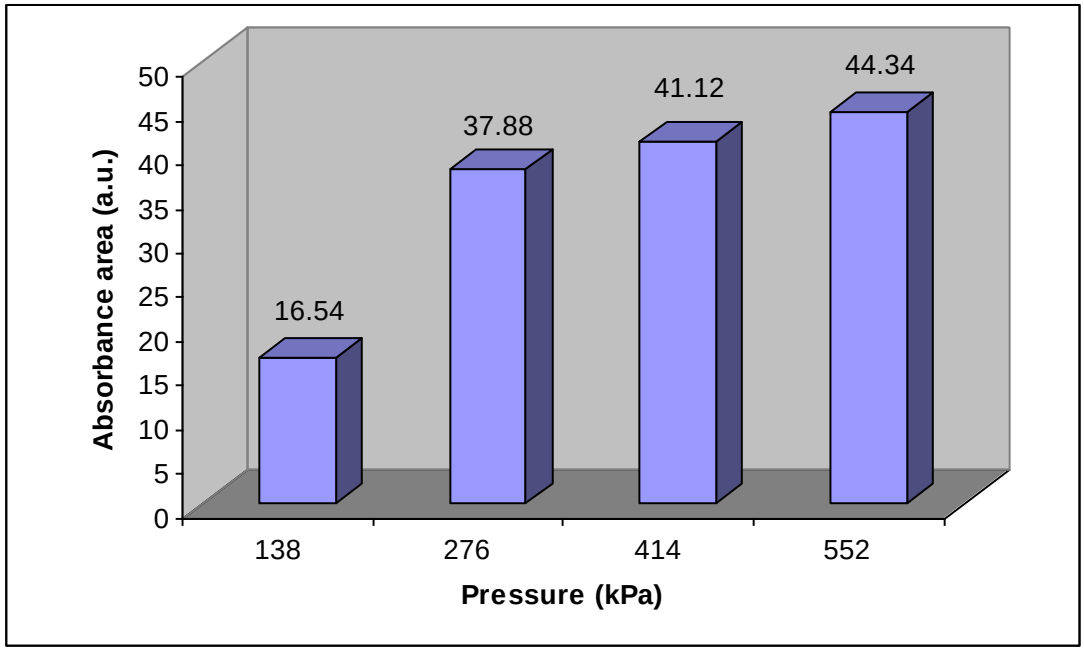

Figure 4.29: Effect of equilibrium CO_2 pressure on the FTIR absorbance areas (1450 – 1420 cm^{-1} region) for the chemisorption peak.

4.5 Summary

The structural characteristics and properties as well as carbon dioxide adsorption characteristics of amine modified mesoporous and microporous materials have been thoroughly studied within the scope of research. The adsorption process of porous materials is generally depends on several parameter such as pore volume, surface area, surface properties and the strength of adsorbate-adsorbent interactions. The incorporation of various alkanoamines on porous materials greatly enhances the CO_2 adsorption performance especially for mesoporous materials. Furthermore, the amines also improved the CO_2-adsorbent bonding and as a result increasing the selectivity of the adsorbent towards CO_2 adsorption. However, effect of amines on porous materials

varies differently towards mesoporous materials and microporous materials. From the study, mesoporous materials' CO_2 adsorption capacity improved significantly when using monoethanolamine as the modifying agent especially on MCM-41 support. By contrast, monoethanolamine modification on microporous materials show reduced CO_2 adsorption capacity. In addition, not all amines are suitable for modification on porous materials. Certain amines with large molecules size would actually decrease the CO_2 adsorption performance of the adsorbent. Therefore, this study proved to be important in order to understand the CO_2 adsorption performance of amine modified mesoporous and microporous materials.

CHAPTER 5

CONCLUSIONS AND RECOMMENDATIONS

5.1 Introduction

Since the findings of porous materials, studies on the general classification, synthesis, properties and potential applications have developed significantly over the past few years. These materials possess the ability for tailoring the surfactant assemblies in order to be used to design novel molecular sieve materials with various engineered structures, surface areas, pore diameters, pore size distribution and composition. Further modifications of porous materials using organic and inorganic chemical substances have resulted in improved performance especially when applied to gas adsorption industry such as CO_2 separation process. Through this study, modification of porous materials using different type of amines acting as the functional group of the adsorbents greatly influence the physical and chemical properties of the adsorbents as well as the adsorption characteristics. This chapter review the findings obtained in this study and give a conclusion remarks in order to completely understand CO_2 adsorption characteristics of amine modified adsorbents. Recommendations for future work are also included for the benefit of advance research development.

5.2 Summary of Research Findings

Amine functional groups are useful for CO_2 removal because of their ability to form ammonium carbamates and carbonates reversibly at moderate temperature. The incorporation of organic amines into porous supports is a great approach for CO_2 adsorption combining good adsorption capacity and selectivity. Modifications of porous materials using amines greatly influence the physicochemical properties of the porous materials and significantly affect CO_2 adsorption characteristics of the amine modified adsorbents.

XRD equipment was used to characterize the structure of the amine modified adsorbents. The patterns of XRD peak can be used to determine how well developed are the as-synthesis and amine modified adsorbents. Furthermore, the intensity of the XRD peak can explains the effect of pore filling and the coating of outer surface of amine modified adsorbents. The nitrogen adsorption isotherms of amine modified adsorbents can further confirm the amines were loaded into the pore channels of the support materials. The decreased of surface area, pore volume and average pore diameter of amine modified adsorbents can be used to explain the pore filling effect of amines. Other than that, the FTIR spectra can also be use to characterize the amine modified adsorbents. The stretching and bending vibration of chemical bonds will further determined the incorporation of amines into/onto support materials.

CO_2 adsorption capacity increases considerably after modification of MCM-41 using different types of alkanoamines. The ratio of CO_2 molecular per available N atom in the presence of hydroxyl group is approximately twice that without hydroxyl group. With the absence of hydroxyl group, 2 moles of amine groups are required to react with 1 mole of CO_2 molecule. However, when hydroxyl groups are present, the reaction is two times as much leading to the formation of stabilized carbamate type zwitterions.

There are two possible reasons for synergetic effect determining the characteristics of CO_2 adsorption on porous materials. First is the high surface area of porous materials and another is the uniform porous channel of porous materials. When amine was loaded onto the materials with high surface area, there will be more CO_2 affinity sites exposed to the adsorbate and thus increasing the adsorption capacity. When the channels of porous materials are filled by amine, the apparent pore size of the parent support will be reduced. Hence, reducing the pore volume and decreasing the maximum CO_2 adsorption capacity. However, at the same time more CO_2 affinity sites are introduced into the pore channel of porous materials. Both these contradicting effects occurred simultaneously and directly affected the adsorption capacity. In the study, MEA modified MCM-41 shows the highest CO_2 adsorption capacity at 40.91 mg/g sorbent while the lowest adsorption was at 12.04 mg/g sorbent by TEA modified MCM-41 sample.

MEA amine had been used to modify MCM-41 support at different concentrations. As a result, at low MEA loading (10 wt%), the amine had little contribution on CO_2 adsorption capacity. The highest adsorption capacity was reached by 20 wt% of MEA with high CO_2 adsorption capacity at 40.91 mg/g sobent which is 120% higher than the parent MCM-41 support. The pore channels of MCM-41 play an important role on the characteristic of CO_2 adsorption capacity. When the channels of the MCM-41 are filled with MEA, the apparent pore size of the MCM-41 will be decreased. At the same time, more CO_2 affinity sites are introduced into the channel. In the case of MEA modified MCM-41, physisorption and chemisorption take place at the same time. The physisorption on the MEA/MCM-41 sample occurs mainly in the pore channels of MCM-41 support, while the chemisorption involves the reaction of CO_2 and MEA in the channels of MCM-41 as well as on the external surface of MCM-41. When the channels of MCM-41 are fully filled with MEA, the highest adsorption capacity can be obtained. When MEA concentration is further increased and the MEA begin to coat on the external surface of MCM-41, the adsorption capacity decreases.

Through this study, microporous supports of NaY and 13X show significantly higher CO_2 adsorption capacity compared to mesoporous materials. This can be explained as materials with the strongest enthalpic interactions with sorbed molecules will show the highest level of adsorption. These tend to be materials with narrow pores (microporous), because small pores increase the interaction between gas and the framework. However, materials with narrow pores also have the highest framework densities and thus the lowest amount of free void space per gram of material. Therefore, at the highest pressure when the pores are nearly filled, the materials with the largest free volumes have more room for quest molecules and consequently show the highest CO_2 uptake. This also explained why upon modification by MEA, microporous supports NaY and 13X resulted in decrease of CO_2 adsorption capacity unlike for mesoporous supports.

The adsorption of CO_2 by porous materials or amines is an exothermic process. Accordingly, the adsorption capacity decrease with the increase of temperature. The CO_2 adsorption capacity at adsorption temperature 25˚C (room temperature) shows the highest value at 82.30 mg/g sorbent. At higher temperature the adsorbate CO_2 molecules tend to be in active energized form and are harder to adsorb compare to molecules at lower temperature which has lower activation energy to be adsorbed.

Interactions between CO_2 molecules adsorbed on the amine modified adsorbents are important in adsorption process. The integrated absorbance areas and the intensities of FTIR spectrums reveal that gas CO_2 interact with amine modified adsorbents. The CO_2 molecule is free rotating and adsorbed (physically and chemically) on the active adsorption sites on adsorbent surfaces as gas phase molecules. The type of amines and the equilibrium pressure of CO_2 adsorbate have high influence on the adsorption especially chemisorption.

5.3 Recommendations for Future Work

In order to further understand the gas adsorption characteristics in amine modified adsorbents, the following recommendations are highlighted for future work. As for structural and properties characterization, Temperature Programmed Desorption (TPD) characterization is highly recommended to obtain the acidity and basicity properties of amine modified adsorbents. Other than that, MAS-NMR Spectroscopy can be use to determine the framework of Si to Al ratio by observing the high-resolution spectra from the solid samples.

Besides that, the gas adsorption isotherms for amine modified adsorbents can be conducted in a wider range of pressure and temperature in order to obtain clearer picture of gas adsorption characteristics and equilibrium model. Meanwhile, in spite of using a single pure adsorbate system, gas mixture adsorption can be carried out to further study the adsorbents selectivity properties.

5.4 Concluding Remarks

Gas adsorption characteristics of amine modified adsorbents have been successively studied in this work from the aspects of characterization, adsorption equilibrium, and adsorption behavior on the gas-porous materials interaction mechanisms. The results from this study provide a significant contribution in designing amine modified adsorbents system for improvement towards development of new adsorbents with the highest quality and efficiency.

REFERENCES

Anon. (2005). AG Foundation Release Natural Gas Outlook to 2020. *Pipeline and Gas Journal*. 232: 6-9.

Astala, R. and Auerbach, S. M. (2004). The Properties of Methylene- and Amine-Substituted Zeolites from First Principles. *J. Am. Chem. Soc.* 126: 1843-1848.

Barton, T. J., Bull, L. M., Klemperer, W. G., Loy, D. A., McEnaney, B., Misono, M., Monson, P. A., Pez, G., Scherer, G. W., Vartuli, J. C., and Yaghi, O. M. (1999). Tailored Porous Materials. *Chem. Mater.* 11: 2633-2656.

Beck, J. S. and Vartuli, J. C. (1996). Recent Advances in The Synthesis, Characterization and Applications of Mesoporous Molecular Sieves. *Current Opinion in Solid State & Materials Science*. 1: 76-87.

Boger, T., Roesky, R., Gläser, R., Ernst, S., Eigenberger, G., and Weitkamp, J. (1997). Influence of The Aluminum Content on The Adsorptive Properties of MCM-41. *Micropor. Mater*. 8: 79-91.

Burleigh, M. C., Markowitz, M. A., Spector, M. S., and Gaber, B. P. (2001). Amine-Functionalized Periodic Mesoporous Organosilicas. *Chem. Mater.* 13: 4760-4766.

Cheng, Q., Pavlinek, V., Lengalova, A., Li, C., He, Y., and Saha, P. (2006b). Conducting Polypyrrole Confined in Ordered Mesoporous Silica SBA-15 channels: Preparation and Its Electrorheology. *Micropor. Mesopor. Mater.* : 263-269.

Cheng, Q., Pavlinek, V., Li, C., Lengalova, A., He, Y., and Saha, P. (2006a). Synthesis and Characterization of New Mesoporous Material with Conducting Polypyrrole Confined in Mesoporous Silica. *Mater. Chem. Phys.* 98: 504-508.

Chhatwal, G. R. and Mehra, H. (1974). *Adsorption and Phase Rule*. India: Goel Publishing House.

Choma, J., Jaroniec, M., Burakiewicz-Mortka, W., and Kloske, M. (2002). Critical Appraisal of Classical Methods for Determination of Mesoporous Size Distributions of MCM-41 Materials. *Applied Surface Sci.* 196: 216-223.

Choma, J., Kloske, M., and Jaroniec, M. (2003). An Improved Methodology for Adsorption Characterization of Unmodified and Modified Silica Gels. *J. Colloid and Interface Sci.* 266: 168-174.

Coade, R. and Coldham, D. (2006). The Interaction of Mercury and Aluminum in Heat Exchangers in a Natural Gas Plants. *Inter. J. Pressure Vessels and Piping*. 83: 336-342.

Dabrowski, A. (2001). Adsorption- From Theory to Practice. *Adv. Colloid Interface Sci.* 93: 135-224.

Daiminger, U., Lind, W., and Mitariten, M. (2004). Adsorption Added Value. *Hydrocarbon Eng. VII*. 2: 83-86.

Delaney, W. S., Knowles, G. P., and Chaffee, A. L. (2002). Preprints of Symposia-American Chemical Society, Division of Fuel Chemistry. 47(1): 65-66.

Derouane, E. G. (1998). Zeolites as Solid Solvents. *J. Molecular Catal. A: Chem*. 134: 29-45.

Desideri, U. and Paolucci, A. (1999). Performance Modelling of A Carbon Dioxide Removal System for Power Plants. *Energy Convers. Mgmt*. 40: 1899-1915.

de Sousa, A. and de Sousa, E. M. B. (2005). Ordered Mesoporous Silica Carrier System Applied in Nanobiothecnology. *Brazilian Arch. Bio. Tech*. 48: 243-250.

Evans, J., Zaki, A. B., El-Sheikh, M. Y., and El-Safty, S. A. (2000). Incorporation of Transition-Metal Complexes in Functionalized Mesoporous Silica and Their Activity toward the Oxidation of Aromatic Amines. *J. Phys. Chem. B*. 104: 10271-10281.

Fajula, F., Galarneau, A. and Renzo, F. D. (2005). Advanced Porous Materials: New Developments and Emerging Trends. *Micropor. Mesopor. Mater*. 82.

Frost, H., Duren, T., and Suurr R. Q. (2006). Effects of Surface Area, Free Volume, and Heat of Adsorption on Hydrogen Uptake in Metal-Organic Frameworks. *J. Phys. Chem. B*. 110: 9565-9570.

Fulvio, P. F., Pikus, S., and Jaroniec, M. (2005). Short-Time Synthesis of SBA-15 Using Various Silica Sources. *J. Colloid Interface Sci*. 287: 717-720.

Gaydhankar, T. R., Taralkar, U. S., Jha, R. K., Joshi, P. N., and Kumar, R. (2005). Textural/Structural, Stability and Morphological Properties of Mesostructured Silicas (MCM-41 and MCM-48) Prepared Using Different Silica Sources. *Catal. Communications*. 6: 361-366.

Ghobarkar, H., Schaf, O., and Guth, U. (1999). Zeolites- From Kitchen to Space. *Prog. Solid St. Chem.* 27: 29-73.

Gray, M. L., Soong, Y., Champagne, K. J., Pennline, H., Baltrus, J. P., Stevens Jr., R. W., Khatri, R.,Chuang, S. S. C., and Filburn, T. (2005). Improved Immobilized Carbon Dioxide Capture Sorbents. *Fuel Proc. Tech*. 86: 1449-1455.

Guli, M., Chen, Y., Li, X. T., Zhu, G. S., and Qiu, S. L. (2007). Fluorescence of Postgrafting Rhodamine B in the Mesopores of Rodlike SBA-15. *J. Luminescence*. 126: 723-727.

Guo, J., Han, A. J., Yu, H., Dong, J. P., He, H., and Long, Y. C. (2006). Base Property of High Silica MFI Zeolites Modified With Various Alkyl Amines. *Micropor. Mesopor. Mater*. 166-172.

Hadi Nur, Lau, C. G., Salasiah Endud, and Halimaton Hamdan. (2004). Quantitative Measurement of A Mixture of Mesophases Cubic MCM-48 and Hexagonal MCM-41 by ^{13}C CP/MAS NMR. *Mater. Lett*. 58: 1971-1974.

Han, A. J., He, H. Y., Guo, J., Yu, H., Huang, Y. F., and Long, Y. C. (2005). Studies on Structure and acid-base Properties of High Silica MFI-Type Zeolite Modified with Methylamine. *Micropor. Mesopor. Mater*. 79: 177-184.

Hiyoshi, N., Yogo, K., and Yashima, T. (2005). Adsorption Characteristics of Carbon Dioxide on Organically Functionalized SBA-15. *Micropor. Mesopor. Mater*. 84: 357-365.

Huang, H. Y. and Yang, R. T. (2003). Amine-Grafted MCM-48 and Silica Xerogel as Superior Sorbents for Acidic Gas Removal from Natural Gas. *Ind. Eng. Chem. Res.* 42: 2427-2433.

Ingle, J. D. and Crouch, S. R. (1988). *Spectrochemical Analysis*. United States of America: Prentice-Hall International Inc. 404.

Inoue, M., Tanino, H., Kondo, Y., and Inui, T. (1991). Formation of Organic Derivatives of Boehmite by the Reaction of Gibbsite with Glycols and Aminoalcohols. *Clays and Clay Minerals*. 39(2): 151-157.

Jaroniec, M., Kruk, M., Hyun, J. S., Ryong, R., Sakamoto, Y., and Terasaki, O. (2001). Comprehensive Characterization of Highly Ordered MCM-41 Silicas Using Nitrogen Adsorption, Thermogravimetry, X-ray Diffraction and Transmission Electron Microscopy. *Micropor. Mesopor. Mater*. 48: 127-134.

Kaggerud, K. H., Bolland, O., and Gundersen, T. (2006). Chemical and Process Integration: Synergies in Co-Production of Power and Chemicals from Natural Gas With CO_2 Capture. *Applied Thermal Eng*. 26: 1345-1352.

Kang, T., Park, Y., Park, J. C., Cho, Y. S., and Yi, J. (2002). Preparation of Chemically Active Mesoporous Adsorbent for Pt(II) and Pd(II) Adsorption from Aqueous Solutions. *Korean J. Chem. Eng.* 19(4): 685-687.

Khatri, R. A., Chuang, S. S. C., Soong, Y., and Gray, M. (2005). Carbon Dioxide Capture by Diamine-Grafted SBA-15: A Combined Fourier Transform Infrared and Mass Spectrometry Study. *Ind. Eng. Chem. Res.* 44: 3702-3708.

Klimova, T., Esquivel, A., Reyes, J., Rubio, M., Bokhimi, X., and Aracil, J. (2006). Factorial Design for the Evaluation of the Influence of Synthesis Parameters Upon The Textural and Structural Properties of SBA-15 Ordered Materials. *Micropor. Mesopor. Mater.* 331-343.

Knowles, G. P., Graham, J. V., Delaney, S. W., and Chaffee, A. L. (2005). Aminopropyl-Functionalized Mesoporous Silicas as CO_2 Adsorbent. *Fuel Proc. Tech*. 86: 1435-1448.

Kruk, M. and Jaroniec, M. (2001). Characterization of Modified Mesoporous Silicas Using Argon and Nitrogen Adsorption. *Micropor. Mesopor. Mater*. 44-45: 725-732.

Kruk, M., Jaroniec, M., and Sayari, A. (1999). Influence of Hydrothermal Restructuring Conditions on Structural Properties of Mesoporous Molecular Sieves. *Micropor. Mesopor. Mater*. 27: 217-229.

Kumar, D., Schumacher, K., Hohenesche, D. F. V., Grün, M., and Unger, K. K. (2001). MCM-41, MCM-48 and Related Mesoporous Adsorbents: Their Synthesis and Characterisation. *Colloids and Surfaces A: Physicochem. Eng. Aspects*. 187-188: 109-116.

Lee, S. H., Lee, J. Y., Park, Y. M., Wee, J. H., and Lee, K. Y. (2006). Complete Oxidation of Methane and CO at Low Temperature over $LaCoO_3$ Prepared by Spray-freezing/Freeze-drying Method. *Catal. Today*. In press.

Llewellyn, P. L. and Maurin, G. (2005). Gas Adsorption Microcalorimetry and Modeling to Characterise Zeolites and Related Materials. *C. R. Chimie*. 8: 283-302.

Luan, Z. and Fournier, J. A. (2005). In Situ FTIR Spectroscopic Investigation of Active Sites and Adsorbate Interactions in Mesoporous Aluminosilicate SBA-15 Molecular Sieves. *Micropor. Mesopor. Mater*. 79: 235-240.

Luan, Z., Fournier, J. A., Wooten, J. B., and Miser, D. E. (2005). Preparation and Characterization of (3-aminopropyl)triethoxysilane-Modified Mesoporous SBA-15 Silica Molecular Sieves. *Micropor. Mesopor. Mater*. 83: 150-158.

Mavrakis, D., Thomaidis, F., and Ntroukas, I. (2006). An Assessment of the Natural Gas Supply Potential of the South Energy Corridor from the Caspian Region to the EU. *Energy Policy*. 34: 1671-1680.

McKittrick, M. W. and Jones, C. W. (2003). Toward Single-Site Functional Materials-Preparation of Amine-Functionalized Surfaces Exhibiting Site-Isolated Behavior. *Chem. Mater*. 15: 1132-1139.

Meisen, A. and Shuai, X. S. (1997). Research and Development Issues in CO_2 Capture. *Energy Convers. Mgmt*. 38: 837-842.

Mercuri, L. P., Matos, J. R., Li, Z., and Jaroniec, M. (2006). Comparative Thermogravimetric and Adsorption Study of Highly Ordered Mesoporous Materials. *J. Colloid Interface Sci*. 296: 377-380.

Mirji, S. A., Halligudi, S. B., Mathew, N., Jacob, N. E., Patil, K. R., and Gaikwad, A. B. (2006). Adsorption of Methanol on Mesoporous SBA-15. *Mater. Lett*.

Murcia, A. B., Fletcher, A. J., Martinez, J. G., Amoros, D. C., Solano, A. L., and Thomas, K. M. (2003). Probe Molecule Kinetic Studies of Adsorption on MCM-41. *J. Phys. Chem. B*. 107: 1012-1020.

Náray-Szabó, I. (1969). *Inorganic Crystal Chem*. Hungary: Akadémiai Kiadó, Budapest.

Parvulescu, V. and Su, B. L. (2001). Iron, Cobalt or Nickel Substituted MCM-41 Molecular Sieves for Oxidation of Hydrocarbon. *Catal. Today*. 69: 315-322.

Philippe, L., Sammon, C., Lyon, S. B., and Yarwood, J. (2004a). An FTIR/ATR in Situ Study of Sorption and Transport in Corrosion Protective Organic Coatings 1. Water Sorption and Role of Inhibitor Anions. *Prog. Org. Coatings*. 49: 302-314.

Philippe, L., Sammon, C., Lyon, S. B., and Yarwood, J. (2004b). An FTIR/ATR in Situ Study of Sorption and Transport in Corrosion Protective Organic Coatings 2. The Effects of Temperature and Isotop Dilution. *Prog. Org. Coatings*. 49: 315-323.

Rege, S. U. and Yang, R. T. (2001). A Novel FTIR Method for Studying Mixed Gas Adsorption at Low Concentrations: H_2O and CO_2 on NaX Zeolite and γ-alumina. *Chem. Eng. Sci*. 56: 3781-3796.

Sherman, J. D. (1999). Synthetic Zeolites and Other Microporous Oxide Molecular Sieves. *Proc. Natl. Acad. Sci.* 96: 3471-3478.

Sing, K. S. W. (1998). Adsorption Methods for the Characterization of Porous Materials. *Adv. Colloid Interface Sci*. 76-77: 3-11.

Sing, K. (2001). The Use of Nitrogen Adsorption for the Characterization of Porous Materials. *Colloid and Surface A: Physicochem. Eng. Aspects*. 187-188: 3-9.

Sing, K. S. W. (2004). Characterization of Porous Materials: Past, Present and Future. *Colloid and Surface A: Physicochem. Eng. Aspects*. 241: 3-7.

Srivastava, R., Srinivas, D., and Ratnasamy, P. (2006). Sites for CO2 Activation Over Amine-Functionalized Mesoporous Ti(Al)-SBA-15 Catalysts. *Micropor. Mesopor. Mater*. 90: 314-326.

Stucky, G. D., Zhao, D. Y., Feng, J. L., Huo, Q. S., Melosh, N., Fredrickson, G. H., and Chmelka, B. F. (1998). Triblock Copolymer Syntheses of Mesoporous Silica with Periodic 50 to 300 Angstrom Pores. *Sci*. 279: 548-552.

Tallon, C., Yates, M., Moreno, R., and Nieto, M. I. (2006a). Porosity of Freeze-dried γ-Al_2O_3 Powders. *Ceramics Inter*. In press.

Tallon, C., Moreno, R., and Nieto, M. I. (2006b). Synthesis of γ-Al_2O_3 Nanopowders by Freeze-drying. *Mater. Research Bulletin*. 41: 1520-1529.

Thommes, M., Köhn, R., and Fröba, M. (2002). Sorption and Pore Condensation Behavior of Pure Fluids in Mesoporous MCM-48 Silica, MCM-41 Silica, SBA-15 Silica and Controlled-Pore Glass at Temperatures Above and Below The Bulk Triple Point. *Applied Surface Sci*. 196: 239-249.

Ustinov, E. A., Do, D. D., and Jaroniec, M. (2005). Adsorption of Argon and Nitrogen in Cylindrical Pores of MCM-41 Materials: Application of Density Functional Theory. *Applied Surface Sci*.

Vartuli, J. C., Malek, A., Roth, W. J., Kresge, C. T., and McCullen, S. B. (2001). The Sorption Properties of As-Synthesized and Calcined MCM-41 and MCM-48. *Micropor. Mesopor. Mater*. 44-45: 691-695.

Wakabayashi, F., Kondo, J. N., Domen, K., and Hirose, C. (1997). FT-IR Study of The Interaction of Oxygen, Argon, Helium, Nitrogen and Xenon With Hydroxyl Groups in H-Y Zeolite at Low Temperatures. *Micropor. Mater*. 8: 29-37.

Weitkamp, J. (2000). Zeolites and Catalysis. *Solid State Ionics*. 131: 175-188.

Xiao, B. L., Wang, H., and He, R. (2002). Aluminum Phthalocyanine Complex Covalently Bonded to MCM-41 Silica as Heterogeneous Catalyst for the Synthesis of Cyclic Carbonates. *J. Molecular Catal. A: Chem*. 186: 33-42.

Xu, X., Song, C., Andresen, J. M., Miller, B. G., and Scaroni, A. W. (2002). Novel Polyethylenimine-Modified Mesoporous Molecular Sieve of MCM-41 Type as High-Capacity Adsorbent for CO_2 Capture. *Energy & Fuels*. 16: 1463-1469.

Xu, X., Song, C., Andrésen, J. M., Miller, B. G., and Scaroni, A. W. (2003). Preparation and Characterization of Novel CO_2 "Molecular Basket" Adsorbents Based on Polymer-Modified Mesoporous Molecular Sieve MCM-41. *Micropor. Mesopor. Mater*. 62: 29-45.

Yang, X. N., Xu, Z. J., and Zhang, C. J. (2006). Molecular Dynamics Simulation of Dense Carbon Dioxide Fluid on Amorphous Silica Surfaces. *J. Colloid Interface Sci*. 297: 38-44.

Xu, X., Song, C., Miller, B. G., and Scaroni, A. W. (2005). Adsorption Separation of Carbon Dioxide from Flue Gas of Natural Gas-Fired Boiler by A Novel Nanoporous "Molecular Basket" Adsorbent. *Fuel Proc. Tech*. 86: 1457-1472.

Zhang, X., Schubert, S., and Agar, D. W. (2005). Studies on the Kinetics of Carbon Dioxide Absorption with Immobilised Amines (IA). *Chem. Eng. J.* 107: 97-102.

Zhao, H. L., Hu, J., Wang, J. J., Zhou, L. H., and Liu, H. L. (2007). CO_2 Capture by the Amine-Modified Mesoporous Materials. *Acta Phys. –Chim. Sin.* 23(6): 801-806.

Zhao, X. S., Lu, G. Q., and Hu, X. (2000). Characterization of the Structural and Surface Properties of Chemically Modified MCM-41 Material. *Micropor. Mesopor. Mater*. 41: 37-47.

Zhao, X. S., Lu, G. Q., and Hu, X. (2001). Organophilicity of MCM-41 Adsorbents Studied by Adsorption and Temperature-Programmed Desorption. *Colloids and Surfaces A: Physicochem. Eng. Aspects*. 179: 261-269.

Zhao, X. S., Lu, G. Q., and Millar, G. J. (1996). Advances in Mesoporous Molecular Sieve MCM-41. *Ind. Eng. Chem. Res.* 35: 2075-2090.

Zheng, F., Tran, D. N., Busche, B. J., Fryxell, G. E., Addleman, R. S., Zemanian, T. S., and Aardahl, C. L. (2005). Ethylenediamine-Modified SBA-15 as Regenerable CO_2 Sorbent. *Ind. Eng. Chem. Res.* 44: 3099-3105.

Zhou, L., Liu, X., Sun, Y., Li, J., and Zhou, Y. (2005). Methane Sorption in Ordered Mesoporous Silica SBA-15 in The Presence of Water. *J. Phys. Chem. B*. 109: 22710-22714.

Zhu, S. M., Zhou, H. S., Hibino, M., and Honma, I. (2003). Metallic Ruthenium Incorporation in the Porous Structure of SBA-15 Using a Sonochemical method. *J. Mater. Chem.* 13: 1115-1118.

APPENDIX A

Calculation of Amines

The following calculation is to determine the exact amount of monoethanolamine to be used in modification of selected adsorbents. The calculation also applies to other type of amines in accordance to the selected amine molecular weight and density.

Selected amine = Monoethanolamine (MEA)

Molecular weight = 61.08 g/mol

Density = 1020 g/L

Molarity of MEA $= \dfrac{1020\dfrac{g}{l}}{61.08\dfrac{g}{mol}}$

$= 16.7M$

To prepare 100 ml of 0.5 M MEA solution:

$M_1V_1 = M_2V_2$

$16.7M(V_1) = (0.5M)(100ml)$

$V_1 = 2.99ml$

$$= \quad 2.99ml \times 1.02 \frac{g}{ml}$$

$$\approx \quad 3.05g$$

To calculate 20 wt% of MEA:

Total adsorbent weight	=	0.5 g
Weight of MEA	=	20 % x 0.5 g
	=	0.1 g
The rest of the adsorbent is MCM-41	=	0.5 g – 0.1 g
	=	0.4 g

From previous calculation we know that there are 3.05 g of MEA in 100 ml of 0.5 M MEA solution. Therefore, to obtain 0.1 g of MEA, the volume of 0.5 M MEA solution need to add to 0.4 g of MCM-41 is:

$$3.05g \rightarrow \quad 100ml$$

$$0.1g \rightarrow \quad \frac{0.1g \times 100ml}{3.05g}$$

$$\approx \quad 3.28ml$$

APPENDIX B

Carbon Dioxide Capture Capacity Measurement

During analysis of experimental results for carbon dioxide adsorption, the temperature of thermal gravimetric analyzer was programmed for each sample as stated below:

Adsorbate flow rate = Static in closed system
Adsorption pressure = 138 kPa

Temperature Program:

- Heat from 50 ^{0}C to 100 ^{0}C at 10 ^{0}C/min.
- Hold at 100 ^{0}C for 1440 minutes.
- Cool from 100 ^{0}C to 50 ^{0}C at 5 ^{0}C/min.
- Hold at 50 ^{0}C for 1440 minutes (until equilibrium).

Sample of calculations to determine carbon dioxide capture capacity of adsorbents are presented below. The calculations also apply to other modified adsorbents.

Sample name	=	MCM-41
Original sample weight	=	19.148 mg
Weight after heating	=	90.5253 % x 19.148 mg
	=	17.334 mg

Weight difference after adsorption = 92.2065 % - 90.5253 %

= 1.6812 %

CO_2 weight = 1.6812 % x 19.148 mg

= 0.322 mg

CO_2 capture capacity = $\frac{0.322 mg}{0.017334 g \cdot sorbent}$

= $18.58 \frac{mg}{g \cdot sorbent}$